

L-1006  
II  
4266

FINAL REPORT

For

**Analysis, Design and Development  
of a Flat Plate Solar Thermoelectric  
Energy Conversion Panel**

12 June 1963 - 12 December 1963

Contract No. NAS5-3400

GPO PRICE \$ \_\_\_\_\_

CFSTI PRICE(S) \$ \_\_\_\_\_

Prepared by

Hard copy (HC) 5.00

Microfiche (MF) 1.00

MELPAR, INC.

3000 Arlington Boulevard

Falls Church, Virginia

ff 653 July 65

For

N66-27323  
167  
CR-75388  
(ACCESSION NUMBER)  
(PAGES)  
(NASA CR OR TMX OR AD NUMBER)

(THRU)  
/ (CODE)  
03 (CATEGORY)

NATIONAL AERONAUTICS AND SPACE ADMINISTRATION  
GODDARD SPACE FLIGHT CENTER  
Greenbelt, Maryland

747-38708

FINAL REPORT

for

ANALYSIS, DESIGN AND DEVELOPMENT  
OF A FLAT PLATE SOLAR THERMOELECTRIC  
ENERGY CONVERSION PANEL

12 June 1963 - 12 December 1963

Contract No: NAS5-3400

Prepared by

MELPAR, INC.  
3000 Arlington Boulevard  
Falls Church, Virginia

Prepared for

National Aeronautics and Space Administration  
Goddard Space Flight Center  
Greenbelt, Maryland



## ABSTRACT

2 0323

This report covers the technical effort on the first phase of a program directed toward the analysis, design, and fabrication of a flat plate solar thermoelectric power generation module. This panel should be capable of producing three to six watts of electrical power per square foot of oriented collector surface, with a weight factor of at least fifteen watts per pound (including support structure) in an earth orbit.

The technical effort covered:

- a. A design analysis.
- b. Mechanical and configurational design of flat plate thermoelectric panels meeting the performance and weight requirements.
- c. Separate testing and selection of thermoelectric materials.
- d. Analysis of behavior of these materials, and the couples made from them.
- e. Fabrication and evaluation of experimental thermoelectric unit couples.
- f. Fabrication and initial testing of flat plate thermoelectric panels.

The design analysis was based upon the performance of experimental thermoelectric couples and demonstrated the practicability of achieving the thermoelectric performance required in a flat plate generator panel. Existing available  $\text{Bi}_2\text{Te}_3$  based alloy materials have been shown to have poorer characteristics than can be deduced from current literature, and extensive work on material evaluation and selection was necessitated.

Mechanical designs for the experimental flat plate thermoelectric generator panels were made, and three types of experimental panels were fabricated from unit couples and evaluated. The unit couples used in the basic unit structure employed in the panels exhibited thermoelectric conversion efficiencies of the order of 5%. This is not overall efficiency since performance was reduced by radiative leakage between the absorber and radiator plates due to inadequate internal low-emissivity coatings. The performance of flat plate panels made from units of this type may be deduced, since the assembly of unit couples into panels incurs little performance degradation.

# TABLE OF CONTENTS

	<u>Page</u>
ABSTRACT	ii
LIST OF ILLUSTRATIONS	iv
LIST OF TABLES	ix
1. INTRODUCTION	1
2. TECHNICAL DISCUSSION	2
2.1 Program Synopsis	2
2.2 Design Analysis	5
2.2.1 Calculation of Panel Design Based on Measured Properties of Experimental Couples	5
2.2.2 Conclusions	11
2.3 Configurational Design	12
2.3.1 Mechanical and Thermal	13
2.3.2 Weight	17
2.3.3 Electrical	19
2.3.4 Final Flat Plate Panel Designs	19
2.3.5 Conclusions	24
2.4 Thermoelectric Material Evaluation and Selection	25
2.4.1 Profiling of Ingot Parameters	26
2.4.1.1 Electrical Resistivity	26
2.4.1.2 Seebeck Coefficient	26
2.4.2 Variation of Electrical Resistivity with Temperature	42
2.4.3 Evaluation of Material Performance through Measurement of $\Delta T_{max}$	42
2.4.4 Conclusions	46
2.5 Fabrication of Experimental Flat Plate Thermoelectric Generator Couples and Panels	49
2.5.1 Experimental Work in Fabrication	49
2.5.2 Conclusions	64
2.6 Testing and Evaluation of Experimental Single Couples	65
2.6.1 Junction Resistance	65
2.6.2 Junction Mechanical Strength	68
2.6.3 Thermoelectric Performance	70
2.6.4 Temperature Cycling	72
2.6.5 Conclusions	77
2.7 Testing and Evaluation of Experimental Flat Plate Thermoelectric Generator Panels	79
2.7.1 Mechanical and Thermal	79
2.7.2 Thermoelectric Performance	83
2.7.3 Conclusions	86
2.8 Summary of Conclusions	86

## TABLE OF CONTENTS (Continued)

	<u>Page</u>
3. NEW TECHNOLOGY	89
3.1 Junction Joining Techniques	89
3.2 Panel Structures	89
4. BIBLIOGRAPHY	91
5. APPENDIX I Detailed Fabrication Processes for the Construction of Experimental Flat Plate Solar Thermoelectric Energy Conversion Panels	I-1

# LIST OF ILLUSTRATIONS

<u>Figure</u>		<u>Page</u>
1	Flat Plate Thermoelectric Generator Design, Type I	20
2	Flat Plate Thermoelectric Generator Design, Type II	21
3	Flat Plate Thermoelectric Generator Design, Type III	22
4	Two-Point Electrical Resistivity Probe Apparatus	27
5	Schematic Representation of Two-Point Resistivity Probe Apparatus	28
6	Average Electrical Resistivity as a Function of Distance Along the Ingot. Ingot 5P	29
7	Average Electrical Resistivity as a Function of Distance Along the Ingot. Ingot 6N	30
8	Average Electrical Resistivity as a Function of Distance Along the Ingot. Ingot N-1	31
9	Average Electrical Resistivity as a Function of Distance Along the Ingot. Ingot N-2	32
10	Average Electrical Resistivity as a Function of Distance Along the Ingot. Ingot N-4	33
11	Seebeck Coefficient Apparatus	35
12	Schematic Representation of Seebeck Coefficient Apparatus	36
13	Average Seebeck Coefficient as a Function of Distance Along the Ingot. Ingot 5P	37
14	Average Seebeck Coefficient as a Function of Distance Along the Ingot. Ingot 6N	38
15	Average Seebeck Coefficient as a Function of Distance Along the Ingot. Ingot N-1	39
16	Average Seebeck Coefficient as a Function of Distance Along the Ingot. Ingot N-2	40
17	Average Seebeck Coefficient as a Function of Distance Along the Ingot. Ingot N-4	41

# LIST OF ILLUSTRATIONS (Continued)

<u>Figure</u>		<u>Page</u>
18	Block Diagram of Equipment Used for Measuring Resistivity as a Function of Temperature	43
19	Resistivity of $\text{Bi}_2\text{Te}_3$ Alloy Ingots as a Function of Temperature	44
20	Test Apparatus for Determination of $\Delta T_{\text{max}}$	45
21	Experimental Unit Couple Generators for Type II and III panels	52
22	Assembly Jig, Thermoelectric Elements to Absorber Plate Subassemblies	54
23	Assembly Jig, Thermoelectric Elements - Absorber Plate Subassembly to Radiator Plates	55
24	Radiator Panel Subassembly, Type I	58
25	Configuration of Type II Panel Radiator Plates	59
26	Configuration of Type III Panel Radiator Plates	60
27	Final Assembly Jig for Panels (Types I, II, and III)	61
28	Cross-Sectional View of Experimental Flat Plate Single Couple (Potting Material not Removed)	66
29	Typical Contact Resistance of Lead to Ni Plated N- and P-Type $\text{Bi}_2\text{Te}_3$ Elements	67
30	Evaluation Apparatus for Experimental Flat Plate Single Couples	71
31	Temperature Cycling Life Test Apparatus	74
32	Initial Temperature Cycling Life Test Data	75
33	Experimental Flat Plate Generator Panel, Type I	80
34	Experimental Flat Plate Generator Panel, Type II	81
35	Experimental Flat Plate Generator Panel, Type III	82
36	Evaluation Apparatus for Experimental Flat Plate Panels	84

# LIST OF ILLUSTRATIONS (Continued)

<u>Figure</u>		<u>Page</u>
37	Heat Input Resistor Array and Heat Sink for Evaluation of Experimental Flat Plate Panels	85
38	Flow Chart of Flat Plate Panel Fabrication Process	I-7
39	Absorber and Radiator Plate Forms Used with Type I Panels	I-8
40	Absorber and Radiator Plate Forms Used With Type II-III Panels	I-9
41	Semiconductor Wafering Machine	I-12
42	Thermoelectric Materials: Ingots, Pellets, and Elements	I-14
43	Multiple Station Nickel Plating Apparatus for Elements	I-16
44	Airbrasive Unit	I-17
45	Drawing of Thermoelectric Element	I-19
46	Thermoelectric Elements: Cut, Ends Blasted, Plated, and Solder Contacted	I-21
47	AC Resistance Test Fixture	I-24
48	Thermoelectric Element, Absorber Plate Subassembly	I-27
49	Absorber and Radiator Plate Forming Dies	I-33
50	Hydraulic Press Used for Forming Absorber and Radiator Plates	I-34
51	Electroless Nickel Plating Apparatus	I-35
52	Drawing of Absorber Plate	I-39
53	Absorber Plates: As Formed, with Elements Attached, and Coated with Gold	I-40
54	Assembly Jig for Radiator Plate Subassembly	I-41
55	Radiator Plate Subassembly	I-44

## LIST OF ILLUSTRATIONS (Continued)

<u>Figure</u>		<u>Page</u>
56	Drawing of Radiator Plates	I-45
57	Drawing of Stainless Steel Support Structure	I-48
58	Stainless Steel Support Structure	I-49

## LIST OF TABLES

<u>Table</u>		<u>Page</u>
1	Design Parameter Tables	8
2	Criteria for Selection of Structural Material	14
3	Calculated Weights of Panel Components for a One Square Foot Panel	18
4	Results of $\Delta T_{\max}$ Measurements on Sections of Thermoelectric Material Ingots	47
5	Thermoelectric Performance of Typical Flat Plate Single Couples	73
6	List of Direct Materials	I-3
7	List of Indirect Materials	I-4
8	List of Equipment	I-5 I-6



## 1. INTRODUCTION

This is the final report for the first phase of a program directed toward the design and development of a thermoelectric flat plate solar power generator. This generator is to be capable of producing three to six watts of electrical power per square foot of oriented absorber surface with a weight factor of at least 15 watts per pound in an earth orbit.

The principle of the flat plate solar energy conversion panel was demonstrated experimentally by the Aeronautical Systems Division (USAF), Wright-Patterson Air Force Base, Ohio.<sup>1</sup>

The thermoelectric materials used in that flat plate panel were lead-telluride N-type and zinc antimonide P-type. The materials indicated are not the optimum materials for use in the temperature range in which the flat plate panel will be operating, in an earth orbit. In this temperature range (approximately 300° to 600°K), these materials show a figure-of-merit,  $Z$ , of approximately  $1.2 \times 10^{-3} \text{ }^{\circ}\text{K}^{-1}$ , resulting in devices with  $Z = 1.0 \times 10^{-3} \text{ }^{\circ}\text{K}^{-1}$  or less. In this temperature range, bismuth telluride alloys exhibit  $Z$  values of  $2.0$  to  $2.8 \times 10^{-3} \text{ }^{\circ}\text{K}^{-1}$  resulting in devices with  $Z = 1.5$  to  $2.5 \times 10^{-3} \text{ }^{\circ}\text{K}^{-1}$ .<sup>2</sup>

The work during this phase of this program covered:

- a. A design analysis.
- b. Mechanical and configurational design of flat plate thermoelectric panels meeting the performance and weight requirements.
- c. Separate testing and selection of thermoelectric materials.
- d. Analysis of behavior of these materials and couples.
- e. Fabrication and evaluation of experimental thermoelectric couples.
- f. Fabrication and initial testing of flat plate thermoelectric panels.

## 2. TECHNICAL DISCUSSION

This discussion is divided into eight subsections in which the technical effort of this program is described, and the resulting data presented and analyzed. The first subsection (2.1) is a concise summary of the technical effort on this program in the first quarter. The remainder of the discussion section (2.2 to 2.7) is concerned with the technical effort of the second quarter. The last subsection (2.8) is a summary of the overall first phase program conclusions. The detailed fabrication processes for the experimental flat plate modules are given in Appendix I.

### 2.1 Program Synopsis (First Quarter)

The work during the first quarter of this program covered:

- a. An examination of the problem to determine the probable hot and cold junction operating temperatures.
- b. The development and testing of thermoelectric junction assembly methods suitable for use in the temperature range.
- c. The evaluation of materials and material requirements from tests on thermoelectric couples and from measurements made directly on thermoelectric materials.
- d. The evaluation of the experimental thermoelectric generator couples.
- e. A design analysis suitable for determination of the basic physical structure of a flat plate generator module using variable radiation heat exchange constants and the characteristics of available thermoelectric material.<sup>3</sup>

Junction assembly techniques permitting  $\text{Bi}_2\text{Te}_3$  hot junction operation as high as  $300^\circ\text{C}$  were developed. Up to six percent thermoelectric conversion

efficiency was observed with hot and cold junctions at temperatures consistent with the temperatures defined by the design analysis ( $T_e = 40^\circ$  to  $80^\circ\text{C}$ ,  $T_h = 200^\circ$  to  $300^\circ\text{C}$ ). Using data from the experimental thermoelectric couples, a design analysis was made which demonstrated that the requirements of the program could be met.

The probable hot and cold junction temperatures were established by assuming a practical thermoelectric generator efficiency. Since the conversion efficiency tends to be on the order of four to six percent, approximately 94 to 96 percent of the absorbed radiation must be reradiated from the cold junction, if radiator and absorber areas are equal. With a maximum of 129 watts per square foot of solar energy density, and assuming achievable values for absorber and radiator coatings, (absorber - absorptivity = 0.9, emissivity = 0.15; radiator - emissivity = 0.95) between 50 and 100 watts per square foot will be absorbed and passed through the generator. This energy will require radiation at the cold side to maintain the desired cold junction temperature. Using the Stefan-Boltzman radiation law and attainable emissivities for the radiator, the approximate cold junction temperature can be deduced.

The hot junction temperature is then determined by that temperature required to provide the maximum performance for the generator, taking into consideration the practical operating temperature range of the thermoelectric material, the generator power output requirements, and the reradiation effects at the absorber.

Techniques were developed to allow operation of experimental thermoelectric couples in the temperature range of  $200^\circ$  to  $300^\circ\text{C}$ . Joints were

made using bismuth (M.P. 271°C) and lead (M.P. 327°C). With the bismuth, the joints were made by alloying directly to the  $\text{Bi}_2\text{Te}_3$  materials; the lead was used as a joint with nickel plated  $\text{Bi}_2\text{Te}_3$ .

Contact resistance studies were made on the bismuth to  $\text{Bi}_2\text{Te}_3$  and lead to nickel-plated  $\text{Bi}_2\text{Te}_3$  contacts to determine their quality. These measurements showed no abrupt change in the resistance slope as the potential drop across the junction was probed. Rather, a smooth transition from the bonding material to the  $\text{Bi}_2\text{Te}_3$  was found, indicating the electrical soundness of the joints.

Direct material measurements were made on as-supplied ingots in order to determine their uniformity and suitability as generator materials. The resistivities of the ingots were measured as a function of temperature. In addition considerable material evaluation was performed on the assembled couples. The couples were also evaluated for efficiency and power output. The material and device characteristics of five individual couples were measured, calculated and analyzed.<sup>3</sup> Couple efficiencies as high as six percent were measured.

The material characteristics and couple performance measured indicate that the minimum performance requirements of the flat plate generator can be met, but that the available  $\text{Bi}_2\text{Te}_3$  materials are not optimized for this generator application and therefore the performances achieved do not represent the level of performance that can reasonably be expected. A higher level of performance can be expected with optimized material. A material that is optimized in the required temperature range with controlled parameters is considered achievable but is beyond the scope of the present program.

## 2.2 Design Analysis

The design analysis was made using data from experimental couples that were fabricated and evaluated during the first quarter of this effort. This data is given in section 2.4.5, ppg 36-39, of the first quarterly report.<sup>3</sup>

### 2.2.1 Calculation of Panel Design Based on Measured Properties of Experimental Couples

In order to make the calculations the following assumptions were made, based upon values which have a reasonable expectation of being achieved.

#### Assumptions:

- a. Absorptivity of absorber surface,  $\alpha_a = 0.90$
- b. Emissivity of absorber surface,  $\epsilon_a = 0.15$
- c. Emissivity of radiator surface,  $\epsilon_r = 0.95$
- d. Thermoelectric conversion efficiency,  $\eta_o = 5\%$
- e. Emissivity of absorber inner surface,  $\epsilon_{a_i} = 0.025$
- f. Emissivity of radiator inner surface,  $\epsilon_{r_i} = 0.020$
- g. Area of absorber,  $A_a = A_r$ , area of radiator

The solar energy absorbed,  $W_a$ , is

$$W_a = W \cdot \alpha_a \quad (1)$$

where:  $W$  = solar constant in earth orbit = 129 watts/ft<sup>2</sup>,

$$\alpha_a = 0.9$$

$$W_a = 117 \text{ watts/ft}^2$$

(with the assumed values for the inner surface emissivities, the heat loss by internal radiation exchange is less than a few percent of the energy input and is neglected in this approximate calculation).

An electrical power output,  $P_{out}$ , from the panel of at least 3 watts/ft<sup>2</sup> is required. To determine the energy to be radiated from the radiator surface the input power,  $P_{in}$ , is determined assuming a value of  $\eta_o = 5\%$ .

$$P_{in} = \frac{P_{out}}{\eta_o} = \frac{3}{.05} \quad (2)$$

$$P_{in} = 60 \text{ watts/ft}^2.$$

Of this energy input, 3 watts/ft<sup>2</sup> is converted and therefore the energy to be dissipated by the radiator surface is 57 watts/ft<sup>2</sup>.

Using Radiative Heat Transfer Tables, the temperature of the radiator,  $T_c$ , is determined.<sup>4</sup> In these tables, values of heat radiated per unit area are given as a function of emissivity and temperature by tabulating the function

$$\dot{q}/A = \sigma \epsilon T^4 \text{ watts/cm}^2 \quad (3)$$

for various values of emissivity and temperature. It is then possible, given the amount of heat to be radiated (57 watts/ft<sup>2</sup>) and the emissivity (in the case of the radiator, 0.95), to find the temperature which the surface will attain if the radiation is to deep space.

In this manner, a temperature of approximately 333°K or 60°C is found for the radiator temperature.

The calculation of the temperature of absorber surface,  $T_h$ , is determined in a like manner. The amount of heat to be reradiated,  $W_{rerad}$ , from the absorber surface must be

$$W_{rerad} = W_a - P_{in} = 117 - 60 \quad (4)$$

$$W_{rerad} = 57 \text{ watts/ft}^2$$

The  $T_h$  required to give reradiation of 57 watts/ft<sup>2</sup> at  $\epsilon_r = 0.15$ , from the tables, is approximately 513°K or 240°C.

The operating temperature difference,  $\Delta T$ , is now defined:

$$\Delta T = 240^\circ\text{C} - 60^\circ\text{C} = 180^\circ\text{C}$$

From the previous measured performance of experimental generator couples at this  $\Delta T$ , an  $\eta_0 = 4.8\%$  (independent of  $T$ ) is found.<sup>3</sup> Therefore, the assumed 5% thermoelectric conversion efficiency is correct. A further check on  $\eta_0$  from the experimental data is given by finding the  $\Delta T$  which gives 5% efficiency. This value is found to be  $\Delta T = 190^\circ\text{C}$ .  $T_h$  is then  $190^\circ\text{C} + 60^\circ\text{C} = 250^\circ\text{C}$ . Table 1 summarizes the effects of varying the thermoelectric efficiency.

The significant thermoelectric consideration in arriving at a solar generator design is the geometry factor,  $A/\ell$ , the ratio of the total area,  $A$ , of thermoelectric material to the length,  $\ell$ , of the thermoelectric material.

$$\text{For electrical power to a matched load } R = R_L, I = \frac{S\Delta T}{R_L + R} = \frac{S\Delta T}{2R}$$

$$P_{\text{out}} = I^2 R_L = \left( \frac{S\Delta T}{R + R_L} \right)^2 R_L = \frac{(S\Delta T)^2}{4R} = \frac{(\bar{S}\Delta T)^2}{16\bar{\rho}} \frac{A}{L}$$

$$\text{since } R_L = R = \frac{4\rho L}{A} \text{ with } A_n = A_p = \frac{A}{2} \text{ and } \bar{\rho} = \frac{\rho_n + \rho_p}{2}.$$

The  $A/\ell$  may be calculated from

$$P_\ell = 3 \text{ watts/ft}^2 = \frac{(\bar{S}\Delta T)^2}{16\bar{\rho}} \cdot \frac{A}{\ell} \quad (5)$$

$$\text{then } \frac{A}{\ell} = P_\ell \times \frac{16\bar{\rho}}{(\bar{S}\Delta T)^2} = 3 \times \frac{16 \times (1.24 \times 10^{-3})}{(326 \times 10^{-6} \times 180)^2} = 17.3$$

$$\frac{A}{\ell} = 17.3$$

TABLE 1

## DESIGN PARAMETER TABLES

Conditions:  $\epsilon_c = 0.15$ ,  $\alpha_c = 0.9$      $\epsilon_r = 0.95$      $A_c = A_r$   
 (for  $3\text{w/ft}^2$ )

Efficiency	Minimum Residual Power	Power to be Radiated	Required Collector Temperature	Required Radiator Temperature	$\Delta T$	Possible Condition	Comments
3%	$100\text{w/ft}^2$	$97\text{w/ft}^2$	$120^\circ\text{C}$	$100^\circ\text{C}$	$20^\circ\text{C}$	No	$\Delta T$ too small for 3% efficiency
4	75	72	200	75	125	Yes	All values in practical range.
5	60	57	240	60	180	Yes	
6	50	47	290	40	250	Yes	



$P_{\ell}$  = power output to a matched load

$\bar{\rho}$  = electrical resistivity averaged for couples between 60°C and 240°C  
 $= 1.24 \times 10^{-3} \text{ } \Omega\text{cm}$

$\bar{S}$  = Seebeck voltage averaged for couples between 60°C and 240°C  
 $= 326 \times 10^{-6} \text{ V}$

Alternatively, for a matched load,  $A/\ell$  may be calculated as follows:

The input power for matched load

$$\begin{aligned} P_{in} &= (K\Delta T + \pi I - 1/2 I^2 R) = (K\Delta T + S_{T_h} T_h \frac{\bar{S}\Delta T}{2R} - \frac{(\bar{S}\Delta T)^2}{8R}) \\ &= \frac{A}{\ell} (\bar{K}\Delta T + \bar{S}_{T_h} T_h \frac{\bar{S}\Delta T}{8\bar{\rho}} + \frac{(\bar{S}\Delta T)^2}{32\bar{\rho}}) \end{aligned}$$

$$\text{Since } I = \frac{S\Delta T}{R_L + R} = \frac{S\Delta T}{2R} \text{ and } R = R_L = \frac{4\rho\ell}{A}$$

$$\text{with } A_n = A_p = \frac{A}{2} \text{ and } \bar{\rho} = \frac{\rho_n + \rho_p}{2}$$

$$\text{Thus } \frac{A}{\ell} = \frac{P_{in}}{\Delta T \cdot k + (S_{T_h} T_h) \frac{\bar{S}\Delta T}{8\bar{\rho}} + \frac{(\bar{S}\Delta T)^2}{32\bar{\rho}}} \quad (6)$$

$$= \frac{60 \text{ watts/ft}^2}{180 \times 1.6 \times 10^{-2} + 5.7 \times 10^{-3} \cdot \frac{320 \times 10^{-6} \times 513}{8 \times 1.24 \times 10^{-3}} + \frac{5.7 \times 10^{-2}}{32 \times 1.24 \times 10^{-3}}}$$

$$\frac{A}{\ell} = 15.4$$

$k$  = Thermal conductivity of the couple averaged between 60°C and 240°C  
 $= 1.6 \times 10^{-2} \text{ w/cm}^{\circ}\text{K}$

$S_{T_h}$  = Seebeck coefficient at  $T_h$   
 $= 316 \times 10^{-6} \text{ V}$

The average of the two calculated values for  $A/\ell$  is 16.35. A value of  $A/\ell = 16$  was chosen for design purposes and is the approximate value required to achieve 3 watts/ft<sup>2</sup> at 5% efficiency, assuming that the contact resistance is negligible.

Next the weight of the thermoelectric material is determined. Using  $A/\ell = 16$  and  $\ell = 0.3$  cm (chosen on the basis of practical handling considerations and estimated),  $A = 4.8$  cm<sup>2</sup>. The volume is then  $V = A\ell = 1.44$  cm<sup>3</sup>.

The density,  $d$ , of Bi<sub>2</sub>Te<sub>3</sub> alloys is 7.8 g/cm<sup>3</sup>. The weight of thermoelectric material,  $Wt. = Vd = 11.2$  grams. The required power output per unit of weight is 15 watts/lb. With 3 watts/ft<sup>2</sup>, the required  $Wt./ft^2$

$$\frac{Wt.}{ft^2} = \frac{3 \text{ watts/ft}^2}{15 \text{ watts/lb}} = 0.2 \text{ lb.} = 90 \text{ grams} \quad (7)$$

The amount of weight allowance for non-thermoelectric materials is approximately 90 g - 11.2 g = 79 grams.

In calculating the number of couples to be used in the design, we must compromise between the conflicting requirements of having a high output voltage (of the order of 3V/ft<sup>2</sup>) and keeping the initial panel structures from becoming too complex. At the operating  $\Delta T$ , approximately 100 couples would be required to give 3V/ft<sup>2</sup>. A compromise for the number of couples,  $n$ , was chosen:  $n = 64$ .

The dimensions of the square elements were calculated from value of  $A = 4.8$  cm<sup>2</sup>, which was previously determined. This  $A$  is total thermoelectric material area. The area of the individual thermoelectric leg,  $A/\ell$ , was determined

$$A/\ell = \frac{A}{2n} = \frac{4.8}{128} = 0.0375 \text{ cm}^2. \quad (8)$$

The width or side dimension,  $x$ , of the leg

$$x = \sqrt{A/\ell} \quad (9)$$

$$x = 0.194 \text{ cm or } 0.076 \text{ inch.}$$

The dimensions of the legs or elements of the couples are then 0.076 in. x 0.076 in. x 0.118 in. (0.194 cm x 0.194 cm x 0.3 cm).

The weights and characteristics of the non-thermoelectric materials are considered in section 2.3.

#### 2.2.2 Conclusions

The design analysis leads to the following conclusions:

a. Given requirements of at least three watts electrical output power per square foot and 15 watts per pound, and with the given solar constant in an earth orbit, the physical laws of radiation, known or estimated properties of materials, the  $A/\ell$  ratio = 16 cm.

b. Assuming the availability of thermoelectric material which can provide a conversion efficiency of 4.8% or better between 60° and 240°C with an  $A/\ell$  = 16 cm, element length = 0.3 cm, and using the non-thermoelectric materials specified in the next section, a flat plate generator panel can be fabricated, that should meet the power requirements of 15 watts/lb provided the non-thermoelectric weight can be reduced to 79 gm/ft<sup>2</sup>.

c. Using 64 couples of 0.3 cm length with square legs of 0.19 cm, sufficient mechanical stability should be provided while satisfying conclusions a and b. The voltage output into a matched load should then be 1.9 v/ft<sup>2</sup> with all couples connected in series.

### 2.3 Configurational Design

The special requirements of a light weight space environment thermoelectric generator in the form of a flat plate makes great and often conflicting demands upon the design. In considering these requirements, it was necessary to make many design compromises to achieve a practical and more nearly optimized mechanical design. It was necessary to choose materials which combine desirable or acceptable thermal and mechanical strength and rigidity properties. In all cases, weight of the materials to be used was extremely important and therefore was emphasized. The electrical conductivity of absorber and radiator plates, solders, platings, etc., were almost equally important, since the electrical resistance of the couple interconnections had to remain a small fraction of the total resistance, in order to achieve maximum efficiencies.

The designs worked out are likely to provide practical and satisfactory solutions to the configurational design problem.

The material chosen for the absorber and radiator plates is aluminum. It can be shown that this is the best choice among the most reasonable candidates. If a merit factor,  $M$ , which defines the criteria for the selection of a plate material, is

$$M = \frac{ks}{\rho d^2}$$

where

$k$  = thermal conductivity,

$s$  = structural strength,

$\rho$  = electrical resistivity,

$d$  = density,

then aluminum can be shown to have the greatest merit factor at both 60° and 200°C (see table 2). This merit factor was deduced by Melpar based upon the obviously important required material characteristics and the estimate of the relative importance of each in the total design.

### 2.3.1 Mechanical and Thermal

Mechanical and thermal design factors are considered together since the more pertinent thermal phenomena manifest themselves in a mechanical manner.

Considering the mechanical factors first, the following requirements must be met:

Structural strength (the panel and component materials must have an acceptable degree of strength and rigidity to withstand assembly, testing and application).

An analysis was made of the mechanical properties of structural materials (absorber and radiator plates, thermoelectric elements, solders, adhesives, the support structure, etc.). The choice of the material for the absorber and radiator plates, aluminum (alloy 1100), is explained in section 2.3. The mechanical properties of the thermoelectric materials are fixed, although it is not uncommon for mechanical properties to vary rather drastically from ingot to ingot. In general,  $\text{Bi}_2\text{Te}_3$  based alloy thermoelectric materials are sufficiently strong to be applied to a flat plate generator design if properly handled.

Solders have been chosen on the basis of compatibility with the other materials used, rather than from considerations of mechanical strength. However, the strengths of the solders (for junctions, Pb and Sn-Pb) are greater than that of the thermoelectric materials and hence are satisfactory.

TABLE 2

CRITERIA FOR SELECTION OF STRUCTURAL MATERIAL

$$M = \frac{k^s}{\rho d^2}$$

	Radiator Temperature, $T_c \sim 60^\circ\text{C}$					Absorber Temperature, $T_h \sim 240^\circ\text{C}$		
	Structural Strength, $s$	Thermal Conductivity, $k$	Electrical Resistivity, $\rho$	Density, $d$	Merit Factor, $M$	Thermal Conductivity, $k$	Electrical Resistivity, $\rho$	Merit Factor, $M$
Cu (Electrolytic)	$3.17 \times 10^6$	3.98	$1.9 \times 10^{-6}$	8.94	$.836 \times 10^{11}$	3.81	$2.35 \times 10^{-6}$	$.642 \times 10^{11}$
Al (Alloy 1100)	2.46	2.22	3.1	2.71	2.40	2.05	4.6	1.49
Ag (Pure)	2.96	4.19	1.35	10.5	.895	3.89	2.6	.403
Mg (Pure)	2.32	1.38	4.7	1.74	2.25	1.34	7.45	1.39
	$\text{g/cm}^2$	$\text{w/cm}^\circ\text{C}$	$\Omega \text{ cm}$	$\text{g/cm}^3$	$\text{w}\Omega \text{ cm}^\circ\text{C}$	$\text{w/cm}^\circ\text{C}$	$\Omega \text{ cm}$	$\text{w}\Omega \text{ cm}^\circ\text{C}$

Adhesives have been chosen on the basis of the bond strength to the material to which they are applied, their temperature application range and their curing temperatures. The principal adhesive, used for the bonding of the radiator plates to one another, was an epoxy (Armstrong, Type A1). Epoxy was chosen because of its excellent bonding strengths to aluminum and because it could be cured at a low temperature as necessitated by other steps in the assembly process.

The support structure, a rigid superstructure, to be used for handling and mounting the panels, was made from stainless steel tubing. The main structural purpose of the support structure was to add rigidity to the whole panel assembly and to overcome any tendency to warp due to uneven heating. Small diameter, thin wall stainless steel tubing provides the greatest strength and rigidity in long sections of any practical structural material.

Thermally, the obvious and important characteristics of materials in this application are: coefficient of thermal expansion and coefficient of thermal conductivity.

The thermal conductivity of the thermoelectric material is a fixed parameter. The thermal expansion of the thermoelectric material is important in the consideration of the configurational design. The materials to be used in close conjunction with the thermoelectric elements should not make too great a thermal mismatch. The absorber and radiator plates to which the elements are attached are of major importance. The coefficient of linear expansion of  $\text{Bi}_2\text{Te}_3$  based alloy materials is approximately  $20 \times 10^{-6}$  per  $^{\circ}\text{C}$ . The coefficient of linear expansion for aluminum is approximately  $23 \times 10^{-6}$  per  $^{\circ}\text{C}$ . The thermal expansion

of the solders used is of secondary importance, since only small sections a few thousandths of an inch thick are used and the materials are generally soft and will tend to flow under stress.

The epoxy adhesive used in the radiator assembly has a coefficient of expansion on the order of  $60 \times 10^{-6}$  per  $^{\circ}\text{C}$ . They are considered acceptable for use on the radiator side since the temperature should not rise above  $100^{\circ}\text{C}$  in normal operation.

The stainless steel support structure has a coefficient of linear expansion of approximately  $17 \times 10^{-6}$  per  $^{\circ}\text{C}$ . Silicone rubber pads (0.030 in. thick), bonded between the structure and the panel, serve as isolators for differential thermal expansion and mechanical shock.

In operation, the panel with the radiator surface mechanically bonded into a single structure will produce some differential expansion when the absorber plate is heated and the radiator plate remains cool. This is adjusted by annealing both the radiator and absorber plates to a "dead-soft" condition. When differential thermal expansion occurs it is absorbed by very slight bending of the plates (especially the 0.004 in. thick absorber plates). This differential expansion effectively occurs as an increase in the spacing between two adjacent thermoelectric elements fastened to the same hot absorber plate and to the unit structure of the cold radiator plates. The joints are not adversely affected by this stress, since the plates bend slightly. An expansion mechanism, a circular dimple surrounding each element, serves to reduce the stress on the thermoelectric element bonds, by acting as a flexible linkage.

Finally, another significant point relating to the absorber and radiator plates (especially the absorber) is the lateral thermal conductance through the



plate. At the absorber side the lateral thermal conductance must be great enough so that no significant temperature drop occurs among the outlying regions of the absorber plates and the immediate region of the thermoelectric element.

### 2.3.2 Weight

Since weight is an extremely important factor in design of the solar thermoelectric flat plate generator, the weight of the materials used must be considered carefully in connection with the role they play in the total assembly. The weight of the thermoelectric material is fixed by the thermoelectric design given in section 2.2. The calculated weights of the materials required for a square foot panel are given in table 3. The total weight of non-thermoelectric materials used in the experimental panels was 108 grams. This is 29 grams greater than the weight specified in section 2.2 and allowed greater reliability in the mechanical properties of the first panels.

The choice of aluminum for the absorber and radiator surfaces is explained in section 2.3. The choice of thickness was based upon using the maximum allowable weight of aluminum to provide the greatest panel strength and rigidity. The stainless steel tubing support structure provided the greatest strength and rigidity in long sections, of any available material of equivalent size and weight and therefore was chosen.

Since the combined weight of the other materials (solder, adhesives, plating, etc.) is small; their choice was based more heavily upon other factors rather than weight.

TABLE 3

CALCULATED WEIGHTS OF PANEL COMPONENTS  
FOR A ONE SQUARE FOOT PANEL

<u>Material</u>	15 watts/lb for 3 watts/ft <sup>2</sup>	15 watts/lb for 4 watts/ft <sup>2</sup>
	<u>weight/ft<sup>2</sup></u>	<u>weight/ft<sup>2</sup></u>
Thermoelectric Material	12 g	12 g
Aluminum Absorber Surface	19.5 (0.003"th.)	26 (0.004"th.)
Aluminum Radiator Surface	26 (0.004"th.)	52 (0.008"th.)
Plating, Coatings, Adhesives, Solder	12	12
Stainless Steel Support Structure	20.5	18
	<hr/>	<hr/>
Total	90 g	120 g

### 2.3.3 Electrical

The structural materials that have electrical requirements are the absorber, radiator plates and the bonding solders. The bonding solders are chosen primarily for their compatibility with the thermoelectric elements and the total fabrication process, although they must be capable of producing low resistance joints to the thermoelectric elements (contact resistivity  $\leq 1 \times 10^{-5}$  ohm/cm<sup>2</sup>).

The absorber and radiator plates (especially the absorber plates, since they are thinner) must be able to handle the currents generated without producing excessive losses due to  $I^2R$ . Resistance in the plates themselves represents approximately four percent of the resistance of a thermoelectric unit couple.

### 2.3.4 Final Flat Plate Panel Designs

A final panel design and alternative designs are shown in detail in figures 1, 2 and 3. The considerations of the foregoing sections (2.2.1, 2.2.2 and 2.3.1 through 2.3.3) were evaluated in producing these designs.

These panels are based upon a radiator surface that is made up of several discrete radiator plates bonded together with an electrically insulating adhesive. This forms a rigid, relatively strong structure which, along with the stainless steel support structure, provides the mechanical strength of the panels. The absorber surface is made up of several discrete absorber plates. These plates are not bonded together and, hence, are electrically, thermally, and mechanically isolated from one another. Since the absorber surface operates at a much higher temperature than the radiator plate, the resulting differential expansion precludes mechanical joining of the absorber surface.

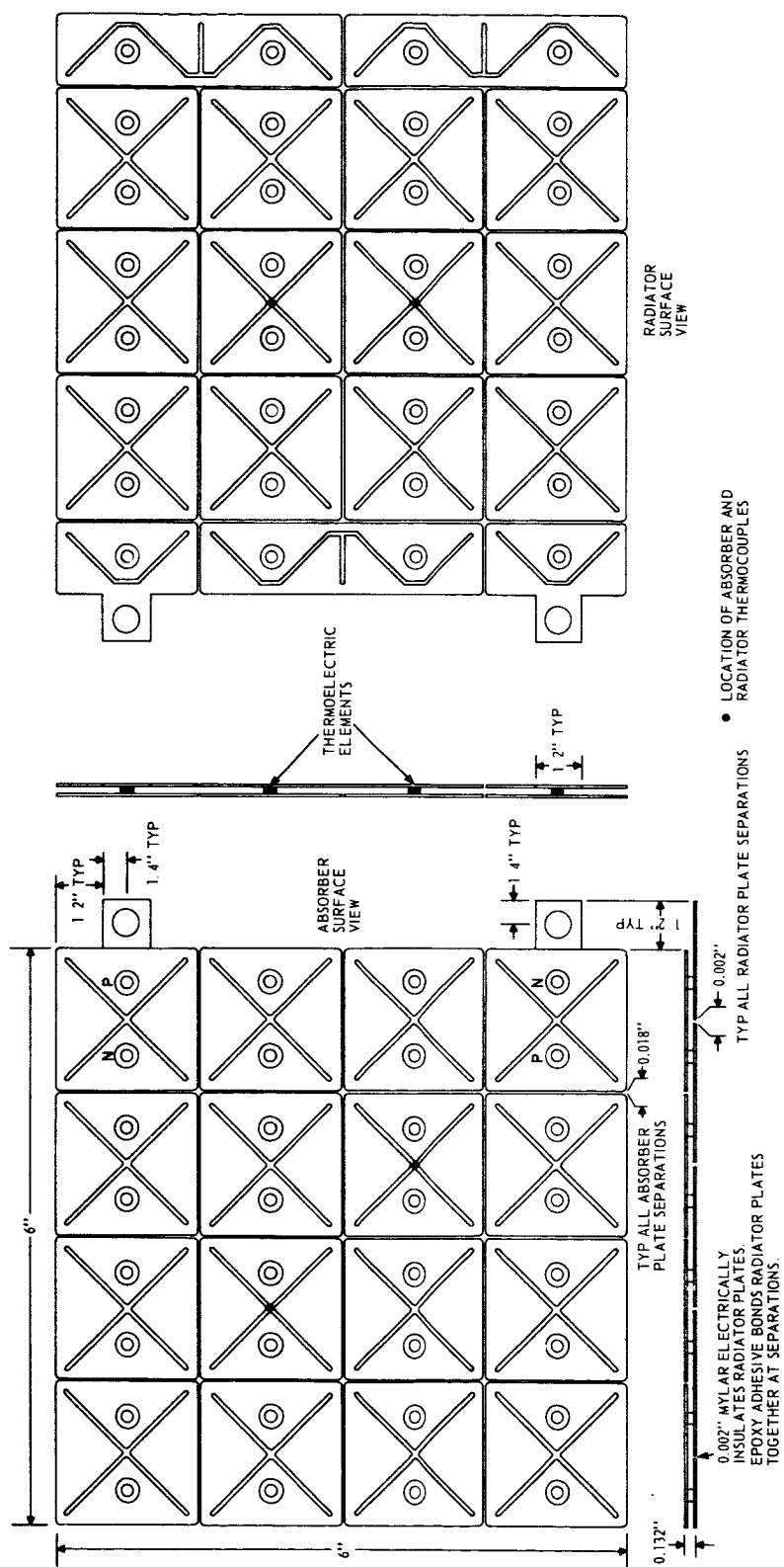


**Figure 1. Flat Plate Thermoelectric Generator Design, Type I**

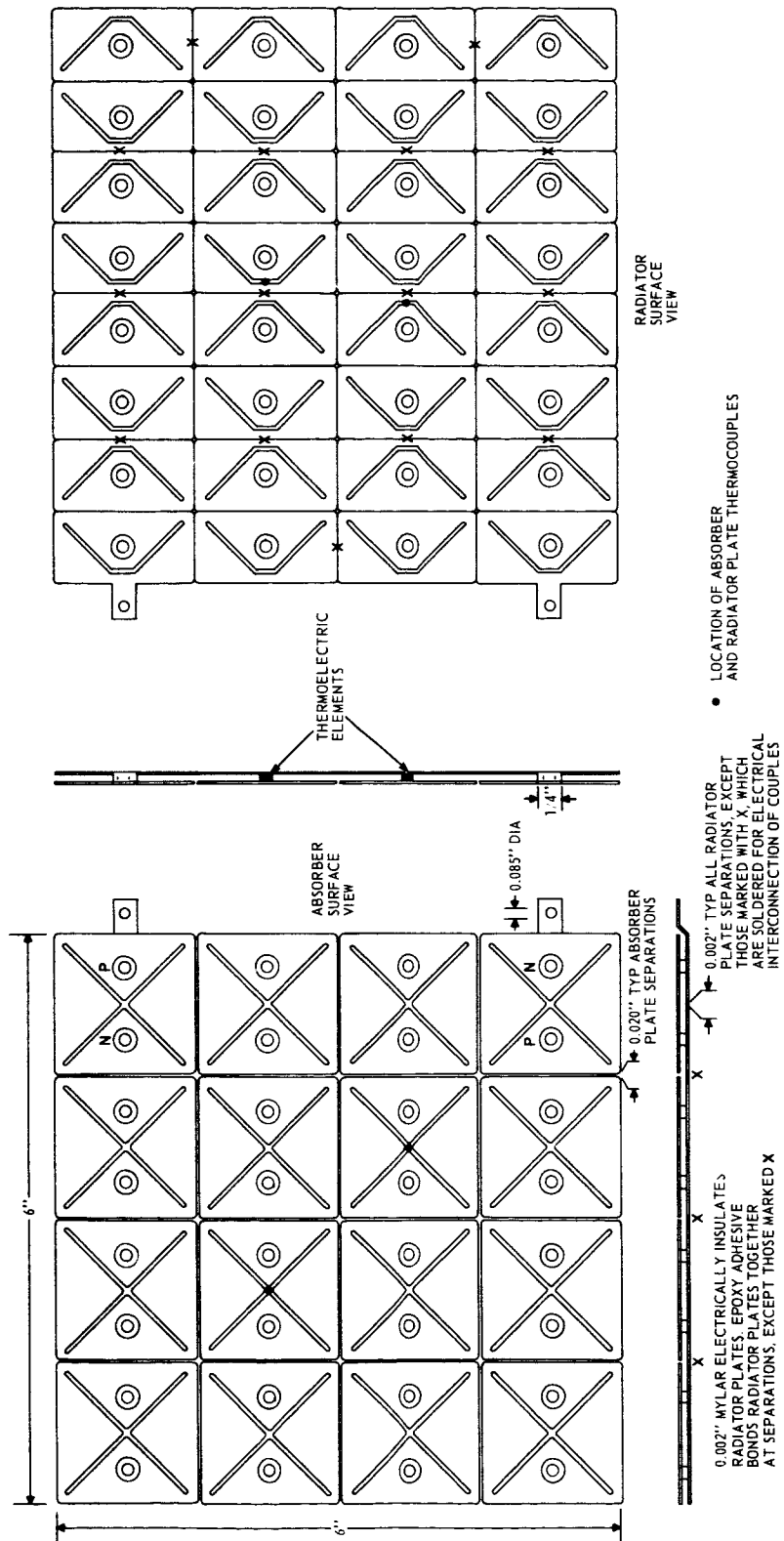


Figure 2. Flat Plate Thermoelectric Generator Design, Type II

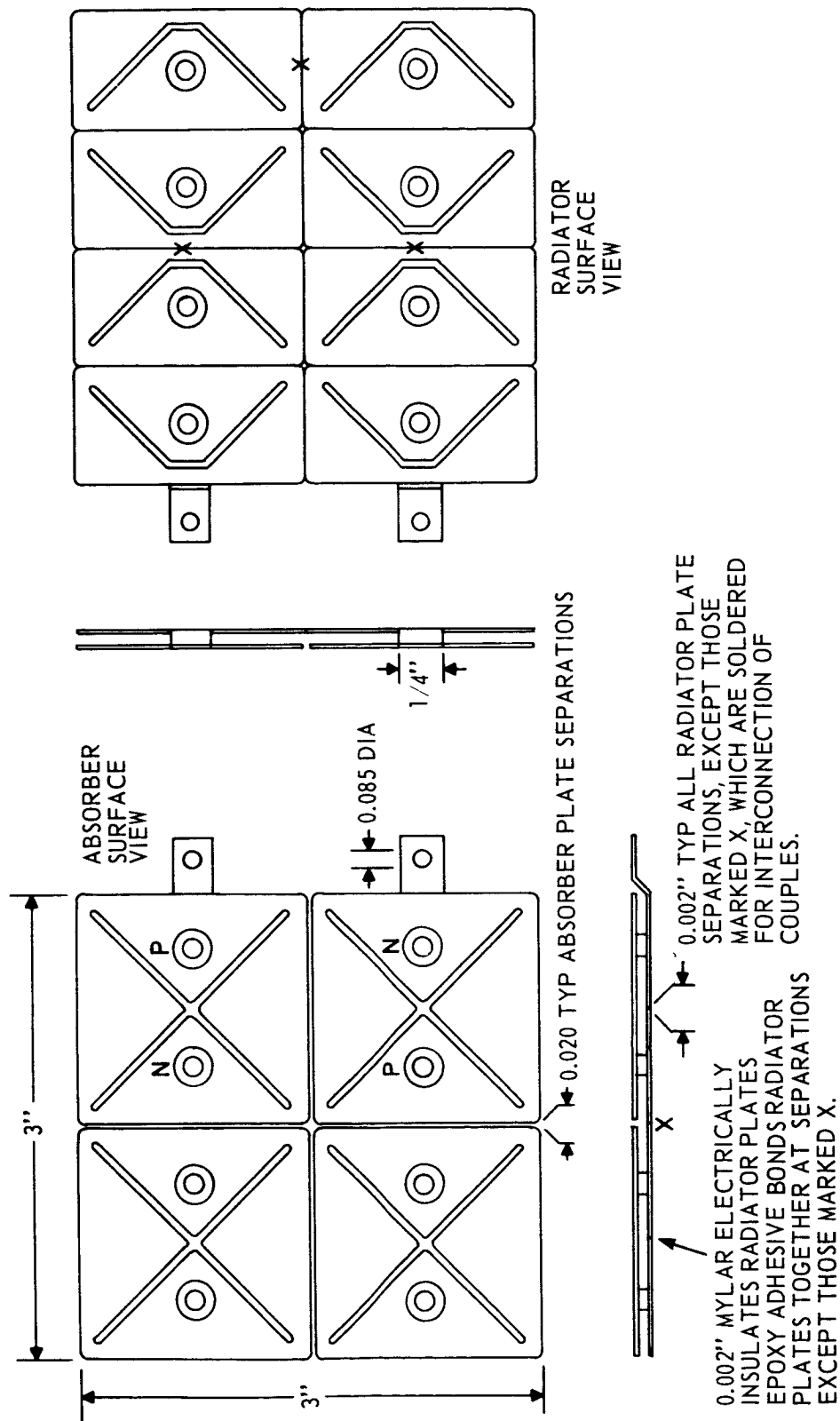


Figure 3. Flat Plate Thermoelectric Generator Design, Type III

The elements are uniformly dispersed throughout the area of the panel. In addition to single couples, three types of panels were constructed:

a. Type I (16 couples): Entire radiator panel prepared and adhesive bonded. Sixteen absorber plate subassemblies soldered simultaneously to the radiator panel. See figure 1.

b. Type II: Sixteen completely fabricated single couples, joined together at the radiator side electrically and mechanically, to form a panel. See figure 2.

c. Type III: Same as Type II, but four couples. See figure 3.

Special features of these designs are:

a. The use of foil with edges turned down all around to increase rigidity and strength of panels.

b. The use of diagonal grooved depressions in the foil to increase rigidity and strength of panels.

c. The plating and tinning a short distance along the length of the thermoelectric elements to increase the bond strength of the solder joints.

d. The use of "dead soft" annealed aluminum to reduce stress on the thermoelectric elements,

e. The use of circular depressions around the thermoelectric elements--aluminum plates joints as a flexible expansion joint.

f. The use of silicone rubber shock isolators between the support structure and the panel.

g. The orientation of the thermoelectric elements so that the diagonal of the element lies in the direction of the thermomechanical stress.

### 2.3.5 Conclusions

Based upon known material properties, the configurational design has been analyzed and it is concluded that:

a. A panel based upon the foregoing designs is practical and should be mechanically and thermally stable.

b. Thermoelectric material deficiencies and/or contact degradation should be the limiting factors in these designs.

c. Four watts per square foot of electrical power from the plate will be necessary to meet the 15 watts per pound weight requirement with the weights for the non-thermoelectric material used as specified in table 2.



## 2.4 Thermoelectric Material Evaluation and Selection

Preliminary work in fabricating experimental generator couples during the first quarter of the program indicated the necessity for testing and selecting the thermoelectric materials to be used in the fabrication of the experimental flat plate generator modules. This work is summarized and described in detail in the following subsections. It was found that great differences exist among ingots of the same type in the commercially available  $\text{Bi}_2\text{Te}_3$  based power generation alloys. In order to select the best ingots and best sections of ingots a testing program was initiated.

Both n- and p-type  $\text{Bi}_2\text{Te}_3$  ingots were probed to produce ingot profiles of Seebeck coefficient and resistivity. The resistivity of certain ingots was measured as a function of temperature as a further aid in choosing the best material. Finally, sections of ingots were fabricated into simple couples so that an approximate "operating condition Z" could be obtained. This was done by measuring the couple as a cooler, operating the hot junction at the proposed operating condition it would experience as a generator ( $\sim 240^\circ\text{C}$ ). A measurement of  $\Delta T_{\text{max}}$  was made. Z was calculated for the  $\Delta T_{\text{max}}$  measurements using

$$\Delta T_{\text{max}} = \frac{Z T_c^2}{2} \quad (11)$$

where:  $T_c$  = temperature of the cold junction.

It was expected that by using these progressively more selective tests, the best material could be chosen from the available thermoelectric material ingots.

#### 2.4.1 Profiling of Ingot Parameters

The first step in thermoelectric material selection was to make room temperature profiles of the electrical resistivity and the Seebeck coefficient.

2.4.1.1 Electrical Resistivity: Each  $\text{Bi}_2\text{Te}_3$  alloy ingot was marked off in centimeters and electrical contacts made to each end of the individual ingots by tinning with tin-bismuth eutectic solder. An ac current of three amperes was passed through the ingot under test, and the potential drop was measured using a two-point probe at each centimeter interval. Four readings were taken 90 degrees apart around ingot at each centimeter interval. These four readings were then averaged giving the voltage value for the particular centimeter interval. Considerable variations were noted around the ingots.

The resistivity was then determined in the usual manner. The diameter of the ingots was 1.2 centimeters and the potential probe spacing was 0.2 centimeters. The apparatus used for these measurements is pictured in figure 4 and schematically presented in figure 5.

Even more dramatic variations of resistivity were found along the length of the ingots as compared to the circumferential variations noted above.

This data is presented in figures 6 through 10, which show the resistivity profiles. Large variations are noted, but the variations do not follow any consistent pattern.

2.4.1.2 Seebeck Coefficient: After completion of the resistivity profiles, the Seebeck Coefficient was measured at four 90-degree intervals around the ingot for each centimeter interval along the length of the ingot. The four

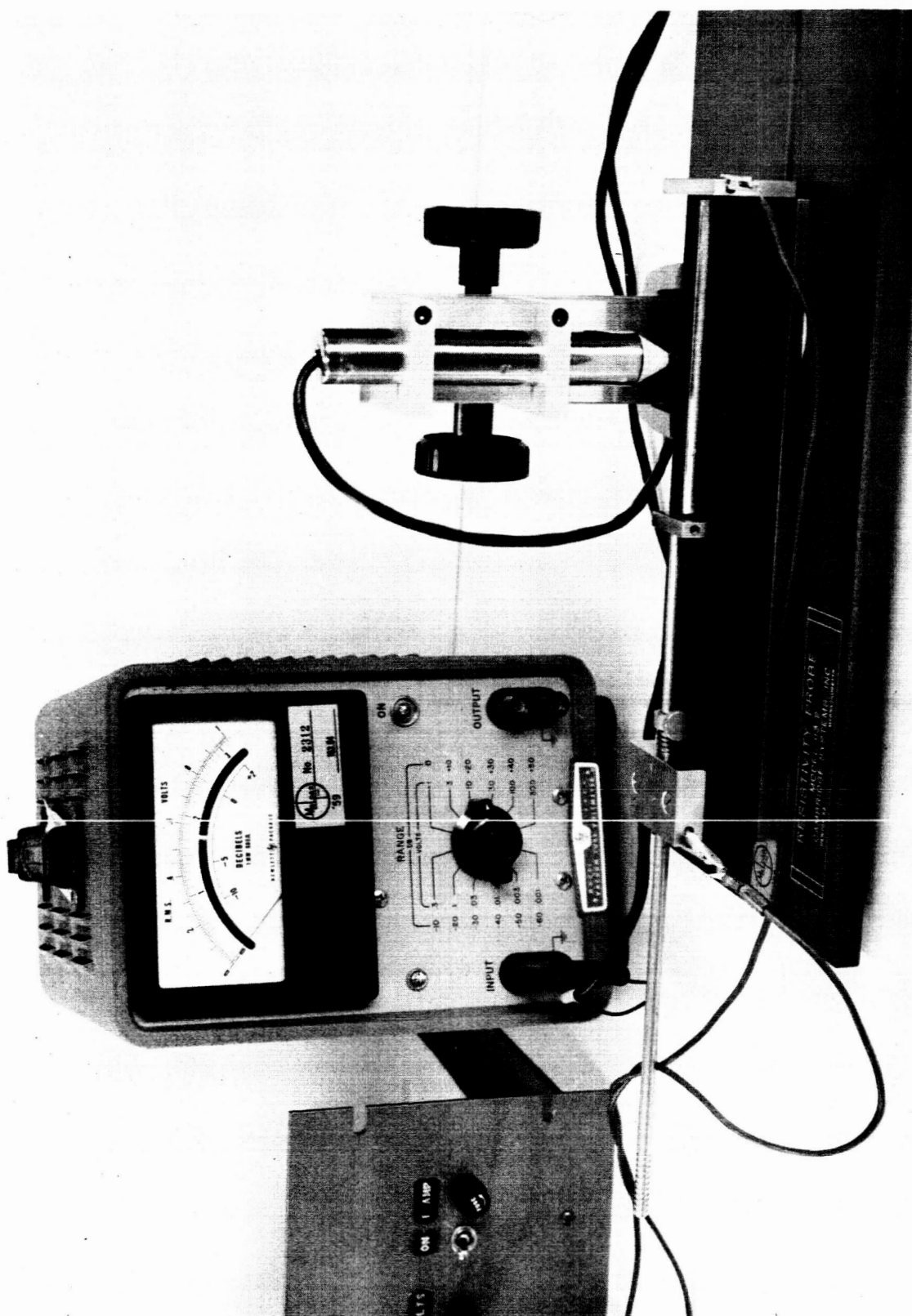


Figure 4. Two-Point Electrical Resistivity Probe Apparatus

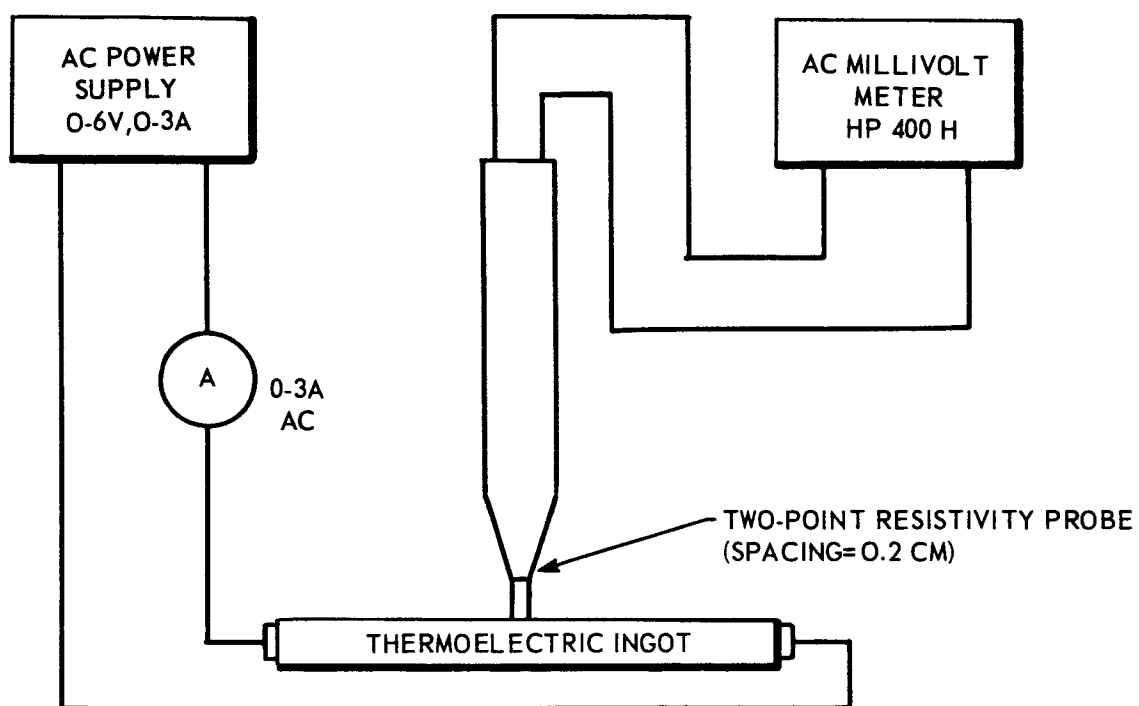


Figure 5. Schematic Representation of Two-Point Resistivity Probe Apparatus

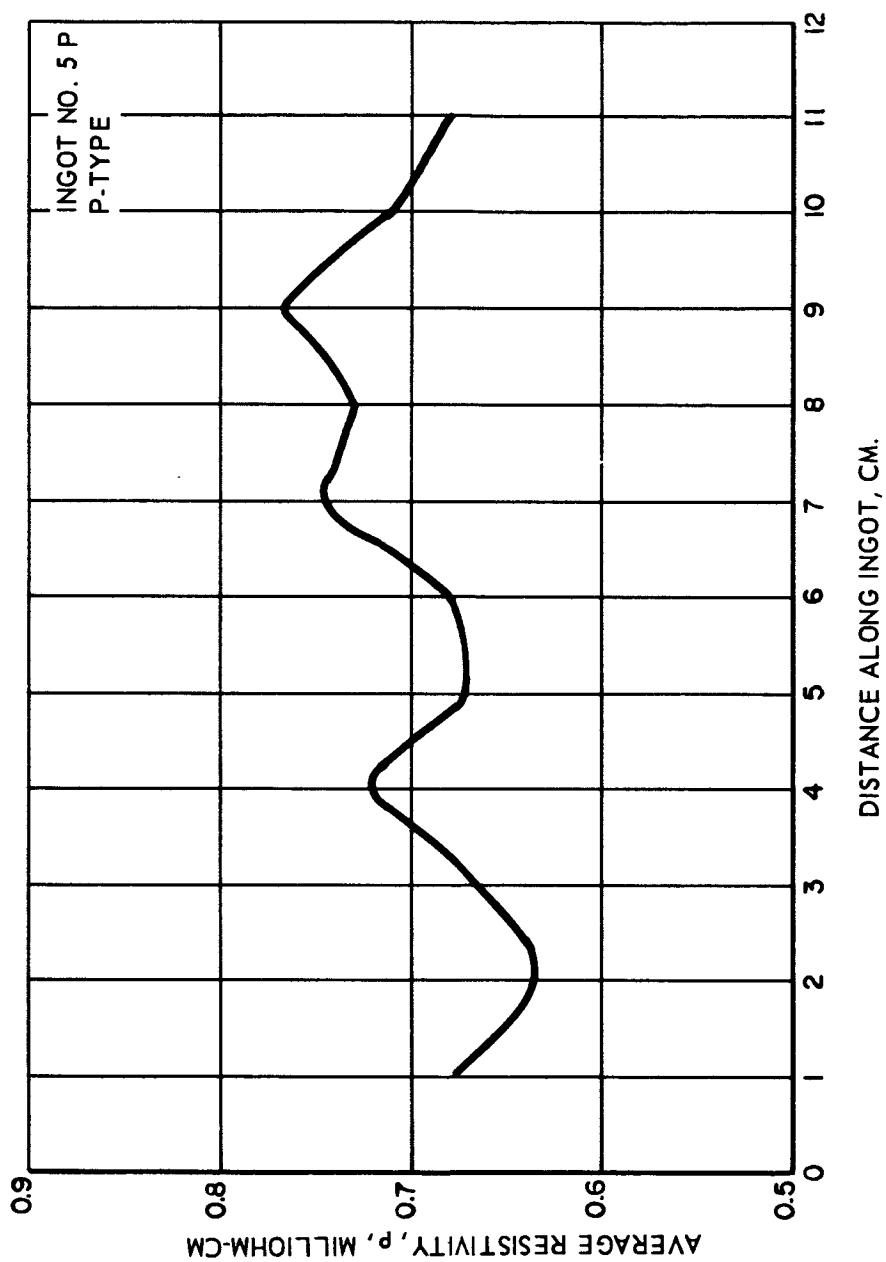


Figure 6. Average Electrical Resistivity as a Function of Distance Along the Ingot.  
Ingot 5P

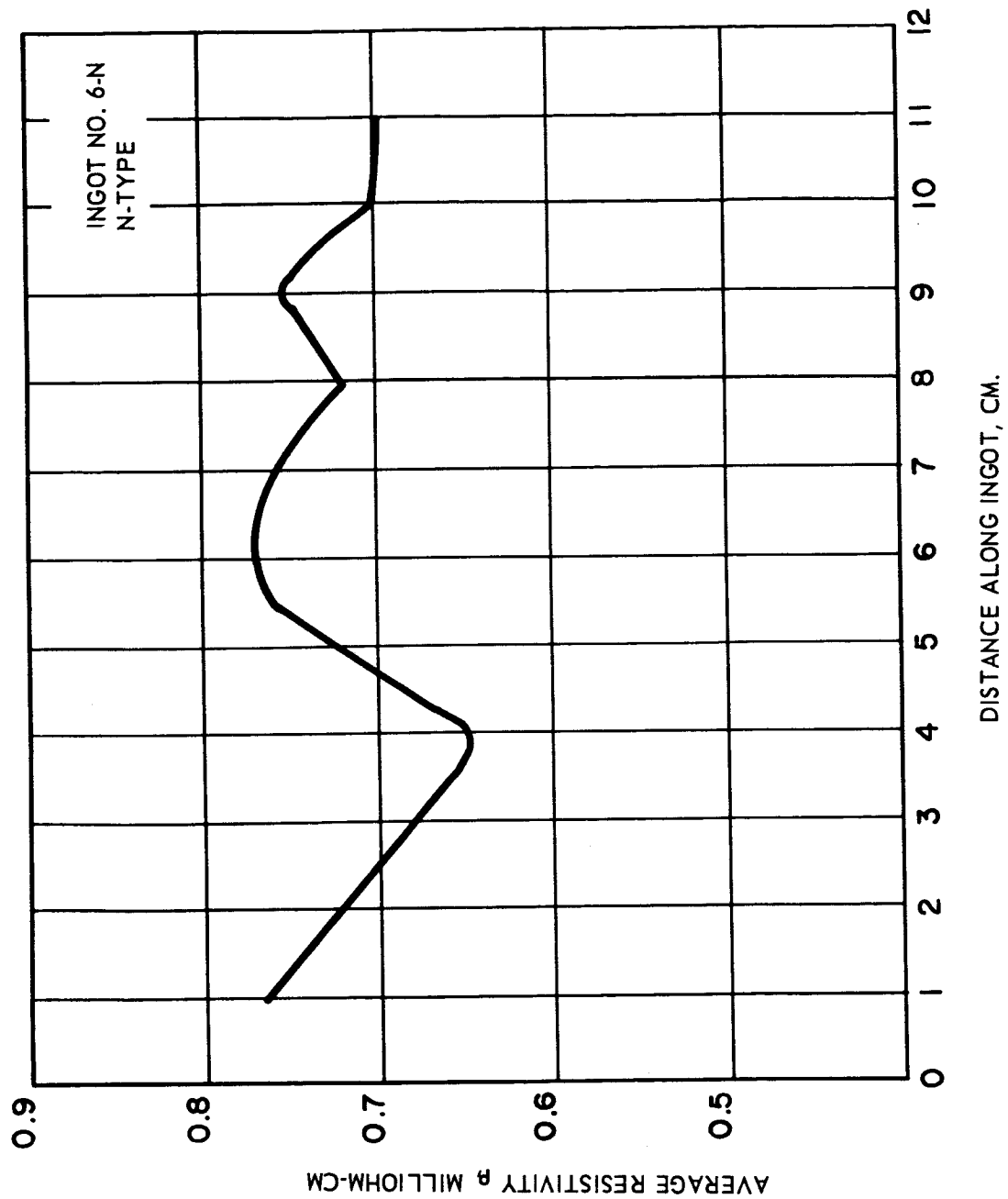


Figure 7. Average Electrical Resistivity as a Function of Distance Along the Ingot.  
Ingot 6N

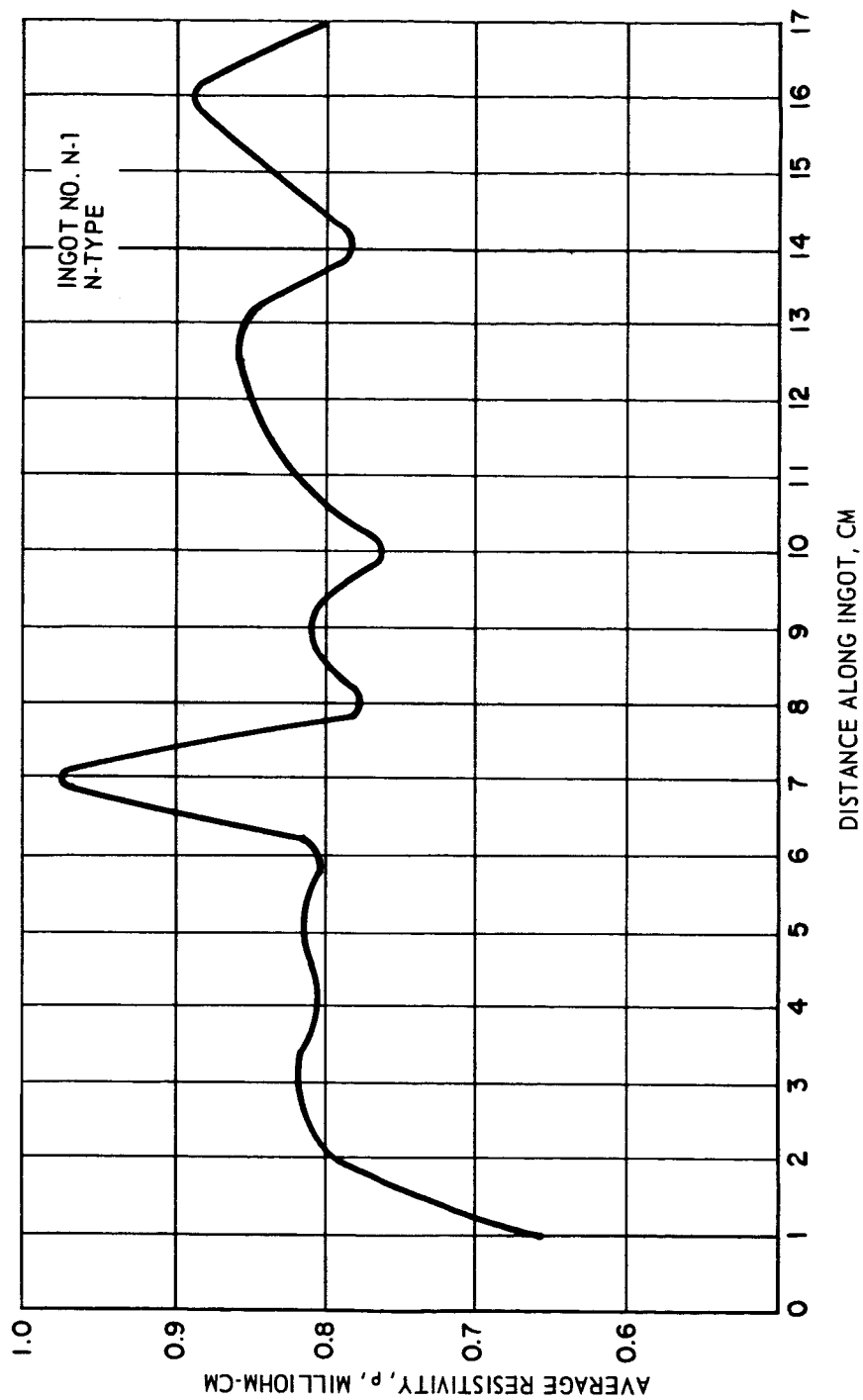


Figure 8. Average Electrical Resistivity as a Function of Distance Along the Ingot.  
Ingot N-1

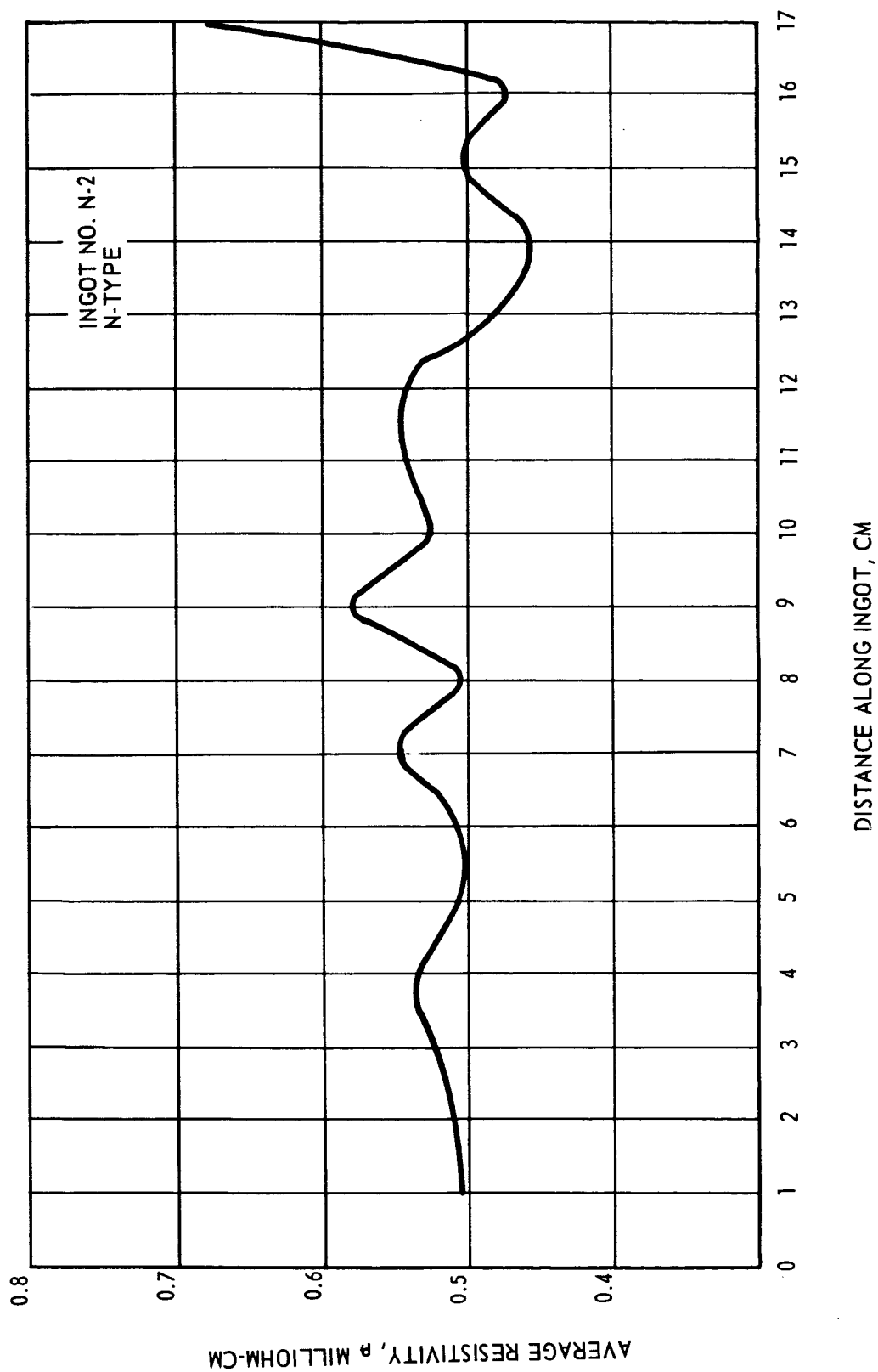


Figure 9. Average Electrical Resistivity as a Function of Distance Along the Ingot.  
Ingot N-2



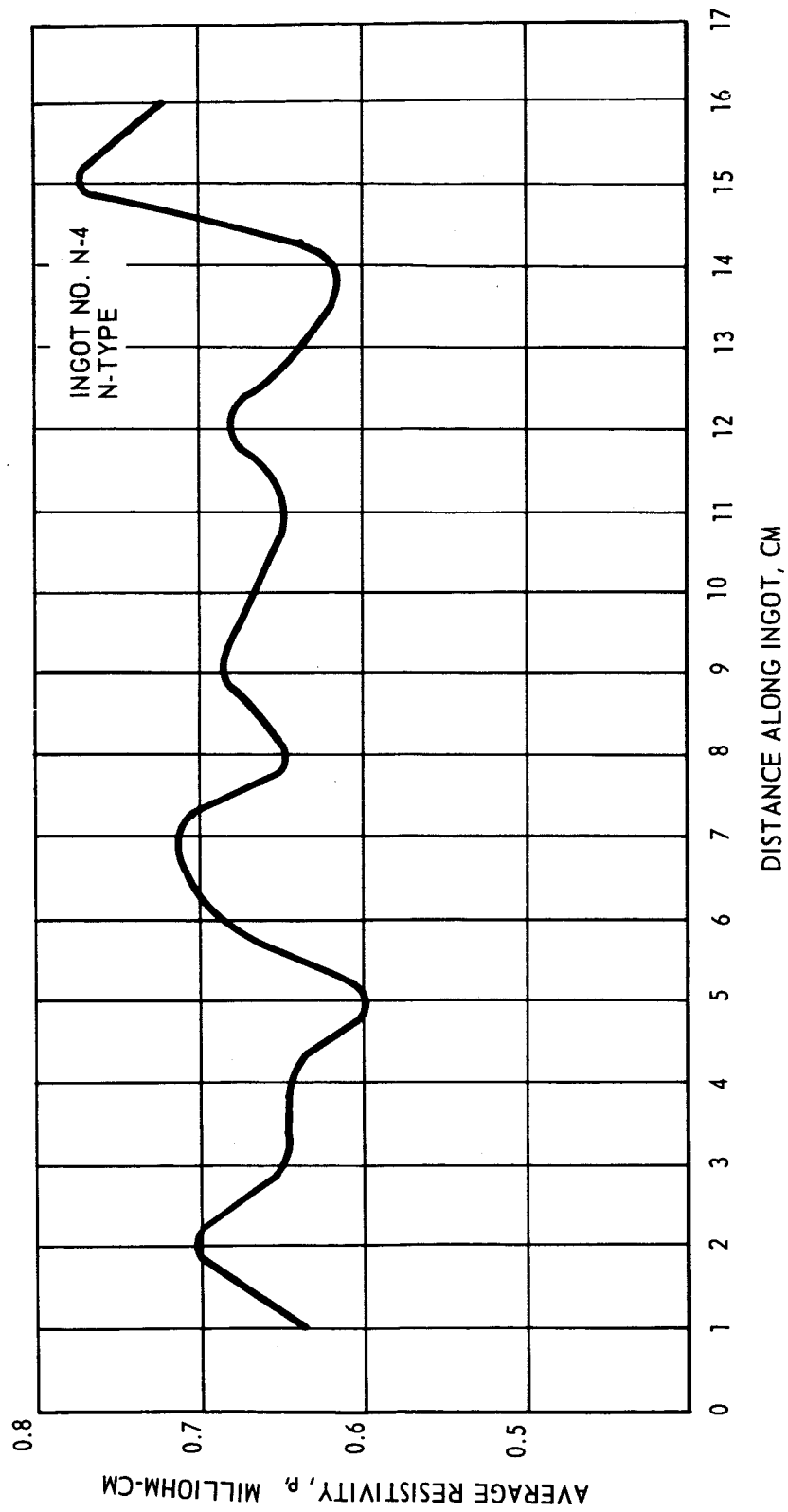


Figure 10. Average Electrical Resistivity as a Function of Distance Along the Ingot.  
Ingot N-4

readings were averaged in a manner similar to the resistivity values. The measurement was made with an "S" Meter, an instrument supplied by Cambridge Systems, Inc., Cambridge, Massachusetts.

Basically, the apparatus consists of a hot probe, the temperature of which can be controlled accurately to some preset value, and a cold "reference" temperature block which is in equilibrium with the ambient temperature. The temperature difference is obtained by locating bridge connected thermistors in the probe tip and reference block, and using the error voltage developed to control power to the hot probe. In order to provide means for accurately measuring the temperature difference, thermocouples are located in the probe tip and the reference block.

The instrument consists of two separate circuits, one for sensing and controlling the temperature of the probe, and a second for switching the low level Seebeck voltage and thermocouple outputs, without introducing stray emf's, to the external meter.<sup>5</sup>

The S-Meter is shown in figure 11. Schematic details of this instrument are given in figure 12.

Profiles of the Seebeck coefficient values for the thermoelectric material ingots are shown in figures 13 through 17. The variation is considerable along the lengths of the ingots, and there is no consistent pattern among the ingots. The variation in value of the Seebeck coefficient around the circumference of the ingots was also present. The correlation between the resistivity and Seebeck coefficient at a given centimeter interval was as expected. The Seebeck coefficient generally increased as the resistivity increased.

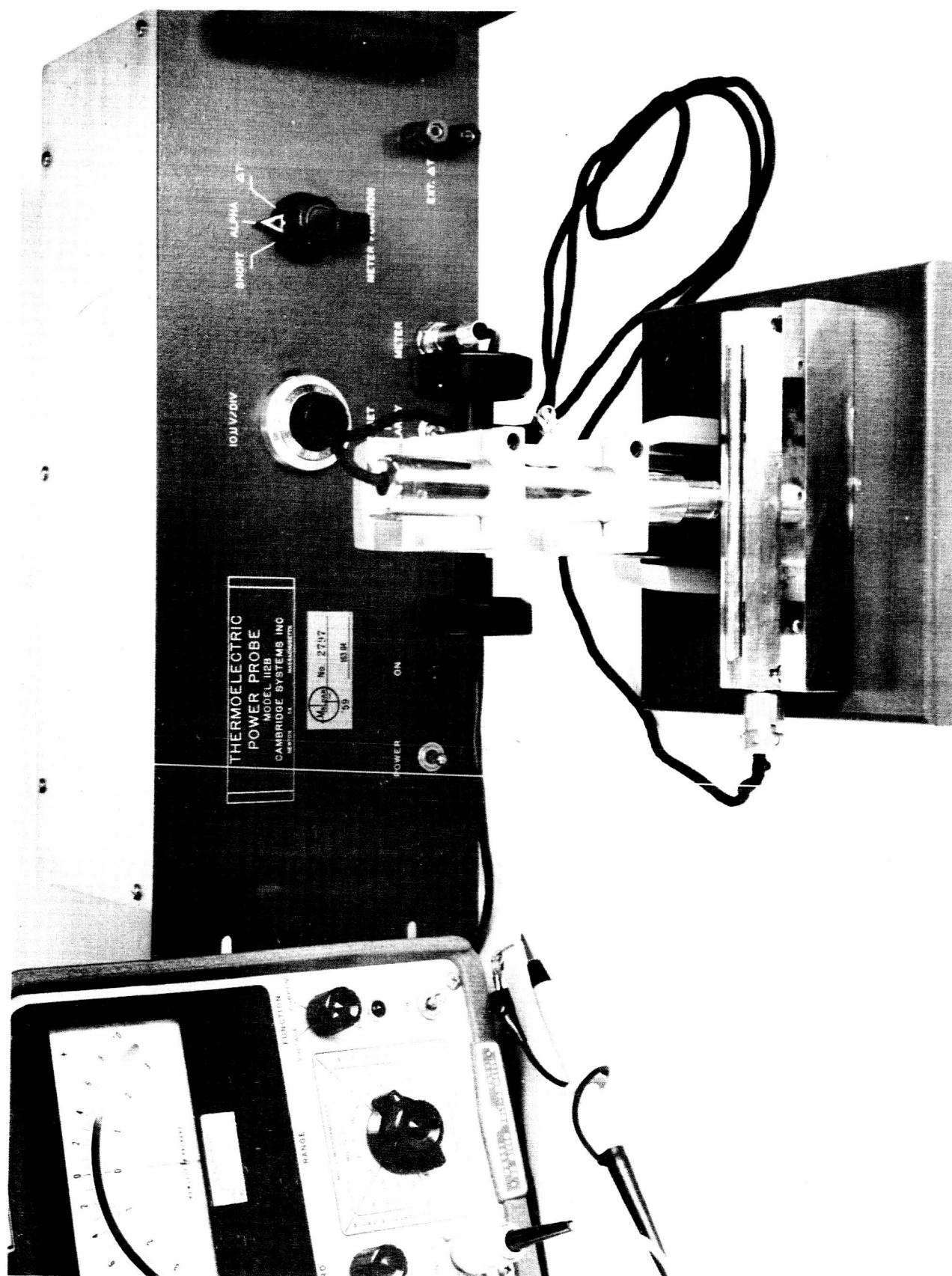


Figure 11. Seebeck Coefficient Apparatus

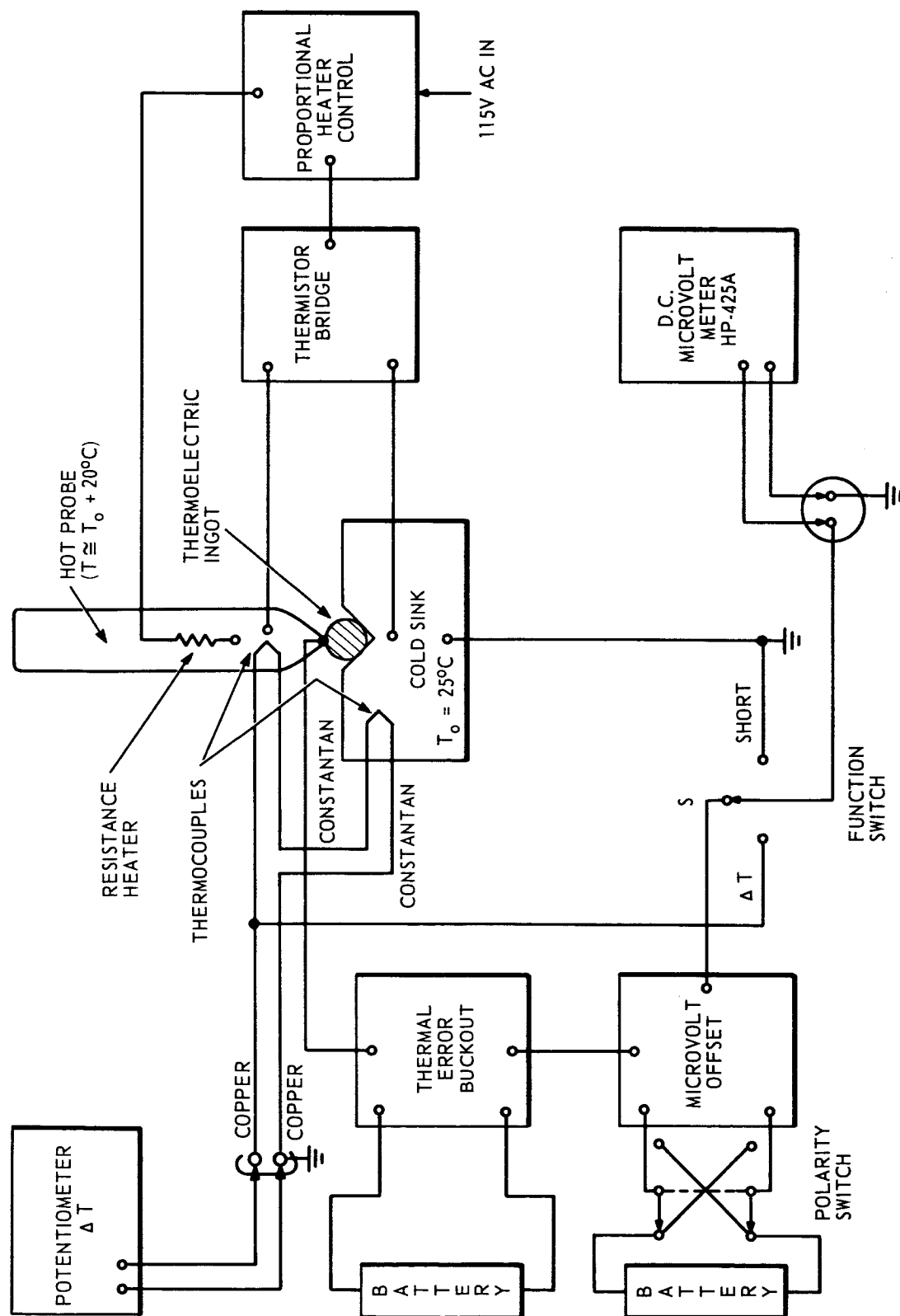


Figure 12. Schematic Representation of Seebeck Coefficient Apparatus

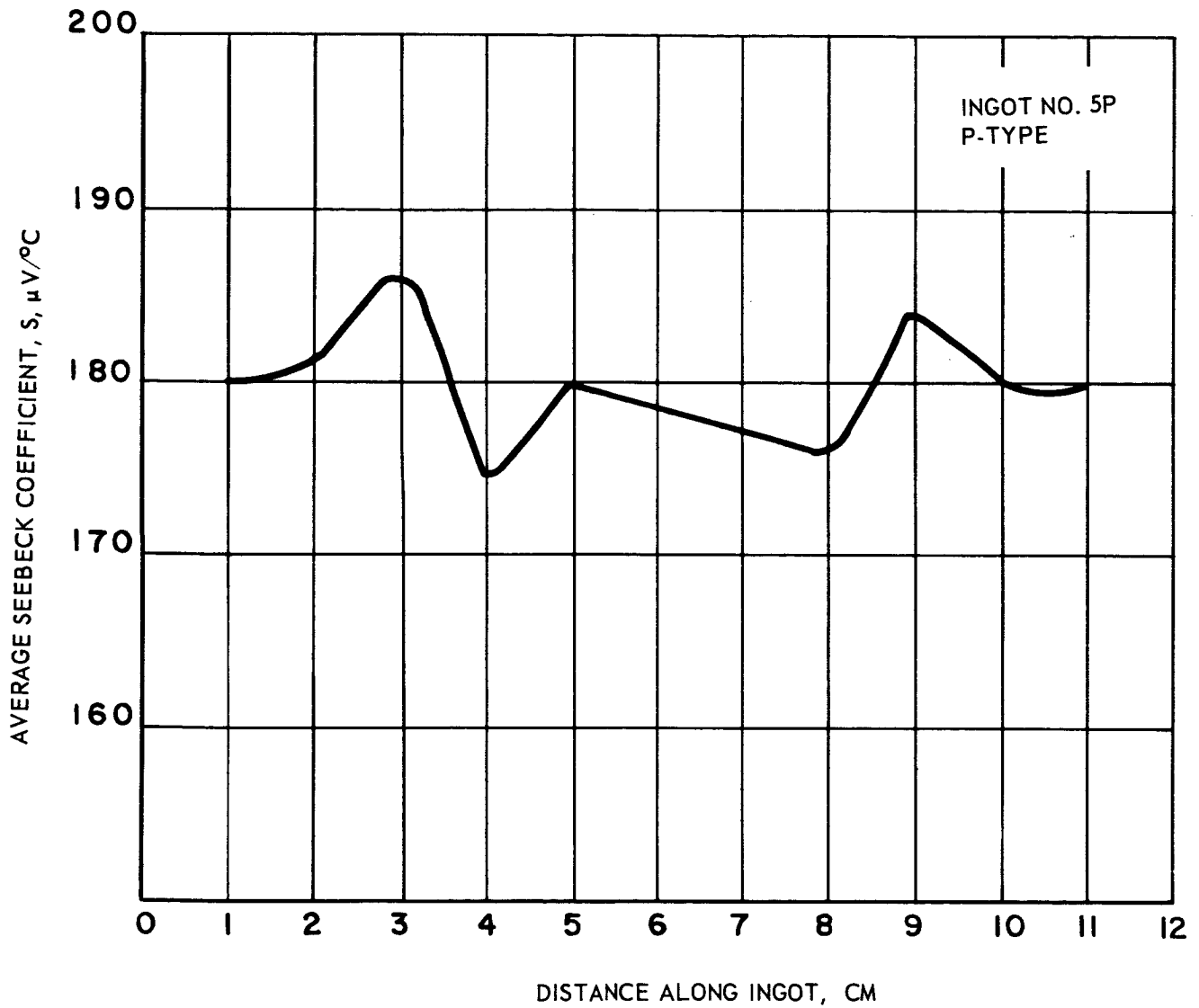


Figure 13. Average Seebeck Coefficient as a Function of Distance Along the Ingot.  
Ingot 5P

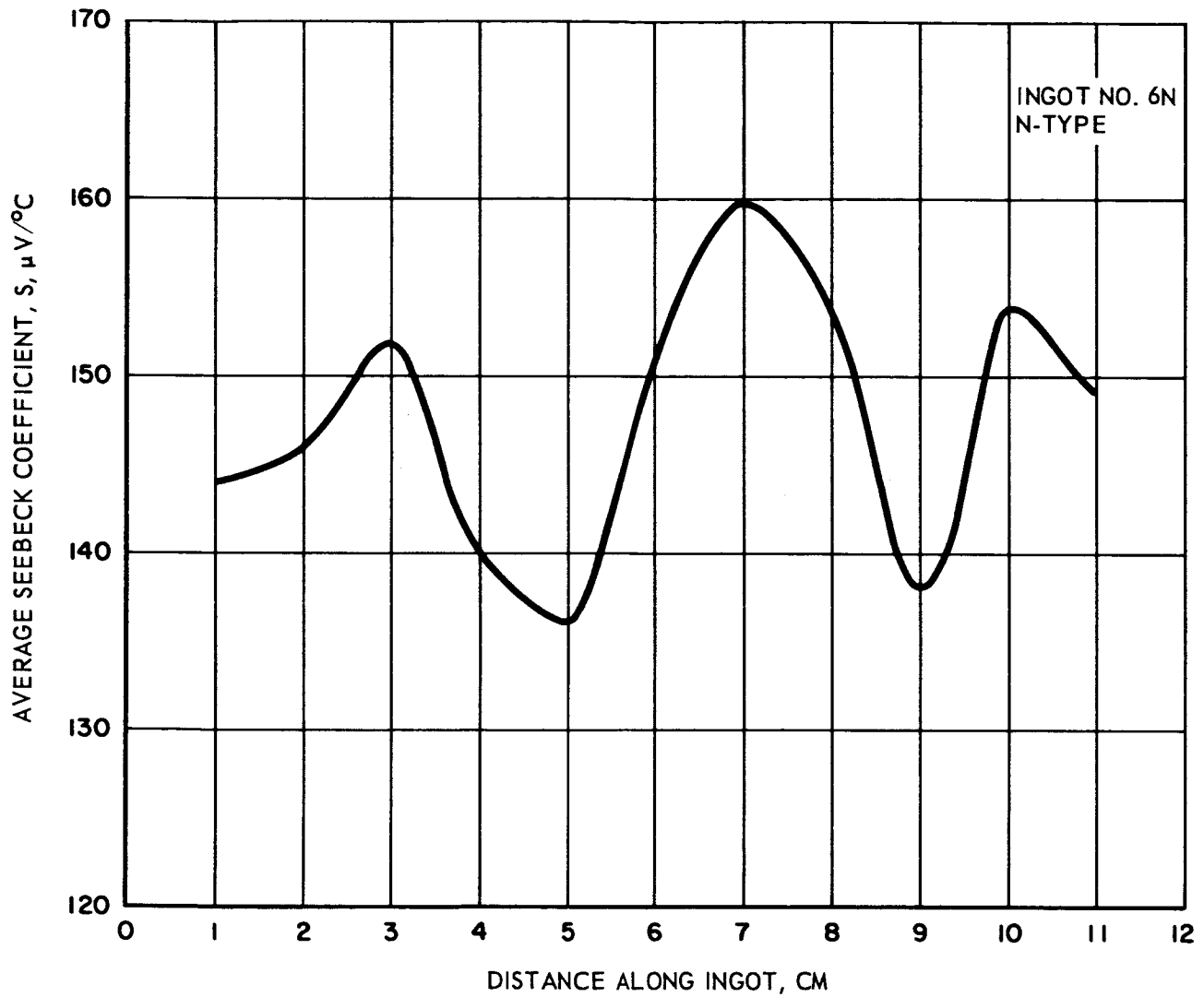


Figure 14. Average Seebeck Coefficient as a Function of Distance Along the Ingot.  
Ingot 6N

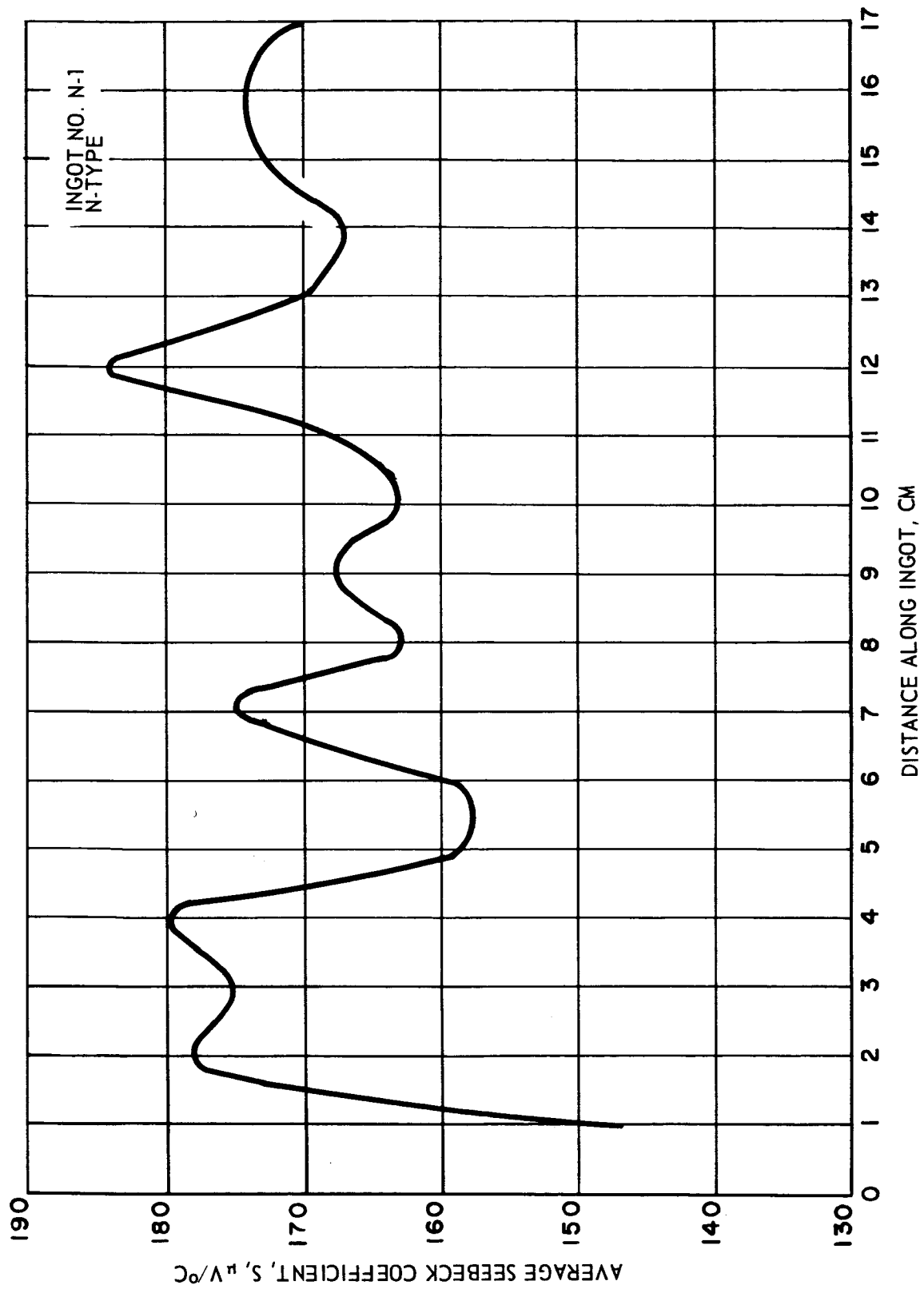


Figure 15. Average Seebeck Coefficient as a Function of Distance Along the Ingot.  
Ingot N-1

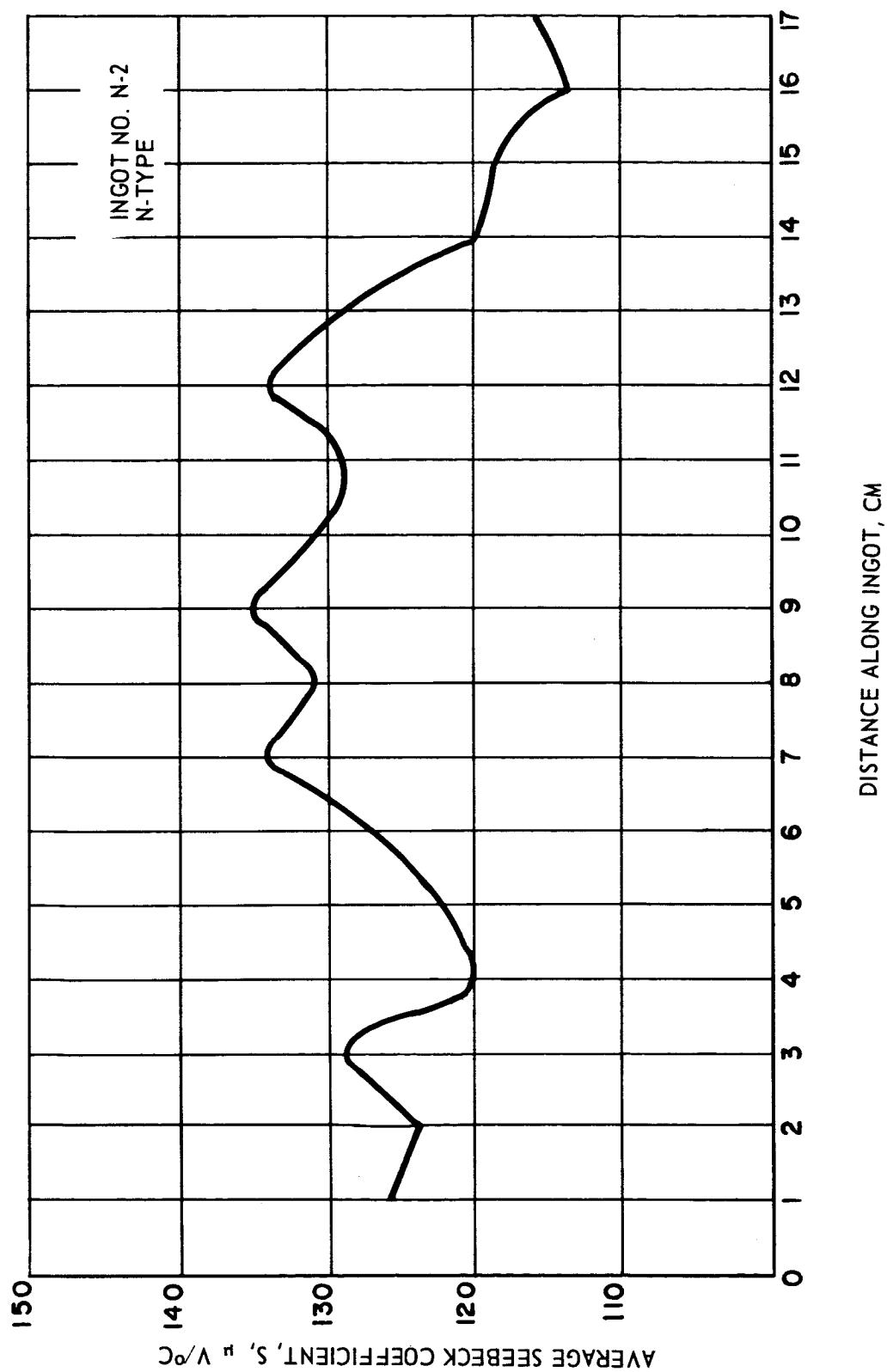


Figure 16. Average Seebeck Coefficient as a Function of Distance Along the Ingot. Ingot N-2



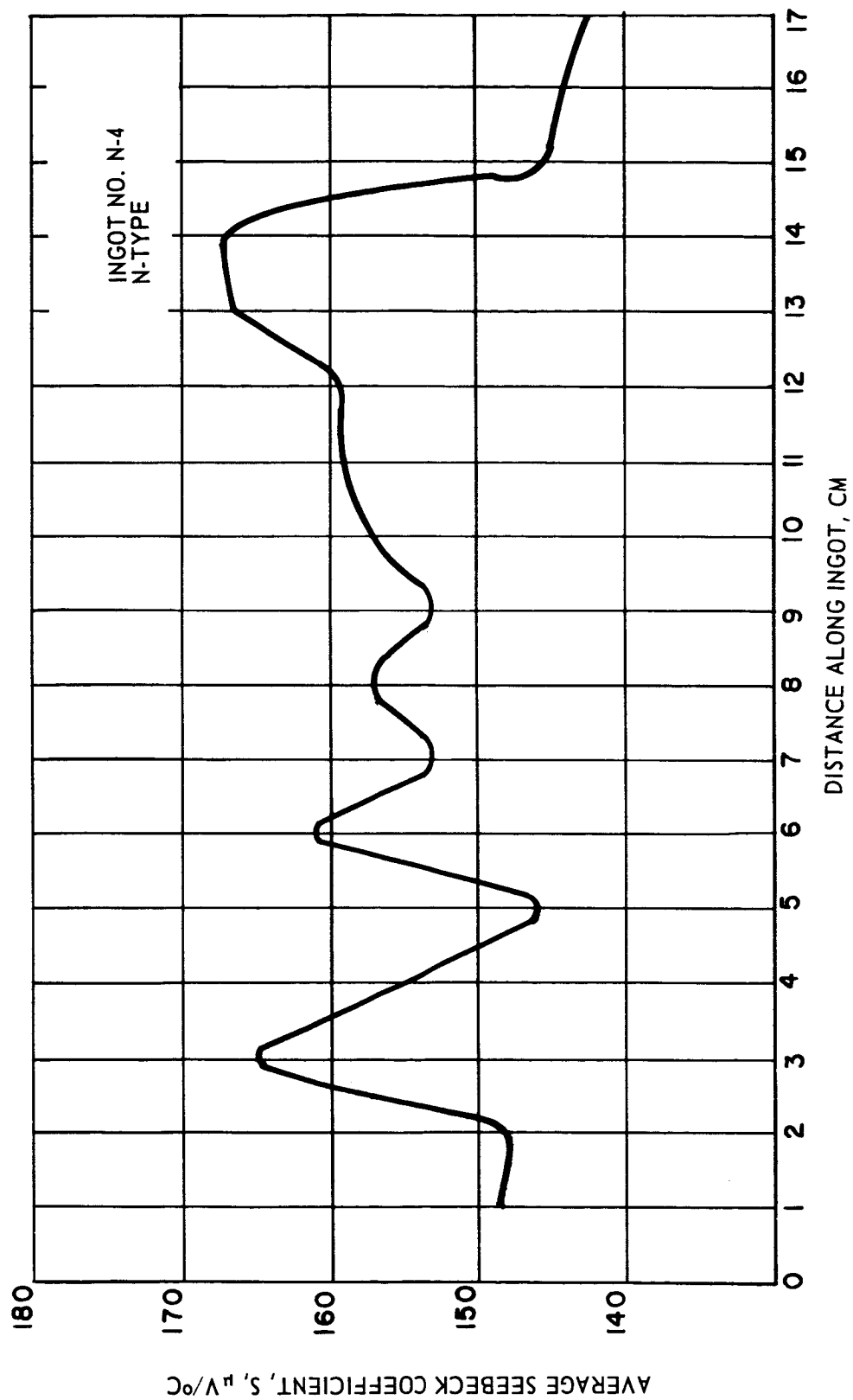


Figure 17. Average Seebeck Coefficient as a Function of Distance Along the Ingot.  
Ingot N-4

#### 2.4.2 Variation of Electrical Resistivity with Temperature

The variation of resistivity as a function of temperature was measured on selected ingots of  $\text{Bi}_2\text{Te}_3$  alloy thermoelectric material. The apparatus used for the measurements is shown as a block diagram in figure 18. The sample ingots were suspended in a controlled oven with thermocouple probes attached to them. Alternating current from an isolation transformer was supplied to the rods by solder connections to the ends, while voltage drops were measured at various points along the rods, but away from the ends. Measurements were taken at several temperatures within the proposed operating temperature range for the flat plate generator.

The results are given in figure 19. Ingot to ingot variation is present in this parameter, also. The resistivities measured in this way are for uniformly heated ingots.

#### 2.4.3 Evaluation of Material Performance through Measurement of $\Delta T_{\text{max}}$

After the thermoelectric material ingots had been profiled for resistivity and Seebeck coefficient and the resistivity measured as a function of temperature, ingots were selected that had regions of the greatest  $S^2/\rho$  values and whose resistivities were of a reasonable value and increased the least with temperature. One centimeter long sections were cut out of the ingots where the greatest  $S^2/\rho$  values showed up on the profile curves. Small sections were cut from these and fabricated into couples. These couples were placed in a vacuum chamber and tested as coolers with the hot junction heated to an elevated temperature. Some of the couples were measured at  $T_h=150^\circ\text{C}$  and some at  $T_h=220^\circ\text{C}$ .  $\Delta T_{\text{max}}$  determinations were made. Figure 20 shows test set-up for the  $\Delta T_{\text{max}}$  measurements.

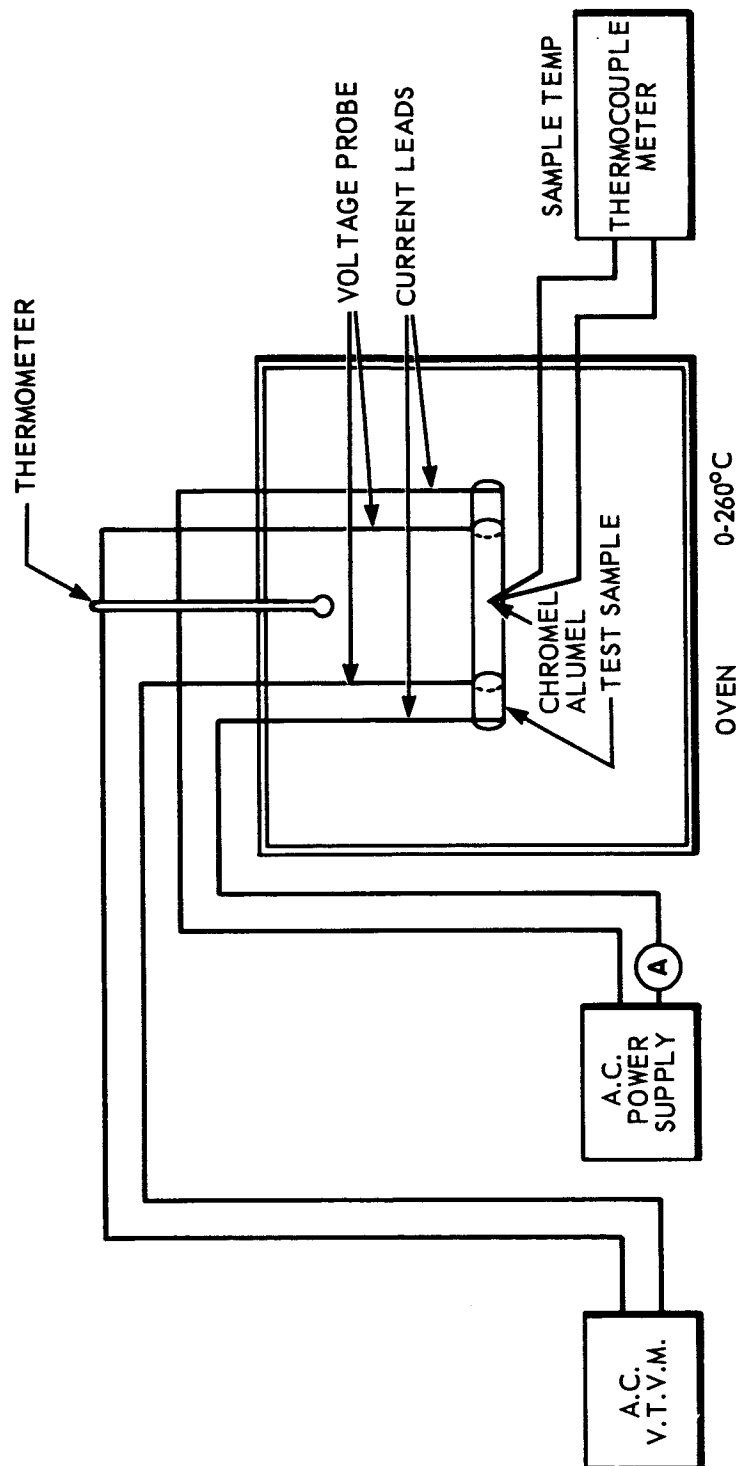


Figure 18. Block Diagram of Equipment Used for Measuring Resistivity as a Function of Temperature

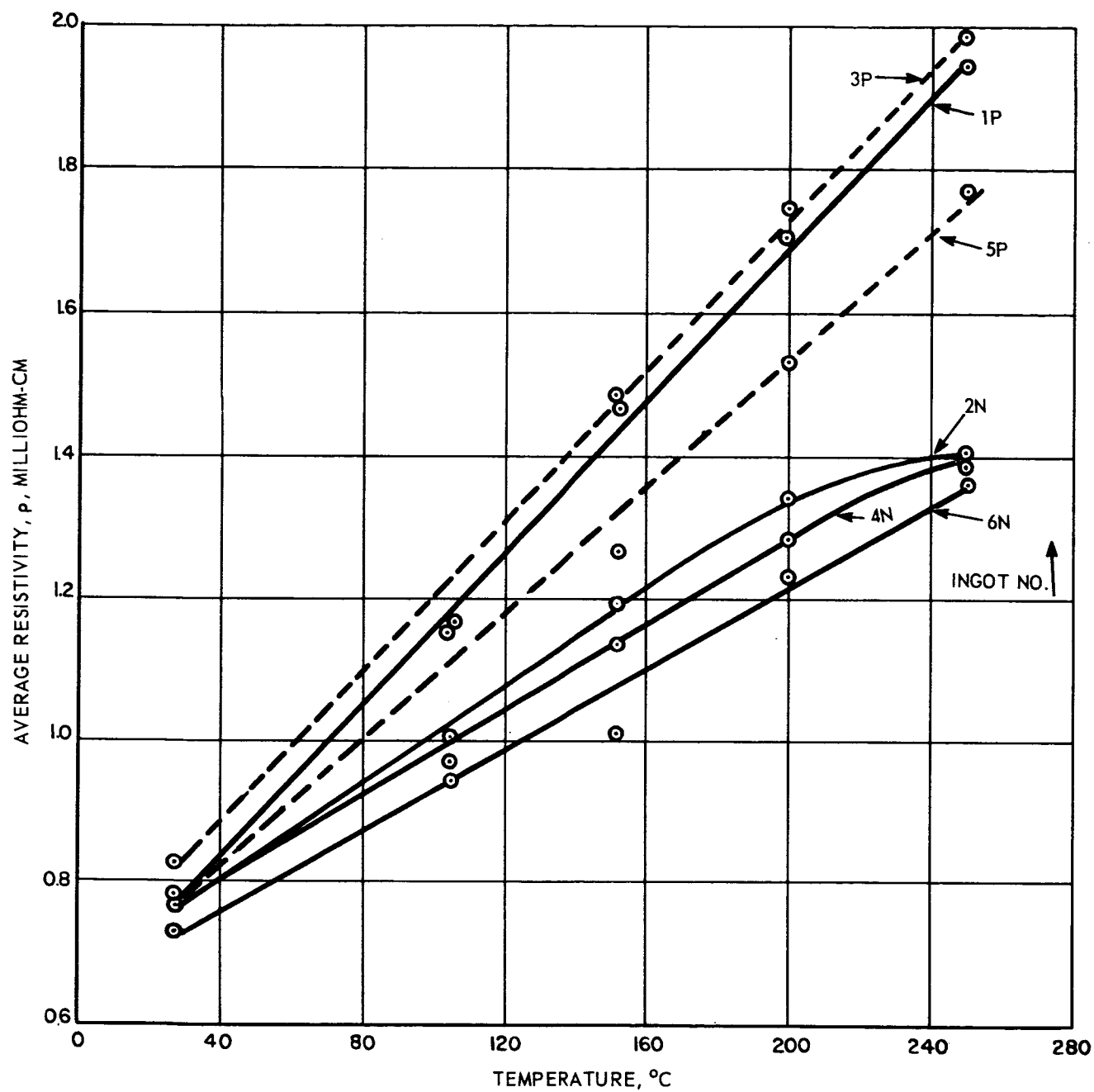


Figure 19. Resistivity of Bi<sub>2</sub>Te<sub>3</sub> Alloy Ingots as a Function of Temperature

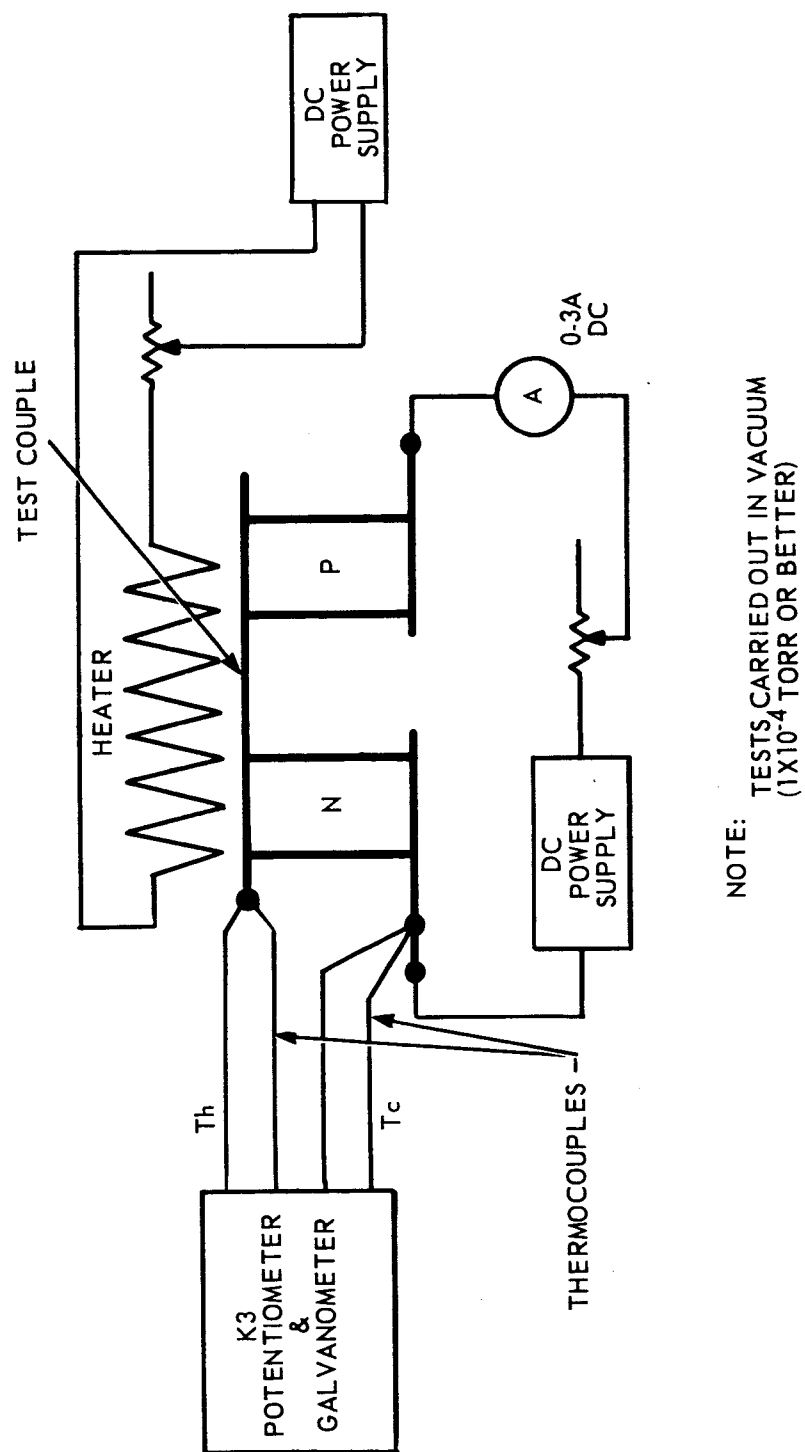


Figure 20. Test Apparatus for Determination of  $\Delta T_{\max}$

The results of these measurements are given in table 4. The validity of these measurements is questioned, however, since the thermocouple placement for measuring the cold junction was improper. This error turned out to be of no consequence, since the scale of material variation was determined to be much smaller than originally supposed. In fact, variations in material parameters were detectable from one location on an individual element to another. This will be discussed further in section 2.4.4.

#### 2.4.4 Conclusions

In the testing, analysis, and selection of the available  $\text{Bi}_2\text{Te}_3$  alloy thermoelectric materials, both n- and p-type, inhomogeneity and unpredictability of parameters extend to the smallest scale tested, i.e., the individual elements (0.076 in. square x 0.118 in. long). The final material tests used were measurements of Seebeck coefficient and resistivity on the individual elements. These were accomplished by the probe techniques. However, on the elements used for the fabrication of the experimental panels, the resistivity could not be checked because reliable readings could be obtained only with tinned elements. The fabrication process precludes the tinning of both ends of the elements at the beginning of the process. Therefore, the only material selection or control factors that could be employed were the Seebeck coefficient and a knowledge of the average ingot resistivity values. The materials cannot be considered as well selected and may or may not represent the best material selection from the available ingots.

TABLE 4

RESULTS OF  $\Delta T_{\max}$  MEASUREMENTS ON SECTIONS  
OF THERMOELECTRIC MATERIAL INGOTS

$$Z = \frac{2\Delta T}{T_c}$$

Test No.	Ingot No.	Section No.	$T_h$	$\Delta T_{\max}$	Z
1.	5P	6	150°C	86°C	$1.55 \times 10^{-3} \text{ } ^\circ\text{K}^{-1}$
	6N	7			
2.	5P	5	220°C	138	2.19
	6N	8			
3.	5P	10	220°C	122	1.77
	6N	4			
4.	5P	5	150°C	104	2.02
	6N	7			

It is concluded that:

a. The available materials are not satisfactory for producing flat plate generator panels of optimized performance. However, at least the minimum required performance is attainable.

b. With materials of the present quality, an extensive materials selection program is meaningless.

c. A program directed towards the development of  $\text{Bi}_2\text{Te}_3$  generator materials with homogenous characteristics and optimized for the temperature range up to 250 to 300°C is needed for the successful achievement of the goals of this program.



## 2.5 Fabrication of Experimental Flat Plate Thermoelectric Generator Couples and Panels

Extensive experimental work was carried out on the fabrication of couples and panels. Major developmental efforts involved were:

- a. The electrical and thermal contacting of the thermoelectric elements to the aluminum absorber and radiator plates.
- b. The mechanics of fabricating unit couples.
- c. The mechanics of fabricating panels.

Other developmental activities were centered upon making existing  $\text{Bi}_2\text{Te}_3$  contacting methods compatible with the new mechanical assemblies, experimentation with the nickel- $\text{Bi}_2\text{Te}_3$  barrier plating, and the coating of internal couple surfaces with a low-emissivity gold film to prevent excessive thermal radiative shunt leakage between plates.

### 2.5.1 Experimental Work in Fabrication

2.5.1.1 Contacting Aluminum Absorber and Radiator Plates: The experimental efforts to make good electrical and thermal contacts to the aluminum plates was divided into two approaches:

- a. Solder bonding by alloying directly to the aluminum.
- b. Solder bonding by nickel plating of the aluminum.

Several techniques were tried in attempting to solder directly to the aluminum. Since the more critical contacts are at the absorber (the hot junction), and lead solder is used as the contacting material at the absorber, the effort was concentrated on the wetting of the aluminum surface with lead. It was learned that lead is one of the more difficult materials with which to solder to aluminum.<sup>6</sup>

The following techniques were tried with the noted results:

a. Use of Zinc as a Wetting Agent: Deposited by thermal decomposition of  $ZnCl$ . Result: Unsatisfactory.

b. Use of Zinc as a Wetting Agent: Alloying of pure zinc into aluminum. Result: Effective as wetting agent for lead to aluminum, but alloying of zinc is difficult to control and requires high temperature.

c. Use of Zinc as a Wetting Agent: Alloying of 95 Zn, 5 Al into aluminum. Result: Effective as wetting agent for lead to aluminum and allows control of zinc alloying, but still requires high temperature processing.

d. Use of Organic-based Fluoride Aluminum Flux: Result: Effective for use with lead, but difficult to control location of wetted area or filleting of solder due to uncontrolled flowing of flux. Makes good electrical and mechanical contacts.

e. Use of Ultrasonic Soldering: Result: Effective, but clumsy in handling and processing small areas. Promising technique, needs more development work.

f. Mechanical Abrasion of Surface: Result: Most satisfactory results were obtained in this manner. Good wetting achieved in controllable size areas. Bonds are electrically and mechanically good. Slower than techniques using aluminum fluxes.

Nickel plating to aluminum for soldering purposes was accomplished using "electroless" plating techniques.<sup>7</sup> See Appendix I. This aluminum soldering method was generally satisfactory, but the process was not sufficiently well controlled, consequently the results obtained were not consistent. The problems encountered were poor bond strength and

high resistance. It is believed that additional work on the process will yield consistently good results.

Satisfactory techniques for soldering elements directly to aluminum and soldering to aluminum by means of a nickel plating have been developed as a result of this study. Each of these techniques has certain advantages and disadvantages. The nickel plating to aluminum prevents any undesirable interaction between the aluminum and the solder, and is easy to solder. However, it does not produce entirely consistent results, and it is an additional layer in a structure in which interfaces should be kept to a minimum, for reasons of thermal and electrical conductance. The direct soldering to aluminum eliminates the extra plating layer, it is strong and of low resistance; but it produces solder-aluminum alloys of unknown physical and chemical properties which may fail mechanically or deteriorate electrically due to thermal fatigue. Life tests of both types of bonds should be conducted.

2.5.1.2 Fabrication of Experimental Single Flat Plate Couples: Methods of making contacts to  $\text{Bi}_2\text{Te}_3$  generator elements were previously worked out.<sup>3</sup> Several experimental single couples of the type shown in figure 21 were constructed using the various aluminum bonding techniques, i.e., direct soldering to aluminum, soldering to zinc-coated aluminum, and soldering to nickel plated aluminum.. This was done to determine the feasibility of using these techniques to bond  $\text{Bi}_2\text{Te}_3$  generator elements to the aluminum absorber and radiator plates. These aluminum bonding techniques were tried with the various combinations of bonding materials found to make satisfactory electrical and mechanical joints to the  $\text{Bi}_2\text{Te}_3$

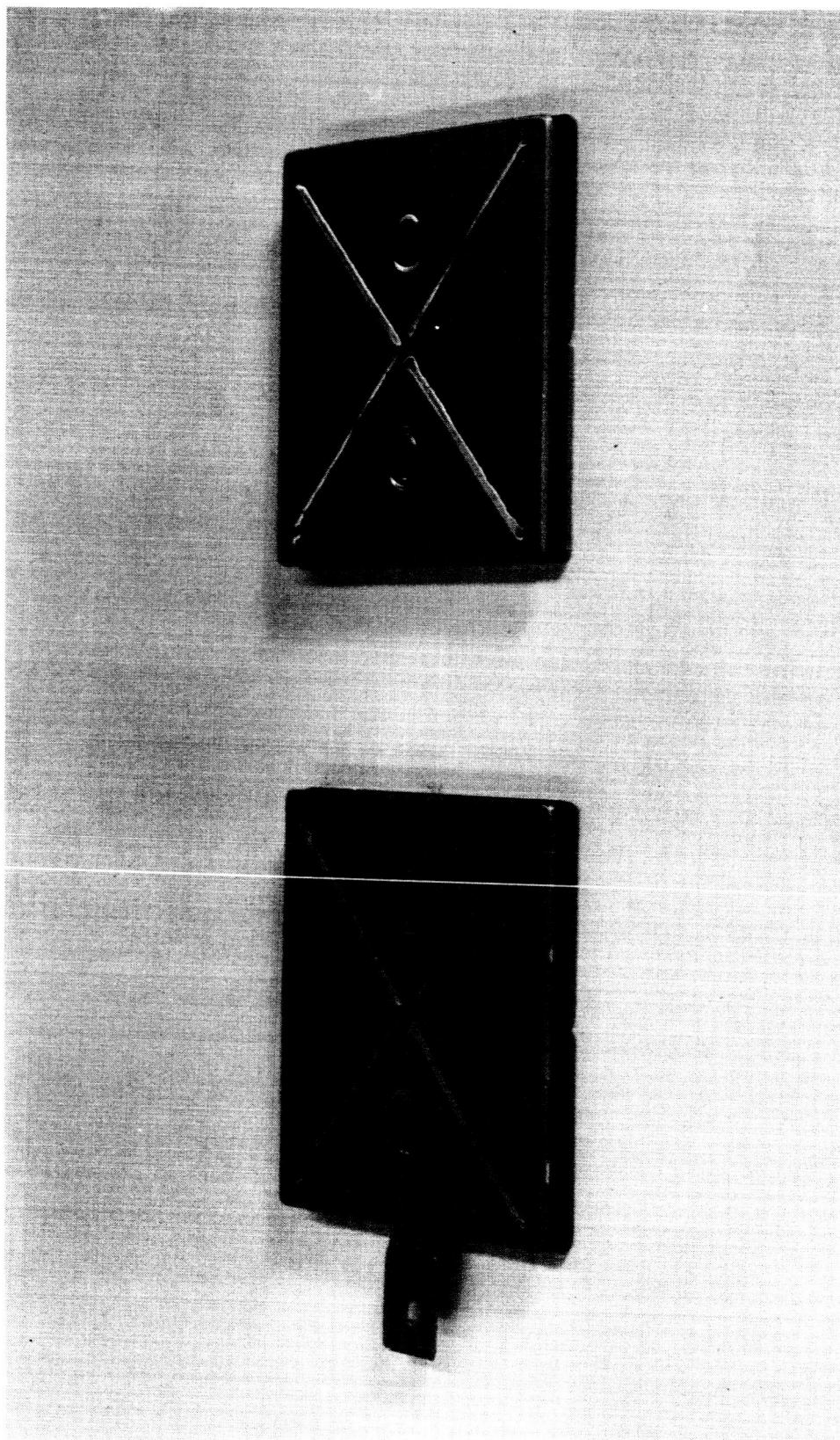


Figure 21. Experimental Unit Couple Generators for Type II and III Panels

generator elements. The most satisfactory means of contacting the  $\text{Bi}_2\text{Te}_3$  generator elements are:

a. Hot Junction: Nickel plated elements with lead solder (M.P.  $327^\circ\text{C}$ ) and elements directly contacted with bismuth solder (M.P.  $271^\circ\text{C}$ ).

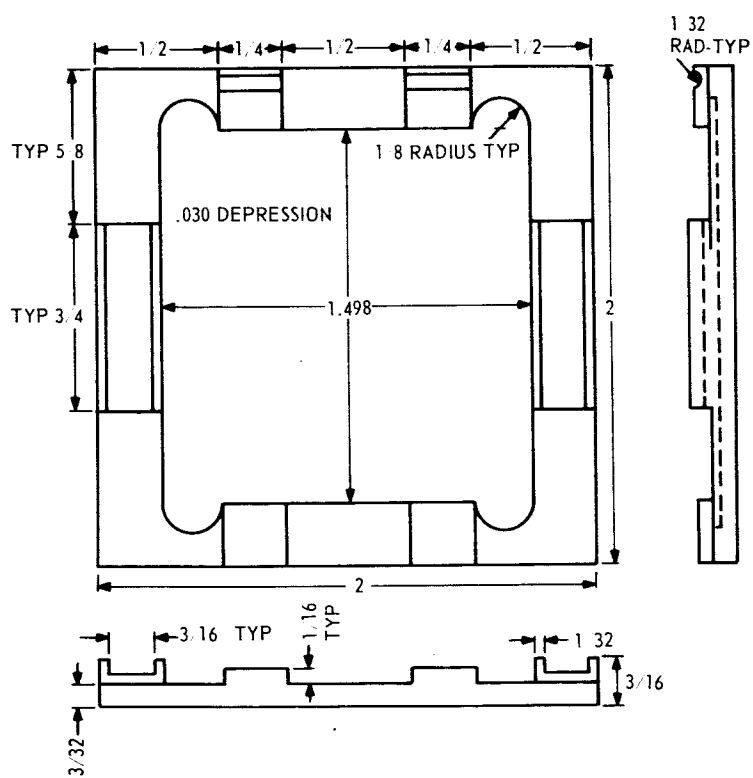
b. Cold Junction: Nickel plated elements with tin-lead eutectic solder (M.P.  $183^\circ\text{C}$ ) and elements directly contacted with tin-bismuth eutectic solder (M.P.  $139^\circ\text{C}$ ). In addition, the two hot junction contacting methods were used successfully for cold junctions.

In the actual fabrication of the couples, the lead and tin-lead solders were found to perform satisfactorily with all of the aluminum bonding techniques. The bismuth and tin-bismuth solders were found to perform satisfactorily with all of the aluminum bonding techniques. However, bismuth could not be joined to aluminum when the organic-base fluoride aluminum flux was used and the zinc-coated aluminum surface resulted in an alloy with too low a melting point ( $254^\circ\text{C}$ ) for reliable use on the generator couples. Direct bismuth to aluminum joints were found to be generally higher in electrical resistance than the other joints. The best results were obtained with the lead and tin-lead solder combinations using nickel-plated elements and unplated aluminum plates.

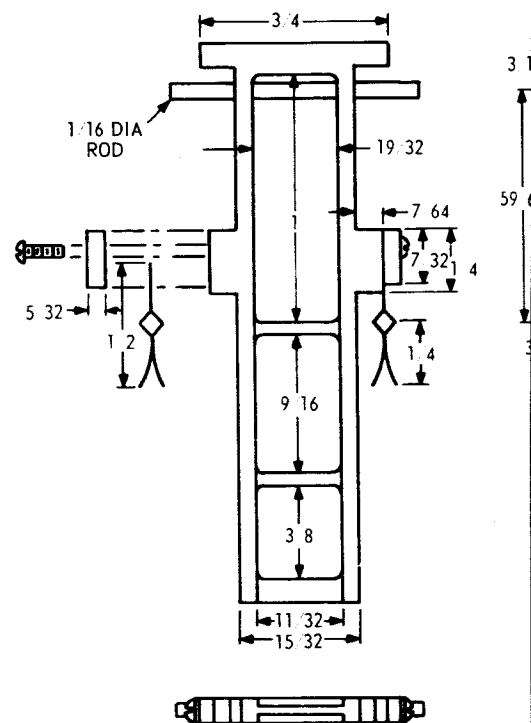
The fabrication of the experimental unit couples was carried out using a specially designed jig to contact the elements to the absorber (hot junction) plates. This jig is illustrated in figure 22.

Another specially designed assembly jig was used to join the absorber plate-thermoelectric element subassembly to the radiator (cold junction) plates. This jig is shown in figure 23. The resulting unit couple

BASE



ARM



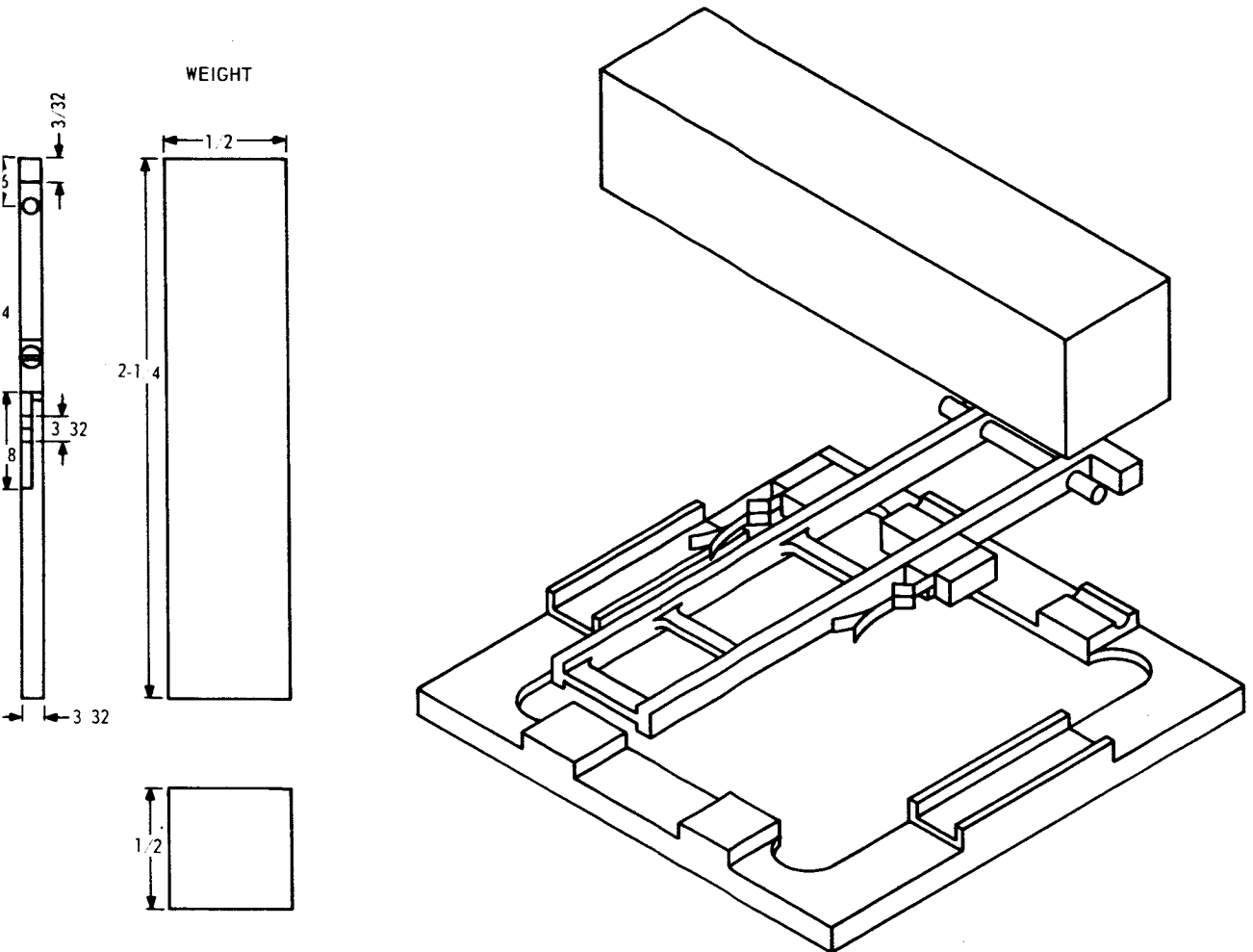


Figure 22. Assembly Jig, Thermoelectric Elements to Absorber Plate Subassemblies

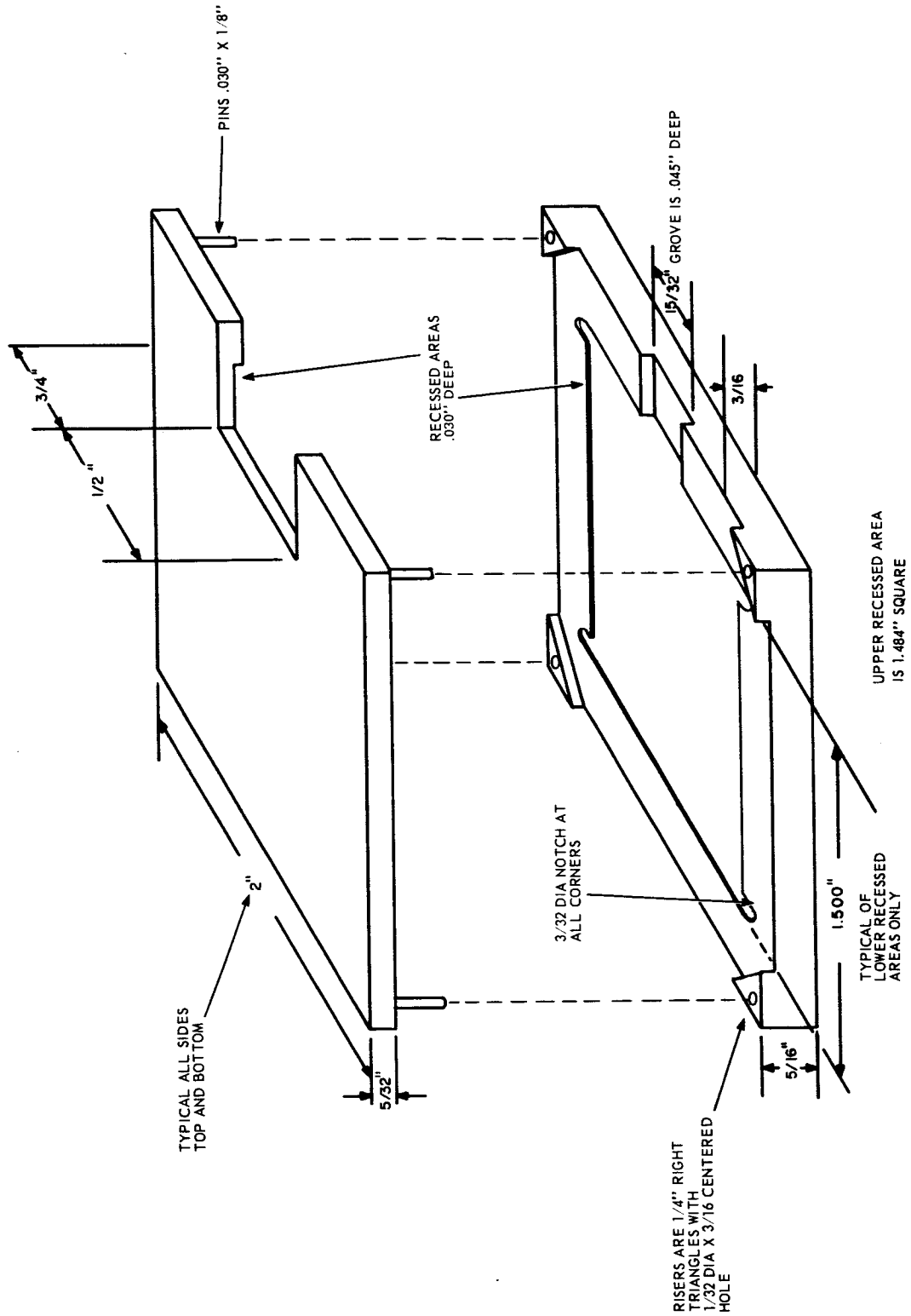


Figure 23. Assembly Jig, Thermoelectric Elements - Absorber Plate Subassembly to Radiator Plates



assemblies could then be tested and subsequently assembled into generator panels.

The final models (i.e., panel types II and III) used nickel plated aluminum absorber and radiator plates. This material was chosen to eliminate the use of the fluoride aluminum flux from the final couple assembly step, where it is extremely difficult to clean away the flux residue, and to facilitate the interconnection soldering of the radiator plates during final assembly of the panels.

2.5.1.3 Fabrication of Experimental Flat Plate Panels: The principal approaches considered for the assembly of flat plate panels were:

a. The simultaneous formation and assembly of all the hot and cold junctions into a complete panel.

b. The simultaneous formation of the hot and cold junctions in a single couple and the subsequent assembly of the single couples into a complete panel.

c. The formation of the hot junctions in individual single couple form (elements to absorber plates) and the subsequent simultaneous formation and assembly (using several of these) of all of the cold junctions into a complete panel (panel type I).

d. The formation of the hot junction in individual single couple form (elements to absorber plates) followed by the formation of the cold junctions in a single couple and the subsequent assembly of the single couples into a complete panel (panel types II and III).

Approaches a. and b. were eliminated because of unsolved technological problems associated with such simultaneous contacting and assembly methods. Approaches c. and d. were both tried and found to be workable. Approach c.

is the easiest method, but d. allows the testing of individual couples which is considered quite advantageous at this stage of the program.

A panel of the type I was fabricated using the methods described in c. and uses the radiator plate subassembly shown in figure 24. Contrasting this, the type II radiator plate construction is shown in figure 25 and type III in figure 26. However, the latter two are not preassembled in this form since the units are fabricated into unit couples. These arrangements are shown for clarity only. The methods described in d. were used for panels of types II and III. In method c., the ac resistances of the elements to absorber plate subassemblies were measured, but there were no means of evaluating the radiator plate contacts before the panel assembly was made. Method d. allowed ac resistance measurements in the absorber plate subassembly stage and after formation into single couples; it also allowed other performance testing before assembly into a panel.

The actual experimental fabrication and assembly of the panels were carried out in a specially designed jig. The jig is slightly modified to accommodate assembly of panel types I, II, and III and is shown in figure 27.

2.5.1.4 Other Experimental Problems: Additional fabrication factors which involved experimentation included plating of a nickel barrier on the contact ends of the thermoelectric elements and coating of the internal surfaces of the aluminum absorber and radiator plates with a gold low-emissivity film.

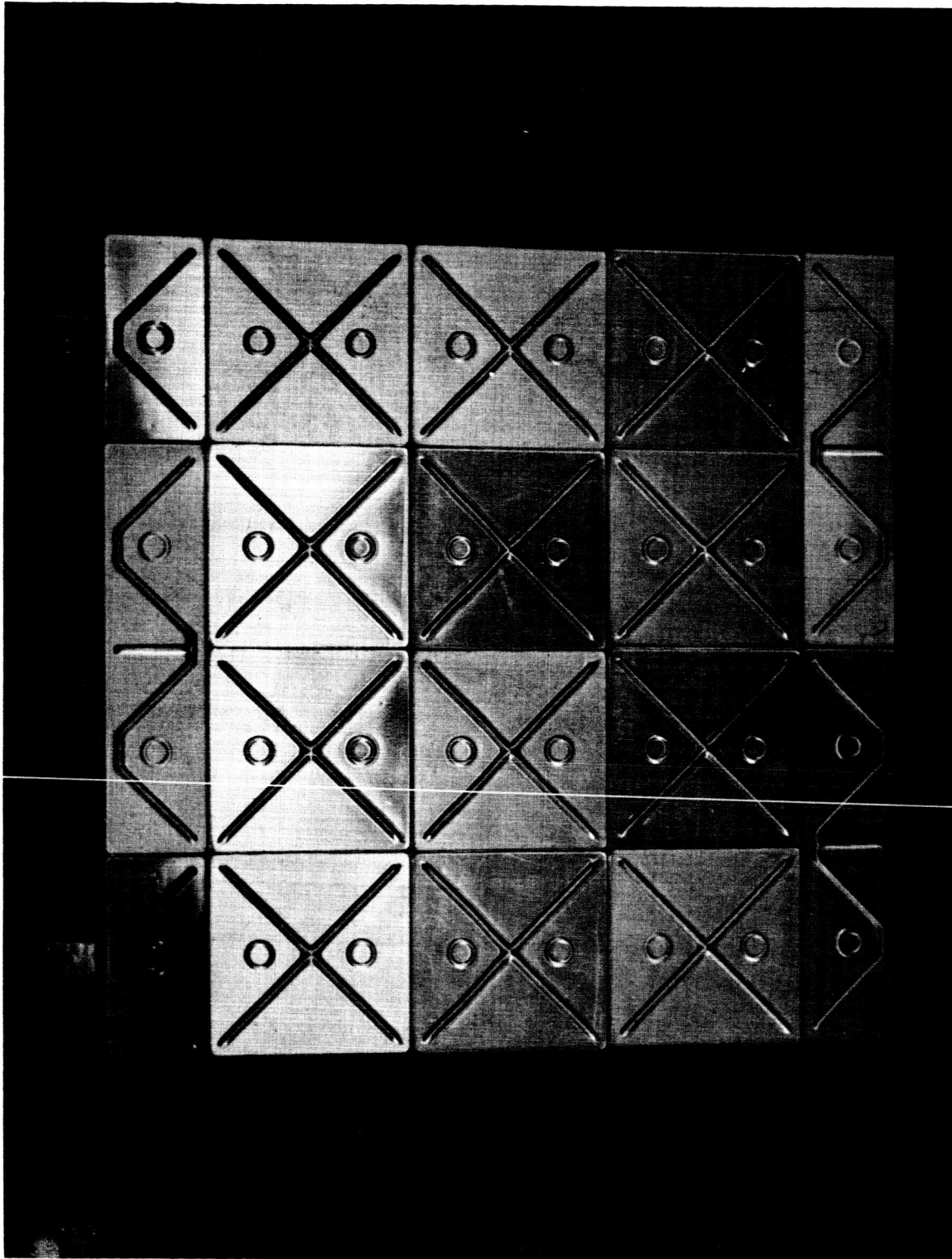


Figure 24. Radiator Panel Subassembly, Type I

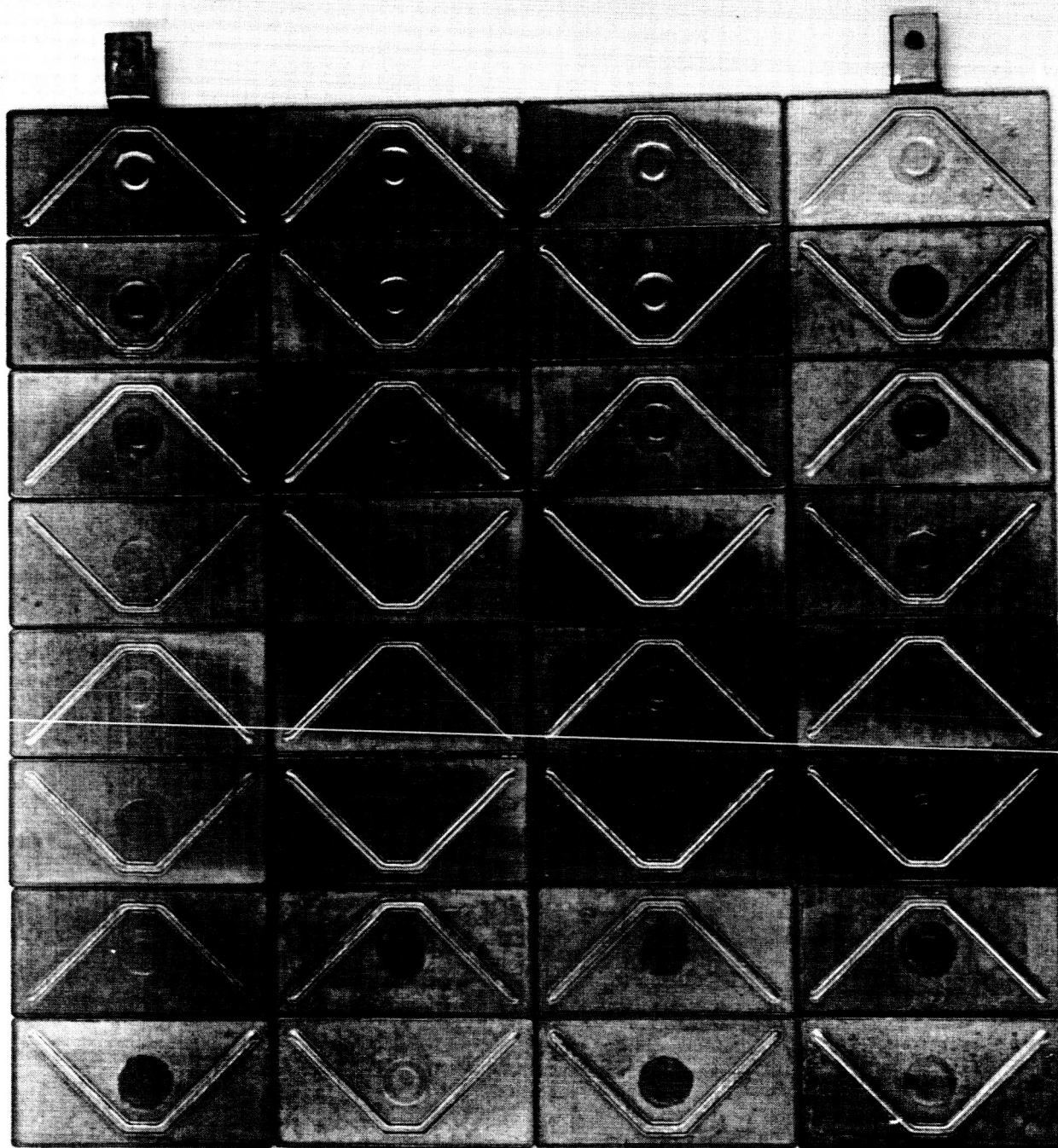


Figure 25. Configuration of Type II Panel Radiator Plates

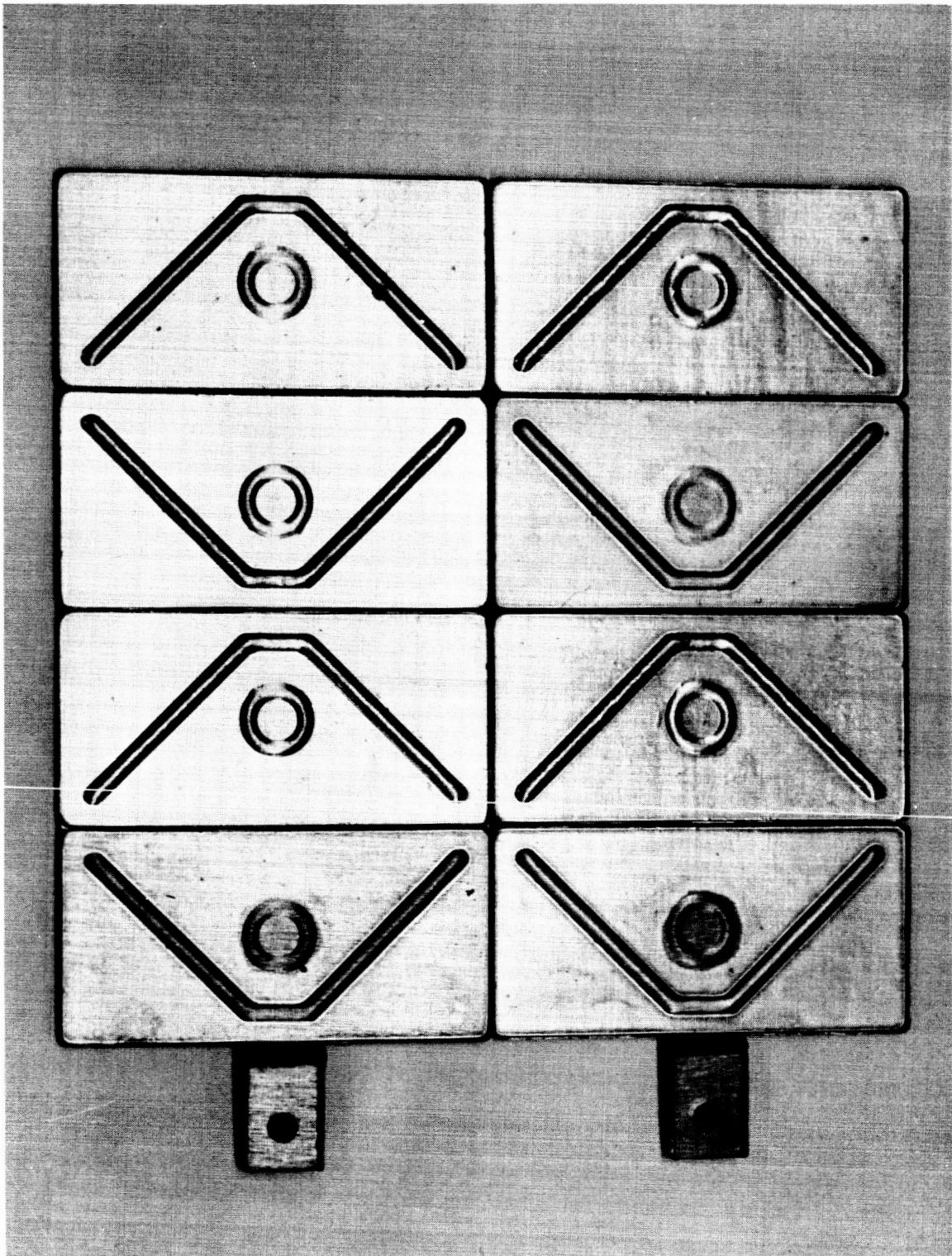
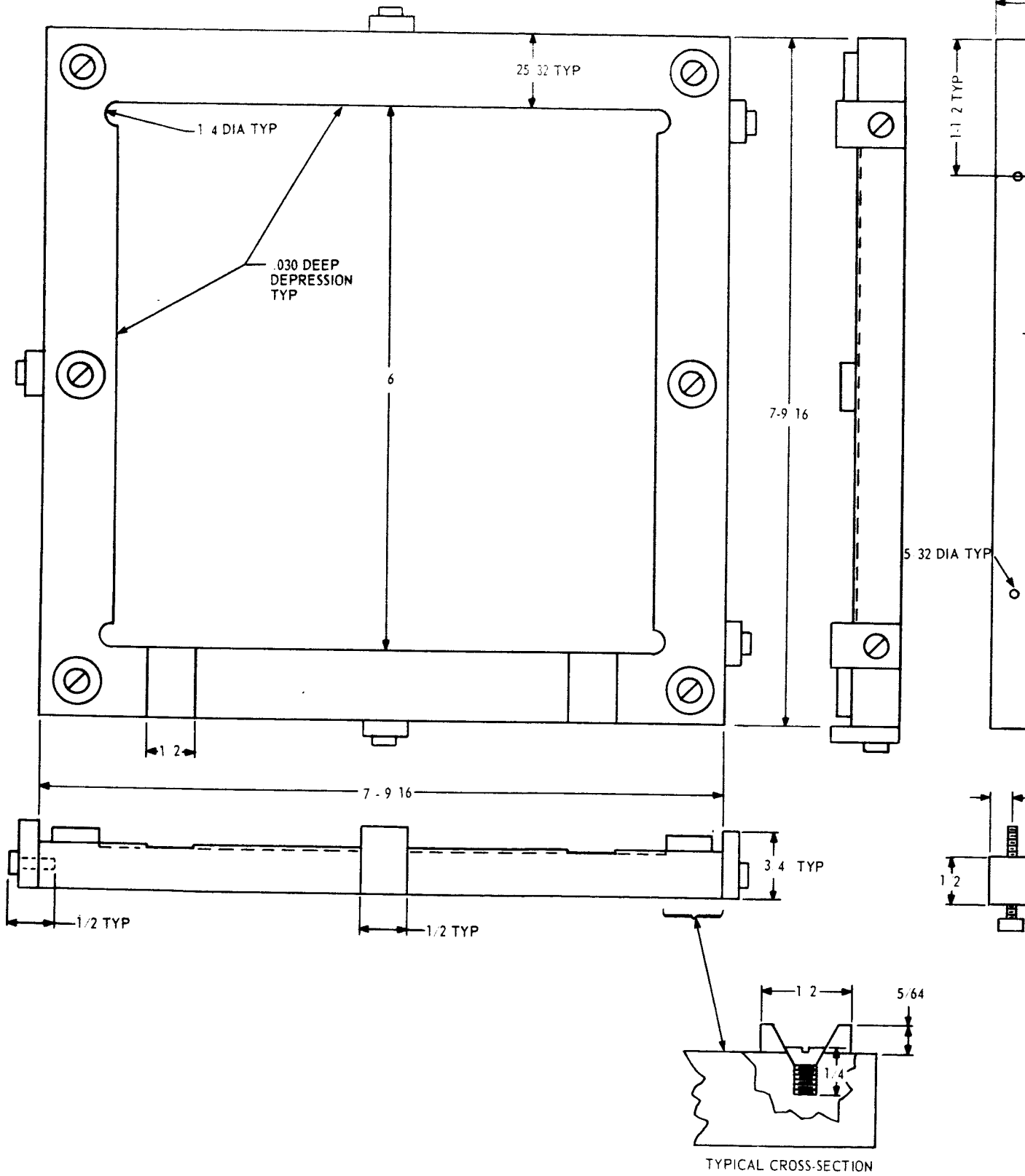


Figure 26. Configuration of Type III Panel Radiator Plates





a. Nickel Barrier Plating: This is a quite critical step in the achievement of reliable  $\text{Bi}_2\text{Te}_3$  generator couples, since many materials act to degrade the performance of  $\text{Bi}_2\text{Te}_3$ . Also an equally important requirement of the nickel barrier is preventing the lead solder from coming into contact with the  $\text{Bi}_2\text{Te}_3$ , since lead forms a low melting alloy composition with bismuth.

The nickel plating bath being used, (Hoover and Strong, Inc., Buffalo, N. Y.), has been demonstrated as satisfactory on the  $\text{Bi}_2\text{Te}_3$  generator materials used in the initial couple testing program; it was also satisfactory on the first flat aluminum plate couples. However, on acquiring a new shipment of  $\text{Bi}_2\text{Te}_3$  generator material from the vendor, it was found that consistently satisfactory barrier platings could not be achieved on the p-type material. This created a serious problem since all of the p-type elements, which were completely processed and ready for assembly into the final panel models, had to be rejected. The plating did not seem to be an effective barrier on the p-type elements to the lead solder, and upon heating resulted in lead getting into the  $\text{Bi}_2\text{Te}_3$  forming an alloy of low melting point. This material was also noted to have a high density of voids and cracks and tended to crack when heated to the processing temperatures. No trouble of this type has been experienced with the n-type material.

Efforts were made to increase the thickness of the nickel  $\text{Bi}_2\text{Te}_3$  barrier plating but this did not solve the problem. The ends of the elements were gently blasted with a fine abrasive, to improve the adherence of the plating. Extensive pre-cleaning and modifications of



conditions were tried without success. The immediate problem was solved by using thermoelectric material from another batch in which the p-type material exhibited this effect to a considerably smaller degree.

A new non-aqueous fluoborate nickel plating bath has been tried but as yet has not been evaluated.

b. Gold Low-Emissivity Coating: This phase of the program does not involve absorber or radiator coatings. However, the accurate evaluation of couples and panels requires that the internal radiation leakage from the absorber to the radiator be minimized. Gold has a quite low total normal emissivity in the temperature range of interest: 0.02 to 0.03 at 250°C.<sup>8</sup>

The first approach to the problem was to use evaporated gold on an anodized aluminum surface. It is necessary to isolate the gold from the aluminum since gold-aluminum compounds form at the hot junction operating temperature which have considerably different physical properties (and therefore, emissivities).

This approach was abandoned when a simpler method was found. A fine gold dispersion in an organic binder, known as Liquid Bright-Gold (Engelhard Industries, Newark, N.J.), which could be painted on and reportedly has similar emissivity characteristics to other forms of gold used for low emissivity coatings was used. According to the supplier, the material is compatible with aluminum due to the formation of a lacquer between the gold and aluminum from the organic binder during the curing cycle.

Plates coated with this material have been exposed to 250°C temperature for several hundred hours with no detectable change in the appearance

or adherence of the gold coating.

#### 2.5.2 Conclusions

The following conclusions are drawn from the experimentation involved with the fabrication of flat plate unit couples and panels:

- a. The use of aluminum is practical from the standpoint of making good mechanical, thermal and electrical contacts.
- b. At this time, the best contacting techniques involve the use of nickel barrier plated thermoelectric elements, nickel plated aluminum plates and lead and tin-lead solder as the bonding materials for the hot and cold junctions, respectively.
- c. At this time, the best assembly method involves the fabrication of single couples and their subsequent testing and fabrication into panels.
- d. From the standpoint of assembly processing, the currently available material is unsatisfactory.
- e. Improved nickel-Bi<sub>2</sub>Te<sub>3</sub> barrier layers are needed. Improvement is expected from the new non-aqueous fluoborate nickel plating process.
- f. The paint on gold low-emissivity coating is an easy process to use, but the results of testing unit couples indicate that the emissivity may not be as low as expected.

## 2.6 Testing and Evaluation of Experimental Single Couples

In the achievement of practical thermoelectric flat plate generator panels, it is first necessary to determine the characteristics of the unit cell of the panel, the single couple. These unit couples are shown in figure 21. The junction electrical resistance, the mechanical strength of the junctions, the thermoelectric performance, and the behavior under thermo-mechanical stresses are among the most important characteristics of the unit couple. The evaluations of these characteristics of unit couples are given.

### 2.6.1 Junction Resistance

The study of junction contact resistance was continued from the first quarter of this program phase. The technique used was that of Mengali and Seiler as described in the first quarterly report on this program.<sup>3,9</sup>

The data taken on cross-sections of unit couples (see figure 28) shows little or no contact resistance due to either the  $\text{Bi}_2\text{Te}_3$  - nickel plating interface or the nickel plating-lead solder interface. The lead-nickel plating (on aluminum) interface showed no detectable contact resistance. On selected samples no contact resistance was found across the nickel plating-aluminum interface. However, it was not unusual to find some contact resistance at the nickel-aluminum interface. Figure 29 is the contact resistance curve of a selected junction and is typical of the better results obtained on an n- or p-type leg at both the hot and cold junctions.

A solution to the problem of inconsistent electrical contacts between the nickel plating and the aluminum is known. The nickel plating characteristics may be improved by pre-coating the aluminum with zinc. A poor electrical contact of this type usually has poor mechanical strength also.

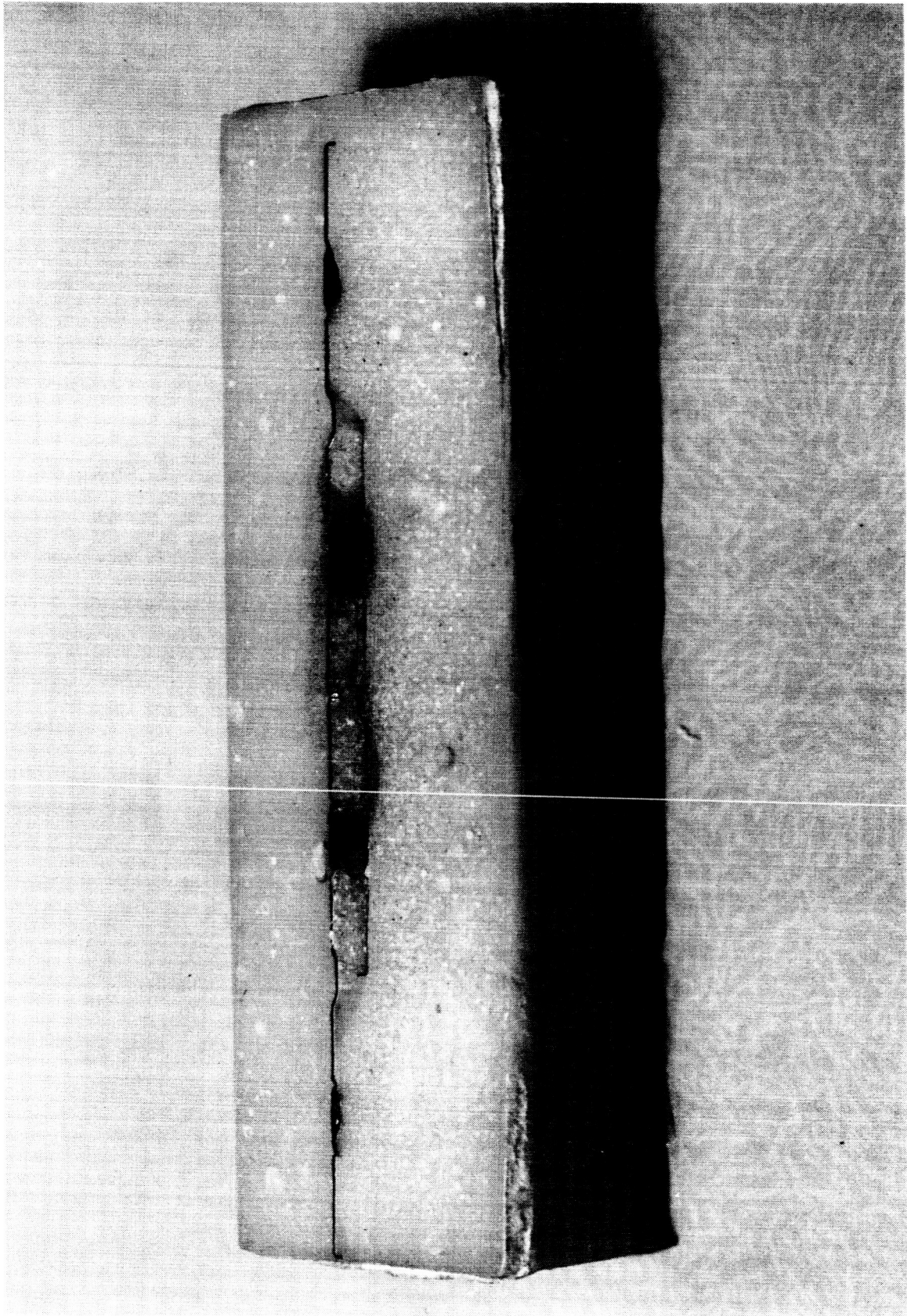


Figure 28. Cross-Sectional View of Experimental Flat Plate Single Couple (Potting Material Not Removed)

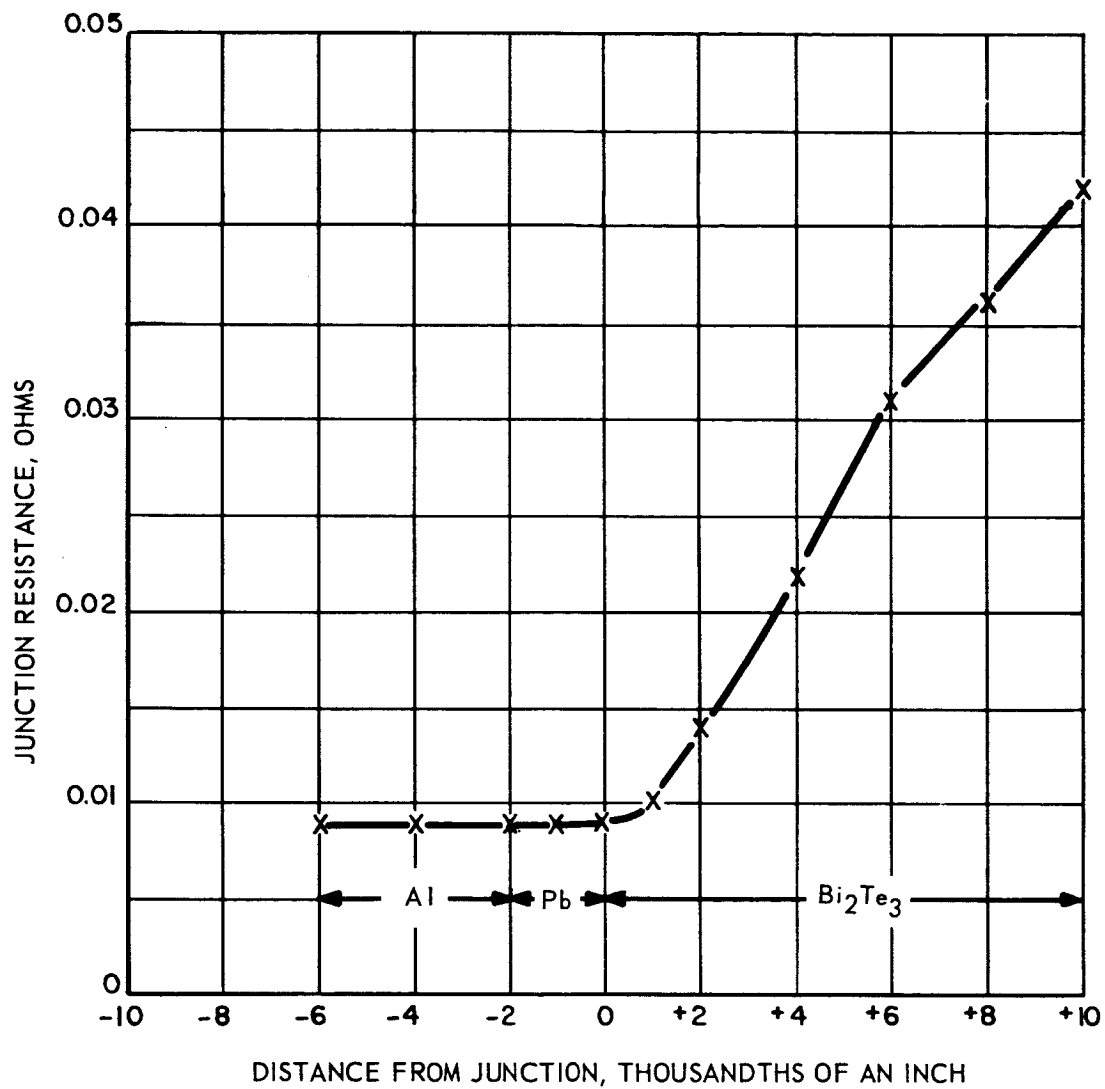


Figure 29. Typical Contact Resistance of Lead to Ni Plated N- and P-Type  $\text{Bi}_2\text{Te}_3$  Elements.

Since zinc is an excellent metallurgical choice for bonding to aluminum and if a suitable technique is developed for coating the desired areas with zinc, the nickel plating on the aluminum may not be necessary.<sup>6</sup> In section 2.5 it should be noted that zinc was used frequently in experiments for bonding to aluminum. A further improvement is the addition of zinc to the lead solder to improve the bonding properties to nickel as well as to aluminum or nickel although satisfactory electrical and mechanical joints are readily achievable. The addition of zinc to the system should improve the contact metallurgically.

The contact resistance of lead to aluminum has been found to be consistently good, although no better electrically than selected nickel plating to aluminum joints. Tin-lead solder for the cold junction gives approximately the same resistance as pure lead.

#### 2.6.2 Junction Mechanical Strength

In considering the mechanical strength of the bonds from the thermoelectric material to the aluminum plates, it is necessary to consider each interface. In all design and processing considerations an attempt was made to minimize the number of interfaces where it was at all practical to do so.

In a good couple the weakest part is the thermoelectric material. Therefore, the bond strengths were determined relative to the fracturing point of the thermoelectric material. Beginning at the nickel plating to  $\text{Bi}_2\text{Te}_3$  bond, the nickel plating bond failed just slightly less often than the thermoelectric material. The majority of the failures were at the p-type elements. No failures were observed at the nickel- $\text{Bi}_2\text{Te}_3$  plate-lead bond, and there were no failures at the aluminum side lead-nickel-aluminum plate bond. Inconsistently bonded nickel plating occurred on the aluminum

plates and some bond failures were noted there. When a failure occurred between the nickel plating and the aluminum, this bond was shown to be by far the weakest, but the number of failures due to this bond were considerably less than the failures due to thermoelectric material fracturing.

From work in the first quarter of this program, and earlier Melpar research it was known that a pure bismuth solder consistently produces bonds to  $\text{Bi}_2\text{Te}_3$  materials which are stronger than the  $\text{Bi}_2\text{Te}_3$  bonds and nickel plate  $\text{Bi}_2\text{Te}_3$  bonds.

The procedure was as follows: Five millimeter diameter thermoelectric elements were held firmly in a holding fixture. A copper rod one-fourth of an inch in diameter and one foot long was bonded to the elements either through bismuth solder or nickel barrier plating and lead solder. Weights were added to the end of the one foot rod until the bond failed. The weight required to break the bond was noted.

The results were:

a. Directly soldered bismuth joint

Element No. 1 (no solder fillet) failed at 95 grams

Element No. 2 (0.005 in. to 0.010 in. fillet) failed at 121 grams

Element No. 3 (0.020 in. fillet) failed at 160 grams,

b. Nickel barrier plated, lead soldered joint

Element No. 1 (no solder fillet) failed at 35 grams

Element No. 2 (0.005 in. to 0.010 in. fillet) failed at 67 grams

Element No. 3 (0.020 in. fillet) failed at 112 grams

The nickel plating joints demonstrated less bond strength than the directly bismuth soldered joints, but in all cases when the joint was

broken the nickel plating pulled away chunks of the  $\text{Bi}_2\text{Te}_3$  material with it. The indications were that the nickel plating was better bonded in some spots than in others. The presence of a fillet along the side of the elements helped the strength of the bonds in both cases, but it was more pronounced in the case of the nickel plated bonds.

### 2.6.3 Thermoelectric Performance

Single couples were evaluated as generators to determine the approximate thermoelectric efficiency attainable in this particular flat plate configuration. The single couples used were of the type illustrated in figure 21. In construction, they were similar to the units used for type I panels, i.e., nickel plated  $\text{Bi}_2\text{Te}_3$  legs soldered directly to the aluminum absorber and radiator plates with lead and tin-lead, respectively. The internal surfaces of the plates were coated with the Liquid Bright-Gold low-emissivity coating to help reduce radiant shunt leakage.

The testing procedure, which is shown in figure 30, was carried out in a vacuum of between  $10^{-4}$  and  $10^{-5}$  Torr. An adiabatic thermal guard system was used. The cold junction was maintained at approximately  $60^\circ\text{C}$  on a heat sink. The thermal input power was provided by a small, flat electrical resistance heater, whose electrical input power ( $I \times V$ ) was measured. The temperature of the hot junction was raised to  $240^\circ\text{C}$ . A thermal guard surrounding the electrical heater and the hot junction was maintained at  $240^\circ\text{C}$  by infrared radiation from a heat lamp. Since the measurements are made in a vacuum and since the power loss from the input heater due to radiation is kept small by the thermal guard, the only remaining losses are by conduction through the input electrical leads to the heater and the radiation loss from the absorber plate to the radiator plate. Both of these losses can be



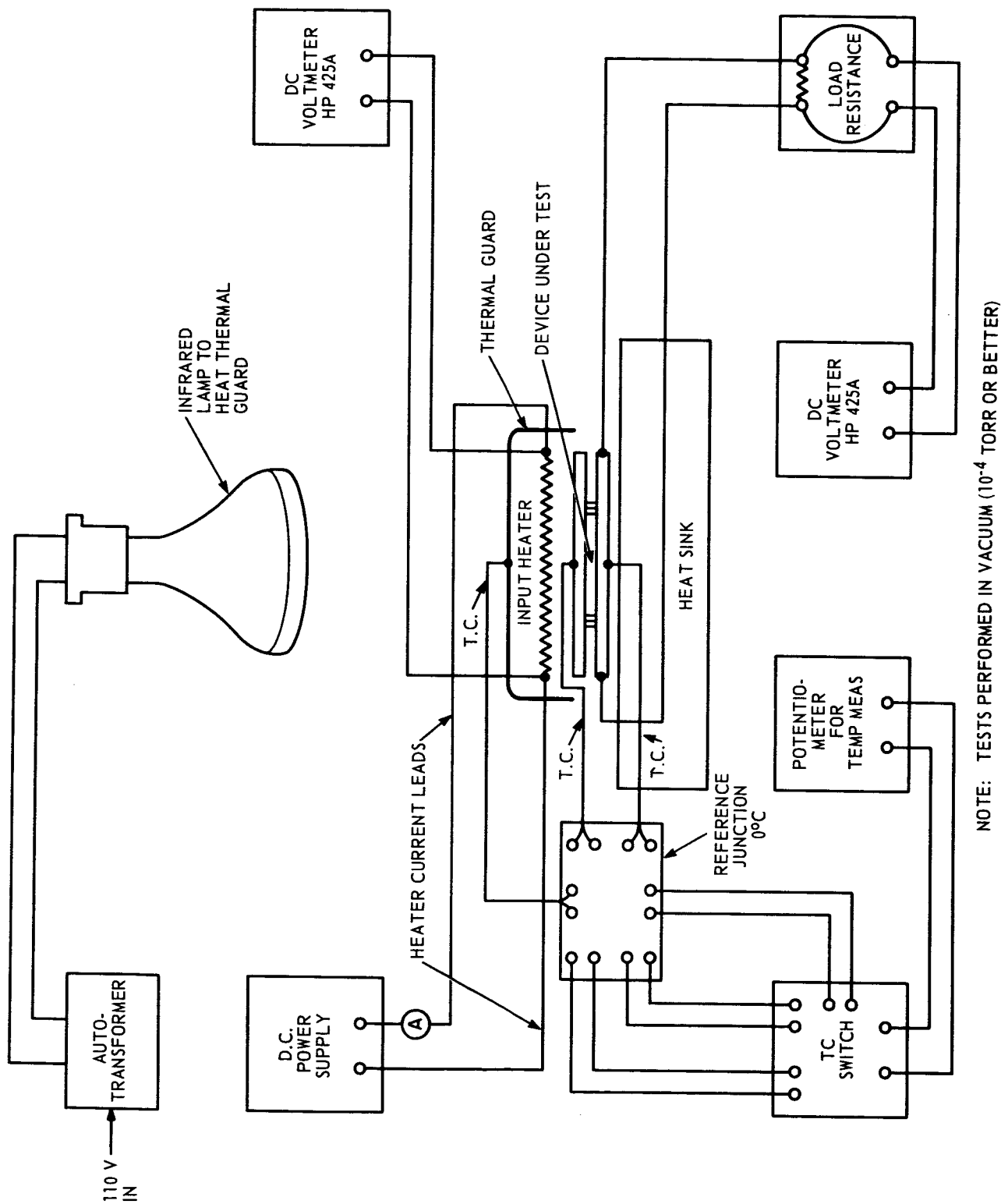


Figure 30. Evaluation Apparatus for Experimental Flat Plate Single Couples

estimated with reasonable accuracy.

The open-circuit output voltage of the couple was measured. The matched-load output voltage and current were measured. The output power and input power were determined and the efficiency calculated. The thermoelectric results for three single couples are given in table 5.

Thermoelectric conversion efficiencies between 4.5% and 5% were obtained when the couples were constructed with small copper straps. When these couples were incorporated into the unit structure shown in figure 21 and tested, efficiencies of the order of half these values were achieved. The obvious conclusion is that the internal gold radiation coatings are not effective leading to thermal conduction leakage. Steps are being taken to solve this problem. Evaporative gold coating techniques may have to be used.

#### 2.6.4 Temperature Cycling

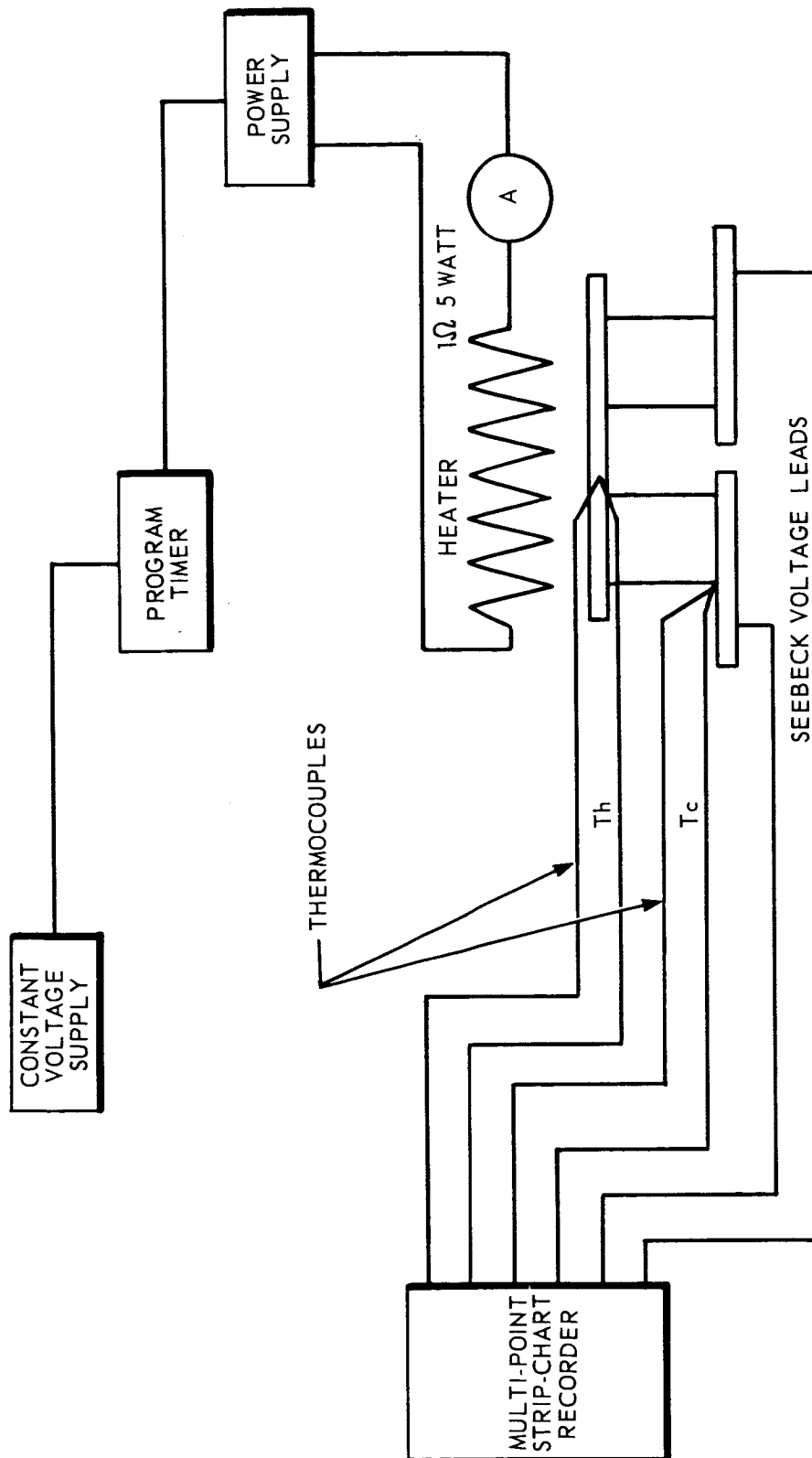
Life testing of the thermomechanical flat plate device properties and thermoelectric material properties by means of temperature cycling of the hot junction from less than 100°C to nearly 240°C was initiated. The tests were carried out in air.

Initially, three flat plate unit couple generator devices were put on the temperature cycling life test. The cycling apparatus is shown schematically in figure 31. A multipoint strip chart recorder was used to continuously monitor the hot and cold junction temperatures and the Seebeck voltage. The cycling was controlled by a programmable time switch. The period of the cycle was approximately 30 minutes. AC resistance measurements were made manually at intermittent intervals.

The results of these initial temperature cycling experiments are given in figure 32. Unit No. 2C failed after handling at 196 cycles (98

TABLE 5  
THERMOELECTRIC PERFORMANCE  
OF TYPICAL FLAT PLATE SINGLE COUPLES

Flat. Plate Couple No.	Measured Thermoelectric Efficiency	Estimated Leakage	Corrected Efficiency
D1	4.49%	0.14%	4.63%
D2	4.75	0.25	5.0
D3	4.55	0.25	4.8



NOTE: TESTS PERFORMED IN AIR.

Figure 31. Temperature Cycling Life Test Apparatus

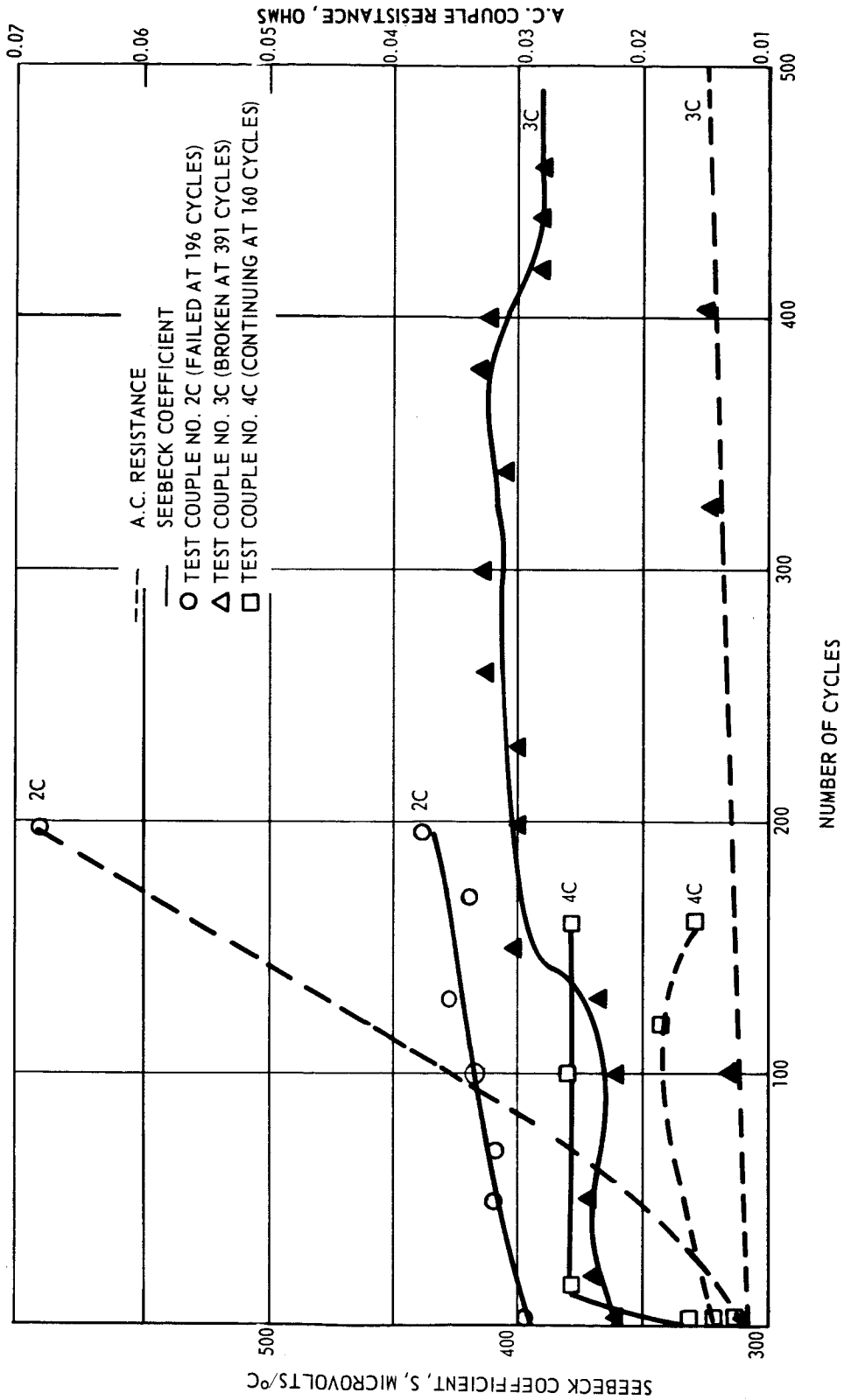


Figure 32. Initial Temperature Cycling Life Test Data

hours). At the end of 98 hours the ac resistance increased over 400% indicating that electrically the bond had effectively failed. The mechanical properties of the bond were also degraded since the bond easily came apart in handling. Examination showed that the main failure spot was the p-type hot junction.

Unit No. 3C exhibited somewhat better performance with an ac resistance increase of only 10% after 100 cycles. At the end of 200 cycles, however, the increase in ac resistance was 24%, indicating probably the same sort of failure mechanism as in Unit No. 2C. At 490 cycles the hot junction heater failed, and the unit was accidentally broken while attempting to replace the heater.

Unit No. 4C is still operative and had increased in ac resistance approximately 12% after 160 cycles; it appears to be similar in performance to unit No. 3C.

The Seebeck coefficient, which is a sensitive gauge of the thermoelectric material parameter changes, was completely overshadowed by the effect of increasing contact resistances at the hot junction, especially at the p-type contact. There seemed to be no significant change in the room temperature Seebeck coefficient or electrical resistivity, so for the present it is assumed that no gross thermoelectric material degradation was incurred during this amount of temperature cycling. The failure mechanism seemed to be a simple failure of the hot junction nickel barrier plating bond to the  $\text{Bi}_2\text{Te}_3$  material; this was especially true at the p-type leg, but it was also present to a lesser extent at the n-type leg. The surfaces appeared to be oxidized or corroded. Trapped plating solution residue may be causing or aiding the reaction.

#### 2.6.5 Conclusions

The following conclusions were derived from the testing and the results of testing of single couples:

a. High efficiency (5%) flat plate form generator couples can be fabricated provided the internal radiation coating problem is solved. High efficiency flat plate panels require one additional assembly step and should be achievable with little or no degradation of performance.

b. Good low contact resistance joints can be made between the  $\text{Bi}_2\text{Te}_3$  materials and the aluminum absorber and radiator plates using nickel plated elements soldered either directly to aluminum or to nickel plated aluminum with lead solder (hot junction) and tin-lead solder (cold junction).

c. A more satisfactory solution than the present nickel plating to aluminum must be found so that consistent results may be obtained. A zinc coating for soldering or a pre-plating zinc coating appear promising.

d. Lead bonding to aluminum and to nickel barrier platings could be improved by the addition of a small amount of zinc to the lead.

e. The presence of a small solder fillet along the sides of the elements definitely increases the strength of the bond.

f. The present nickel plate to  $\text{Bi}_2\text{Te}_3$  bond strength is only slightly greater than the fracturing strength of the thermoelectric material. Mechanically it is not bonding well enough. Temperature cycling life test data indicate rapid electrical and mechanical deterioration of the present nickel plated barrier contacts. A new non-aqueous fluoborate nickel bath shows promise of considerable improvement of mechanical bond strength as well as more effective barrier action due to finer grain size. A thin

nickel shoe soldered to the  $\text{Bi}_2\text{Te}_3$  may be necessary at the hot junction if the nickel plating cannot be made sufficiently adherent.

g. No thermoelectric material degradation is detectable at this time from the temperature cycling life test.

h. Based upon observations and handling of the single couple assemblies during processing and testing, it is believed that they are thermomechanically sound and that stresses due to differential expansion, are taken up in the flexibility of the expansion ring surrounding the element contacts and the flexibility of the soft aluminum plates, themselves. The increase in ac resistance on thermal cyclic testing is attributed more to a chemical change (oxidation) due to the temperature at the interface of the nickel and  $\text{Bi}_2\text{Te}_3$  and less to mechanical stresses.

i. Improved testing techniques must be developed that provide more reasonable and gentle mechanical handling methods. Although the panels have considerable built-in relative ruggedness, strength and rigidity, the absolute magnitude of the force necessary to cause damage at certain points is quite small.



## 2.7 Testing and Evaluation of Experimental Flat Plate Thermoelectric Generator Panels

The experimental flat plate thermoelectric generator panels are to be evaluated in two ways:

- a. For their thermomechanical stability, and
- b. For their thermoelectric performance.

The test setups and the available results are given in the following subsections.

### 2.7.1 Mechanical and Thermal

The individual unit couple assemblies are thermomechanically sound. When they are mechanically joined together, however, this is not necessarily true. The final flat plate assemblies (see figures 33, 34 and 35) must be cycled to their hot and cold junction temperatures several times to demonstrate their thermomechanical stability.

This thermomechanical cycling test is performed in a vacuum with the panels supported by their support and mounting structures only. The hot junction is heated radiantly with a small bank of infrared lamps to the temperature of the hot junction. ( $240^{\circ}\text{C}$ ). The heat is applied at a uniform rate over the entire hot surface of the flat plate. The cold junction is in close proximity to, but not touching a surface cooled with liquid nitrogen. The temperature of this surface is controlled by controlling the liquid nitrogen flow to the back side of the surface. This temperature is adjusted so that the cold junction temperature is approximately  $60^{\circ}\text{C}$  when the hot junction is approximately  $240^{\circ}\text{C}$ . The panel will be free to warp, distort, or be subject to various thermal stresses as is its nature.

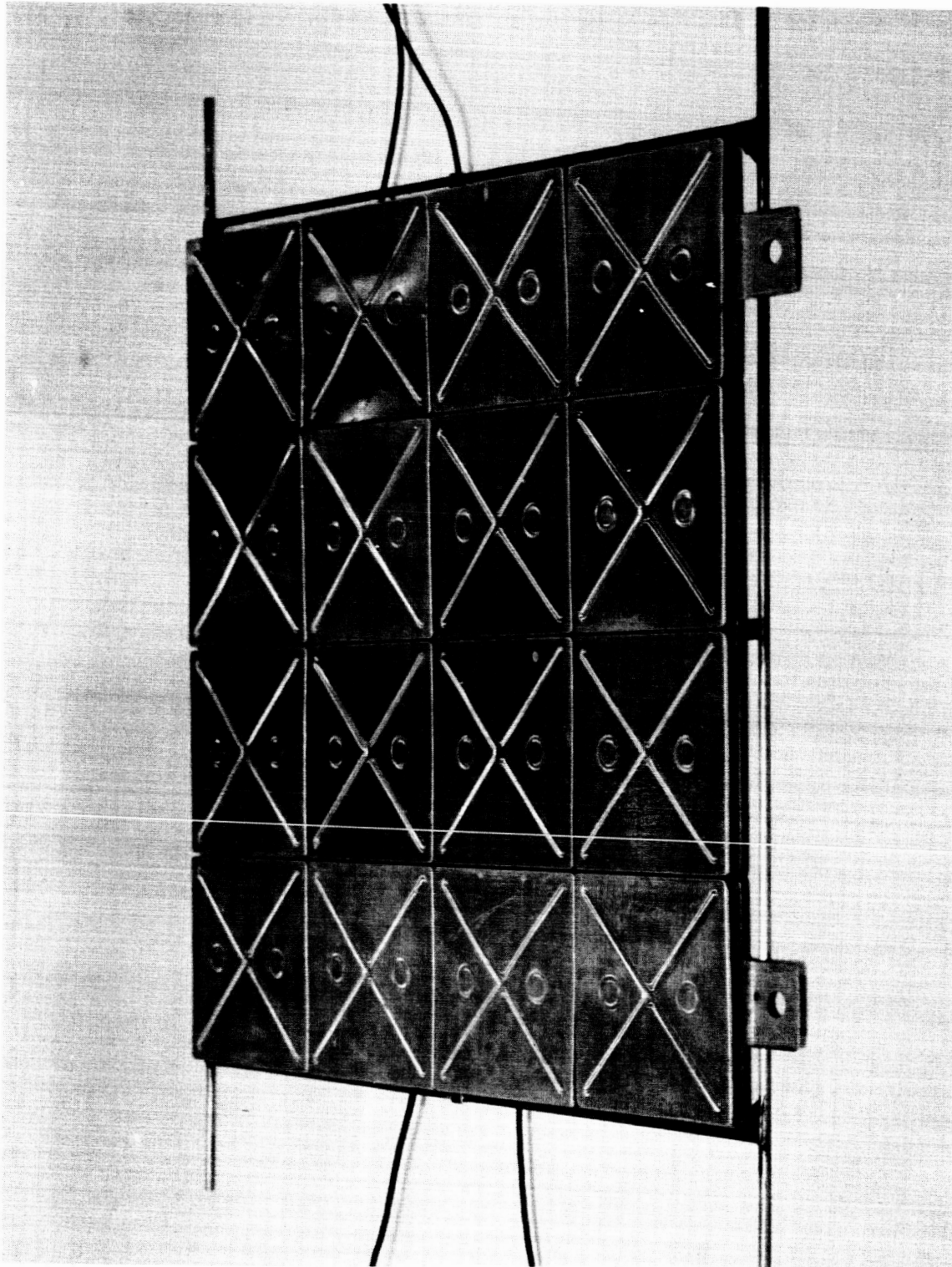


Figure 33. Experimental Flat Plate Generator Panel, Type I

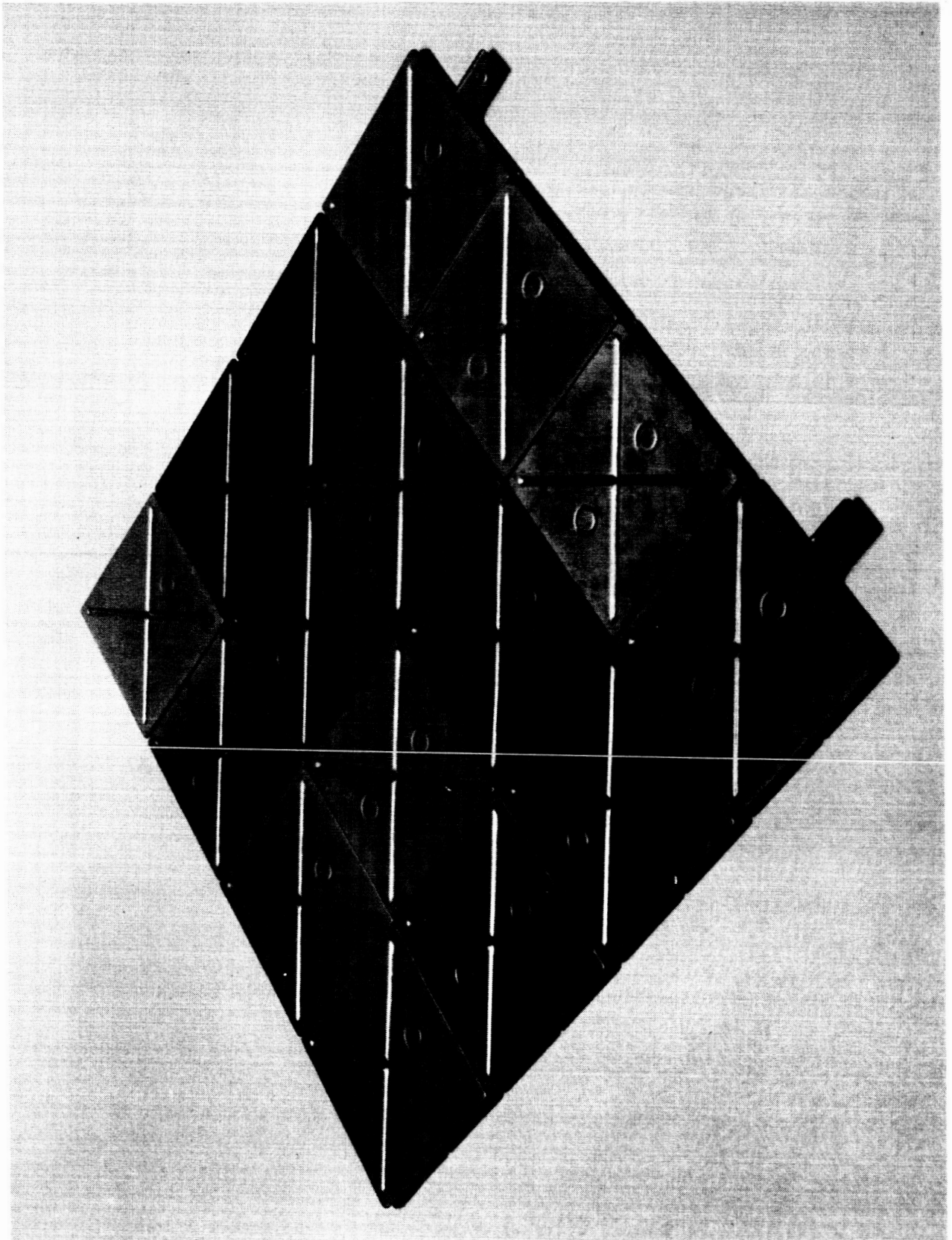


Figure 34. Experimental Flat Plate Generator Panel, Type II

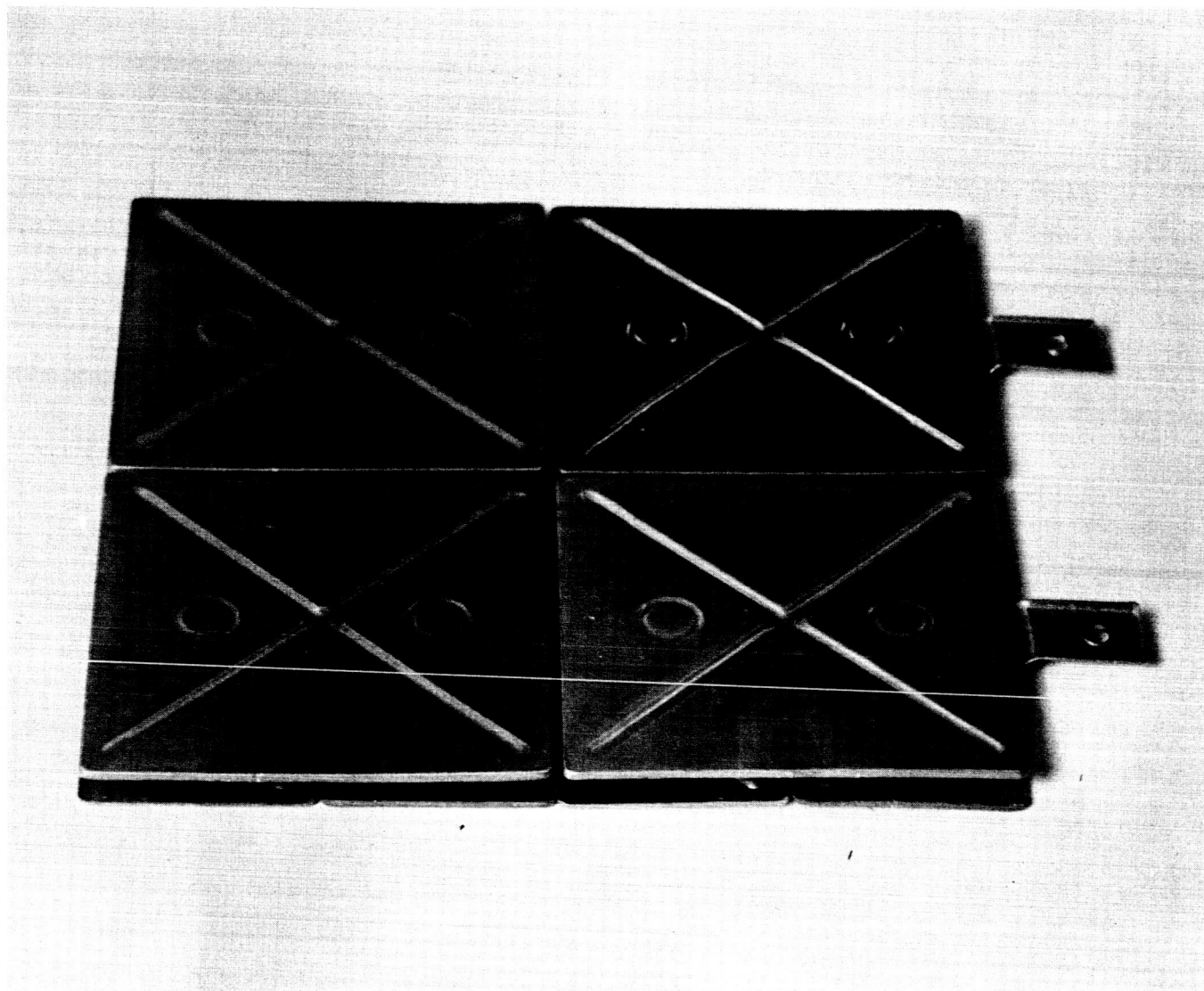


Figure 35. Experimental Flat Plate Generator Panel, Type III

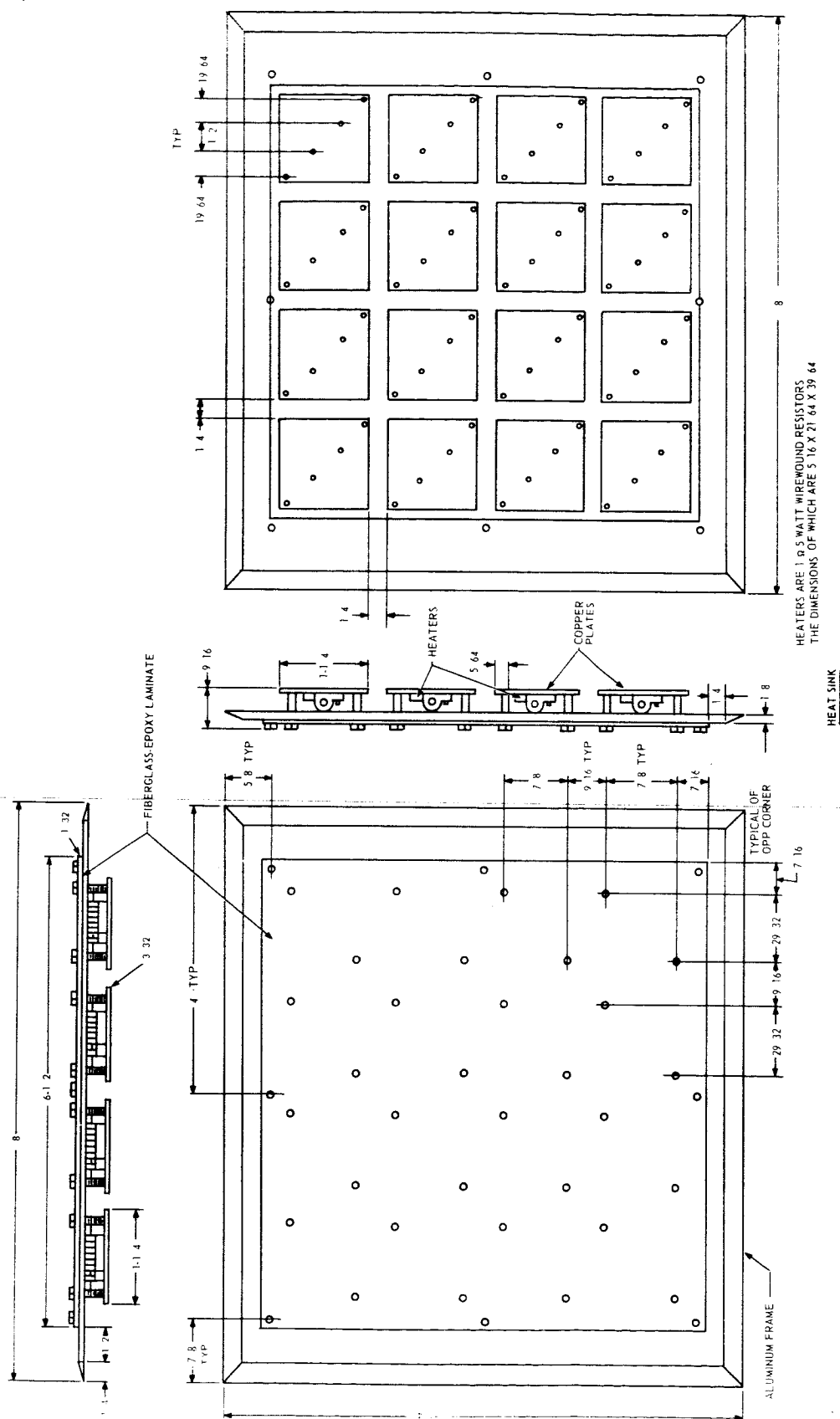
The results of these tests are not yet complete and will be presented in the next quarterly report. One panel was cycled three times in the testing fixture described in section, 2.7.2. These results are not conclusive, however, since the test fixture supports the panel rigidly from both sides. After three cycles ranging from room temperature to 240°C and return, the panel showed no warping or distortion, due to the cycling, when removed from the test fixture.

#### 2.7.2 Thermoelectric Performance

The measurement of the thermoelectric conversion efficiency of the flat plate generator panels is now discussed. The testing principle and procedures are similar to those described in section 2.6. for single couple thermoelectric performance (See figure 36). The test is performed in vacuum using the adiabatic radiation shielding method so that radiant heat leakage from the electrical heaters is reduced to an insignificant level. The main difference between the single couple testing and the panel testing setups is that in this procedure an array of heat input resistors of identical resistances ( $\pm 1\%$ ) connected in series are used for the heat input. The resistor value is one ohm (rated at five watts). One resistor is used for each couple in the panel so that an equal amount of heat is provided for each couple. The sink which is water cooled and the heat input resistor array are shown in figure 37. A thermal guard is used, as in testing the single couples described in section 2.6. The thermal guard is similarly heated with an infrared lamp to 240°C to achieve the adiabatic conditions required.

The open-circuit and matched load output voltages are measured along with the electrical input heater power. The output power and efficiency are calculated.

INPUT POWER HEATER ARRAY



HEATERS ARE 1.5 WATT WIREWOUND RESISTORS  
THE DIMENSIONS OF WHICH ARE 5.16 X 21.64 X 39.64

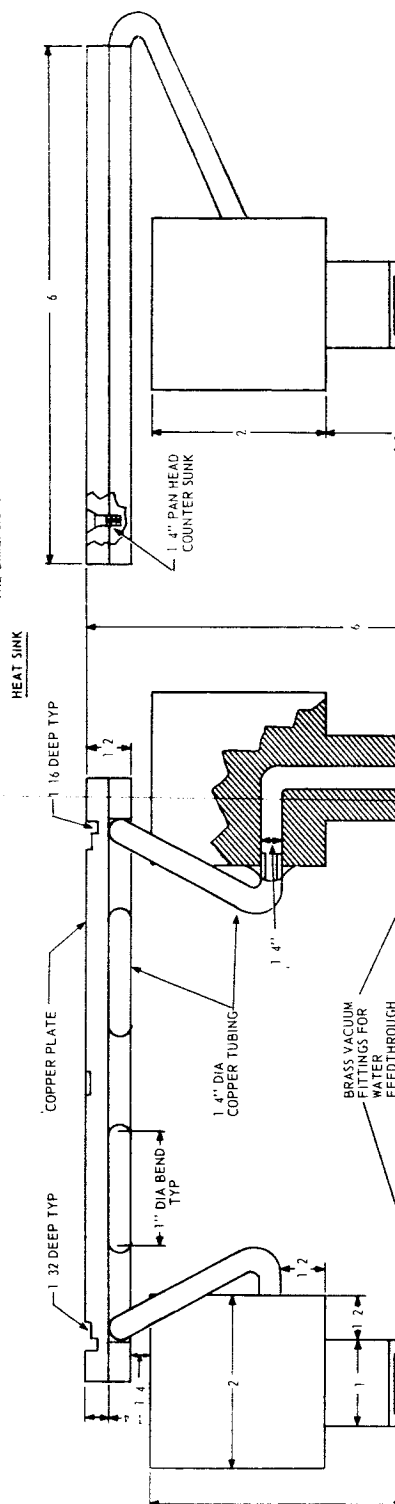
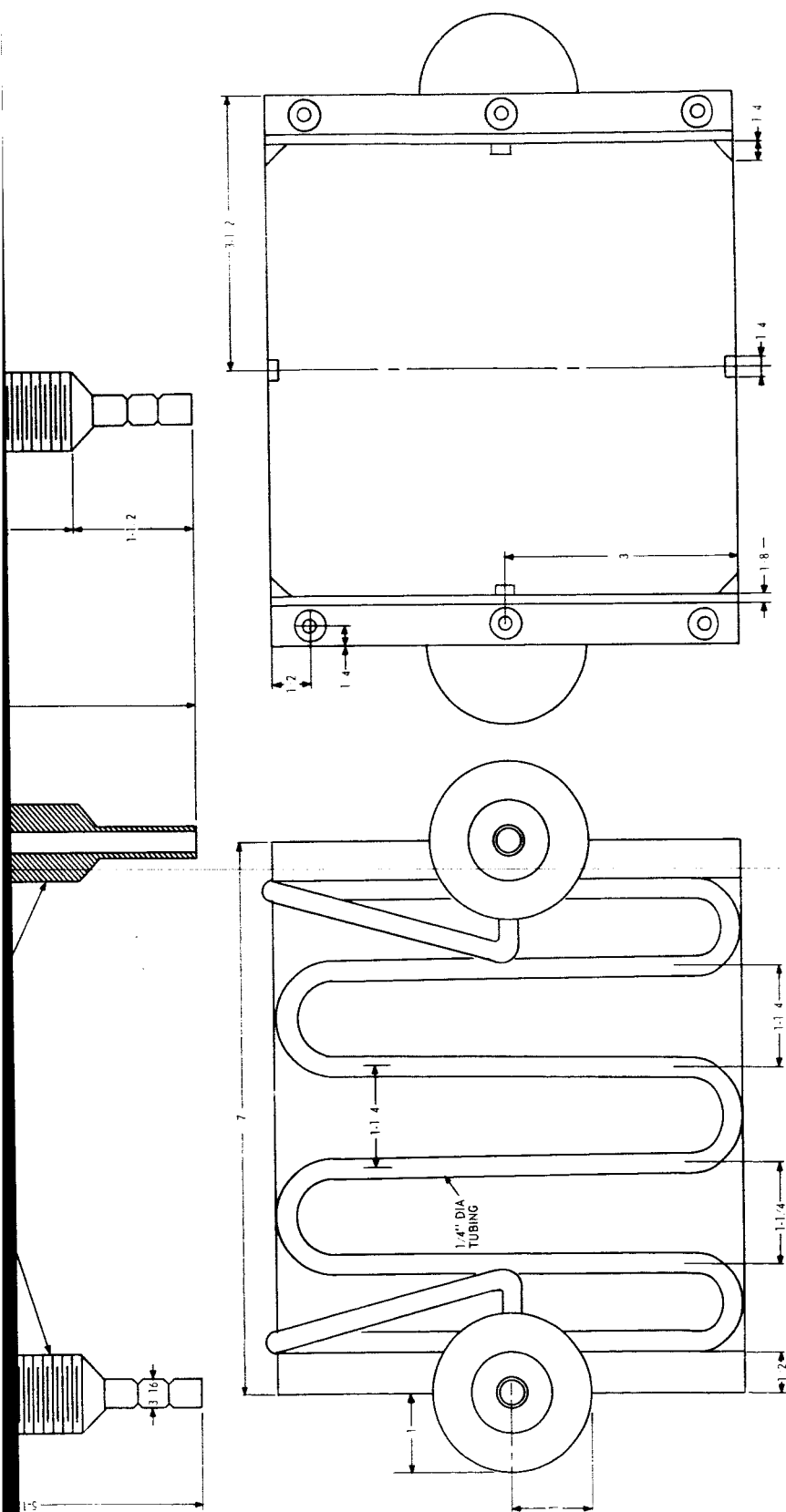


Figure 36. Evaluation



Apparatus for Experimental Flat Plate Panels



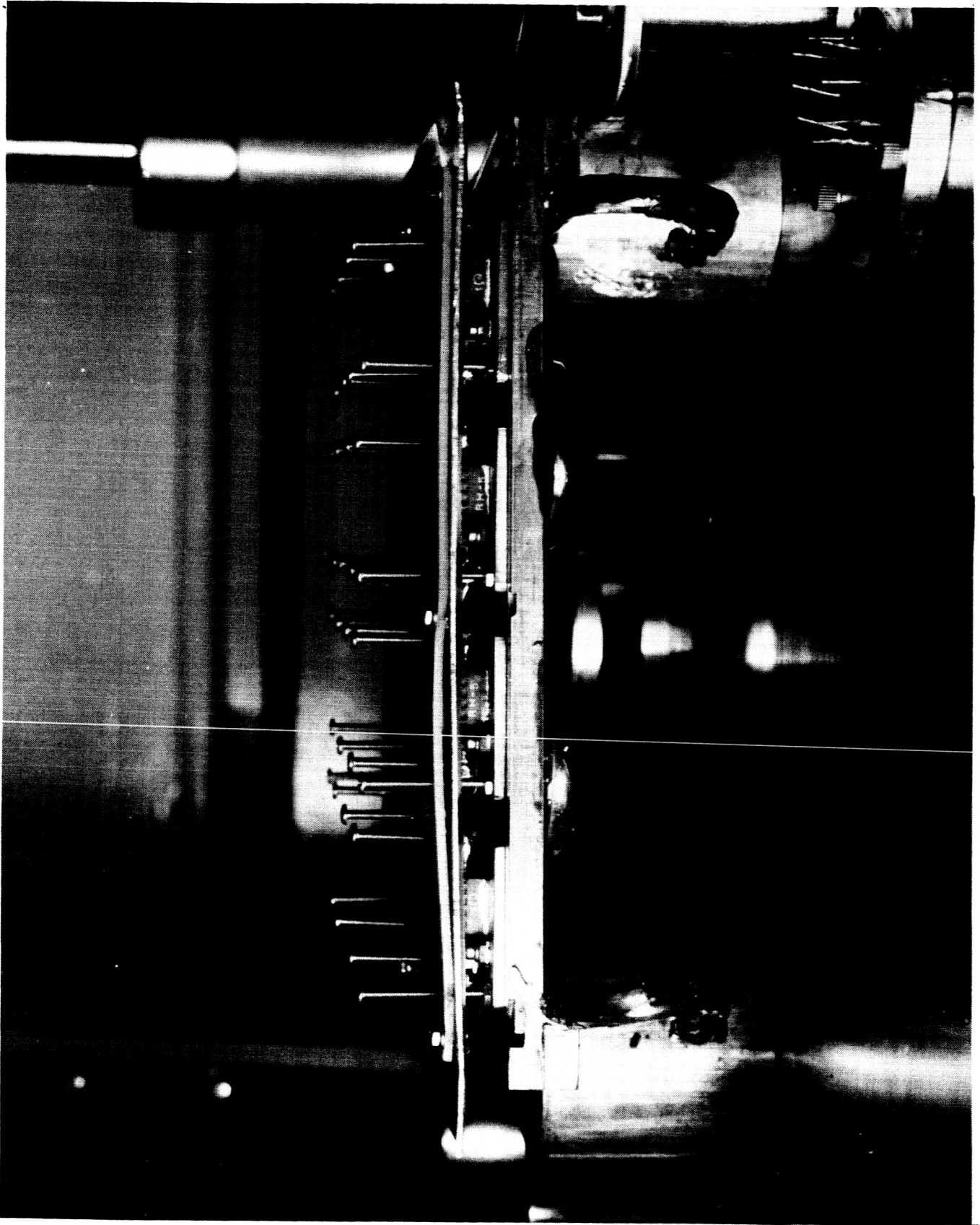


Figure 37. Heat Input Resistor Array and Heat Sink for Evaluation of Experimental Flat Plate Panels.



The results of panel evaluations are not yet complete and will be reported in the next quarterly report.

### 2.7.3 Conclusions

Conclusions concerning the testing and evaluation of the flat plate generator panels are:

a. The panel design seems to be mechanically stable under thermal stress conditions produced by the operating temperatures. (This is however based upon very limited testing.)

b. Although thermoelectric conversion efficiency tests have not been completed on assembled panels, it is reasonable to assume that efficiencies similar to those achieved in the flat plate form unit couples can be achieved in the assembled panels. Once performance is proven in single couples, the assembly into panels should incur little or no performance change.

c. The life of the panels under strenuous conditions of temperature cycling will almost certainly be the same as for the single couples. No improvement in this area for the panels is expected until the nickel  $\text{Bi}_2\text{Te}_3$  barrier plate bonding problem is solved. The performance results should be indicative, though, of the improved life performance that can be achieved once the contacting problem is solved.

### 2.8 Summary of Conclusions

Overall conclusions based upon the results of the technical effort to date are summarized below:

a. Design and Construction: The required thermoelectric material A/ℓ is 16 cm based upon 3-watts per square foot power output. Given suitable

thermoelectric materials and the proper choice of non-thermoelectric structural materials, a practical flat plate solar generator can be designed and constructed that will meet the performance requirements. The ability to achieve reliable low cost panels will be limited by thermoelectric material deficiencies and/or contact degradation.

b. Thermoelectric Material Evaluation: The available  $\text{Bi}_2\text{Te}_3$  alloy thermoelectric generator materials are not satisfactory for achieving optimized panel performance, although the minimum required performance is attainable (3 watts/ft<sup>2</sup> and 15 watts/lb.). Because of the gross inhomogeneity of the available thermoelectric materials, a materials selection program is meaningless unless performed on each leg to be used. This results in a considerable expenditure of effort to produce the 16 couple flat plates shown in figure 33.

c. Flat Plate Generator Fabrication: Good electrical contacts can be made between the thermoelectric legs and the aluminum plates. These contacts, however, were found to degrade after thermal cycling in air due to bond degradation of the nickel- $\text{Bi}_2\text{Te}_3$  barrier plating. Improved nickel- $\text{Bi}_2\text{Te}_3$  plating barriers are required. A liquid paint-on gold coating emissivity-control simplifies the unit construction procedure, but may have emissivity values too high resulting in excessive thermal radiation loss between plates.

d. Flat Plate Generator Evaluation: High efficiency flat plate unit couples can be fabricated when a satisfactory method for internal radiation leakage control is achieved. When this is achieved, high efficiency flat plate generator panels should be obtainable with little or no degradation of performance. It is felt that the thermomechanical characteristics of the

couples and panels are good. More data is required to verify this.

e. General: A program directed toward the development of  $\text{Bi}_2\text{Te}_3$  generator materials with homogenous characteristics and optimized for a temperature range of up to  $250^\circ$  or  $300^\circ\text{C}$  is needed for the successful achievement of the goals of this program. The deficiencies of the thermoelectric materials are troublesome at every step of the fabrication program and the performance characteristics are less than those that could reasonably be expected for materials of this type in this application.

### 3. NEW TECHNOLOGY

The items which can be considered as new technology fall into two categories. They are: junction joining techniques and panel structures. These are described in the succeeding paragraphs.

#### 3.1 Junction Joining Techniques

A method for constructing  $\text{Bi}_2\text{Te}_3$  based thermoelectric generator alloys into useful thermoelectric structures which will operate at  $300^\circ\text{C}$  has been developed.<sup>3</sup> This technique involves the use of an electrolytic nickel plating onto the contact ends of the thermoelectric elements and the soldering of the plated elements to the aluminum absorber plates with lead (100%) solder.

Thermoelectric flat plate generator devices constructed in the manner stated above have been operated and tested at  $300^\circ\text{C}$ . These devices, if reliability and long life can be achieved in this operating temperature range, constitute an improvement in the state of the art of low temperature thermoelectric generators. They would be suitable for all applications now contemplated for  $\text{Bi}_2\text{Te}_3$  alloy generators.

#### 3.2 Panel Structures

A method has been developed for producing a lightweight panel structure, which serves as electrical interconnections for the thermoelectric elements, as absorbers of radiant heat energy, as radiators of waste heat energy, and as mechanically rigid structures. The structural material of the panel is aluminum. It was chosen because of its light weight, its high electrical and thermal conductivity, and its structural strength.

The design features which make it useful are ridging and perpendicular angling of the edges to produce a rigid structure from what essentially is

a foil material. The material is annealed to a soft state to allow stresses to be absorbed throughout the material. Flexible circular dimples are placed around rigid joints to allow flexure of the rigid joint, thereby reducing the amount of stress applied to the rigid joint.

These design features would seem to be useful for use in all solar thermoelectric flat plate structures. The unit thermoelectric couple structure shown in figure 21 should enable the manufacture of units which can be fabricated into panels of several square feet.

4. BIBLIOGRAPHY

1. "Solar Thermoelectric Generators for Application Outside the Earth's Atmosphere." ASTIA Report No. AD-269180 (1960).
2. Satterthwaite, C.B. and R.W. Ure, Jr., Physical Review, 108, p. 1164 (1957).
3. "Development of a Flat Plate Solar Thermoelectric Energy Conversion Panel." First Quarterly Report, Contract No. NAS5-3400, National Aeronautics and Space Administration (1963).
4. Mullin, P.A., and N. Fuschillo, "Radiative Heat Transfer Tables," Technical Note, TP3-277/7/63/50, Melpar, Inc., Falls Church, Va.
5. "Hot Probe Measurements of Semiconductor Thermoelectric Power." Electronics, 8 December, 1961.
6. Hansen, M., "Constitution of Binary Alloys.", McGraw-Hill (1958).
7. Brenner, A., "Electroless Plating Comes of Age.", Metal Finishing, p. 68, November 1954.
8. American Institute of Physics Handbook, 2nd Edition, p. 6 - 158 (1963)
9. Mengali, O.J., and M.R. Seiler, "Contact Resistance Studies on Thermoelectric Materials.", Reprint, Battelle Memorial Institute, Columbus, Ohio.

APPENDIX I

DETAILED FABRICATION PROCESSES  
FOR  
THE CONSTRUCTION OF EXPERIMENTAL FLAT PLATE  
SOLAR THERMOELECTRIC ENERGY CONVERSION PANELS

## APPENDIX I

### DETAILED FABRICATION PROCESSES FOR THE CONSTRUCTION OF EXPERIMENTAL FLAT PLATE SOLAR THERMOELECTRIC ENERGY CONVERSION PANELS

The following is a detailed process report on the fabrication of experimental flat plate thermoelectric generator panels. A list of materials, direct and indirect plus a list of equipment used in the process precede the process. These are given in tables 6, 7, and 8, respectively. The process flow chart is shown in figure 38.

This process deals with the specific methods used to fabricate panel types II or III, because the construction used in types II and III is believed to be superior to that used in panel type I. The main difference in the process between these types is the form and interconnection methods for the radiator sides. In type I, whole, square radiator plates are used (see figure 24) and are completely bonded together with epoxy adhesive. All the thermoelectric element-absorber plate subassemblies are then soldered simultaneously to the type I radiator subassembly.

This is contrasted to the type II - III panel construction where half radiator plate subassemblies are used (see figure 25) and the couples are constructed individually. They are subsequently joined together to form panels by using epoxy adhesive and making the appropriate electrical interconnections. Figure 39 shows the individual absorber and radiator plate used in type I construction. Figure 40 shows the same for type II - III construction.



TABLE 6

LIST OF DIRECT MATERIALS

1.  $\text{Bi}_2\text{Te}_3$  Alloy Power Generation Material, n-type
2.  $\text{Bi}_2\text{Te}_3$  Alloy Power Generation Material, p-type
3. Aluminum Absorber Plates, Alloy 1100
4. Aluminum Radiator Plates, Alloy 1100
5. Lead Solder, pure (99.9% or better)
6. Tin - Lead Solder (63%-37%)
7. Indalloy No. 5 Solder, Indium Corp. of America
8. Lead - Silver Solder (97.5%-2.5%)
9. Liquid Bright-Gold, Type 8342, Engelhard Industries, Newark, N.J.
10. Thermocouples, 40 gauge, Chromel-Alumel (Instrumented Models)
11. Mica, 0.040" x 0.040" x 0.0005", (Instrumented Models)
12. Silicone Adhesive, (Instrumented Models), Type S-32, General Electric Co.
13. Epoxy Adhesive, Type A-1 (with Activator A), Armstrong Products Co., Warsaw, Ind.
14. Silicone Rubber Adhesive, Type A-4000, with Activator, Dow-Corning
15. Silicone Rubber, for support structure isolation
16. Mylar Film, 0.002 inch thick
17. Stainless Steel Tubing, type 304S, 0.050 inch dia. - 0.009 inch wall thick
18. Stainless Steel Sheet, type 304, 0.010 inch thick

TABLE 7

LIST OF INDIRECT MATERIALS

1. Glycol Pthylate Adhesive
2. Airbrasive Abrasive, No. 1, S.S.White Manufacturing Co., New York, N.Y.
3. Kodak Metal-Etch Resist
4. Kodak Metal-Etch Resist Thinner
5. Kodak Metal-Etch Resist Developer
6. Flux, Divco No. 229, Division Lead Co., Summit, Ill.
7. Nickel Plating Solution, Hoover and Strong, Inc., Buffalo, N.Y.
8. Electroless Nickel Plating Solution<sup>7</sup>
9. Tile Mounting Blocks, Merrill Engineering Co., Fanwood, N.J.
10. Cotton Swabs
11. Lint-Free Paper
12. Mylar Film, 0.0005 inch thick
13. Silicone Rubber Adhesive Metal Primer, Type SS4004, Dow-Corning
14. Trichloroethylene, C.P.
15. Acetone, C.P.
16. Methanol, C.P.
17. Deionized Water
18. Hydrofluoric Acid, Reagent
19. Ammonium Hydroxide, Reagent
20. Sodium Hydroxide, Reagent
21. Forming Gas (10% H<sub>2</sub> - 90% N<sub>2</sub>)
22. Nitrogen, Pure
23. Natural Gas
24. Silicon Carbide Abrasive Paper, 600 Grit

TABLE 8

LIST OF EQUIPMENT

1. Semiconductor Wafering Machine, WMA-2 MicroMech Manufacturing Co., Union, N.J.
2. Diamond Slicing Wheel, 5-1/2 inch dia., 0.020 inch thick
3. Diamond Slicing Wheel, 3-1/2 inch dia., 0.010 inch thick
4. Hot Plate, 700 watts, Type 1900, Thermolyne Corp., Dubuque, Iowa
5. Micrometer, 1 inch calibrated in tenths of thousandths
6. Tweezers, fine point, type 3C
7. Self-closing Tweezers, Cornet, Cover Glass
8. Holder for Airbrasive Blasting, for Thermoelectric Elements
9. Artist Brush, Size 00000, M. Grumbacher, New York, N.Y.
10. Microscope, Stereoscopic, Type 0.7X-3X, Bausch and Lomb
11. DC Power Supply, Model H, Electro Products Laboratories, Chicago, Ill.
12. Airbrasive Unit, Model C, S.S.White Manufacturing Co., New York, N.Y.
13. Soldering Iron, 47-1/2 watts, with Nickel Clad Tip, Electron Industries, Hawthorne, Calif.
14. Flux Applicator, Glass Rod, 0.040 inch dia. x 3 inches long
15. Soldering Jig, Elements to Absorber Plates, (see figure 22).
16. Oven, Controlled Temperature, Model OV-185A, Blue-M Electric Co., Blue Island, Ill.
17. AC Power Supply, 0 - 6V, 3A
18. AC Voltmeter, Model 400H, Hewlett-Packard Co.
19. AC Ammeter, 0 - 3A
20. AC Resistance Test Fixture, (see figure 48).
21. Soldering Jig, Element-absorber Plate Subassembly to Radiator Plate Subassembly, (see figure 23).

TABLE 8 (Continued)

22. Assembly Jig, Final Panel Assembly, (see figure 27).
23. Blow Pipe Torch, No. 3-A, National Welding Equipment Co., Richmond, Calif.
24. Absorber Plate Forming Die, (see figure 50).
25. Hydraulic Press, Model B, Fred S. Carver, Inc., Summit, N.J.
26. Vapor Degreaser, Lab Model
27. Electroless Nickel Plating Apparatus, (see figure 52).
28. Annealing Furnace, Controlled Atmosphere, 5000 watts
29. Radiator Plate Forming Dies, (see figure 50).
30. Assembly Jig, Radiator Plate Subassembly, (see figure 55).
31. Soldering Jig, Support Structure Subassembly, (formed to hold pieces while soldering).
32. Propane Torch
33. Surface Temperature Thermometer, Model 573C, Pacific Transducer Corp., Los Angeles, Calif.

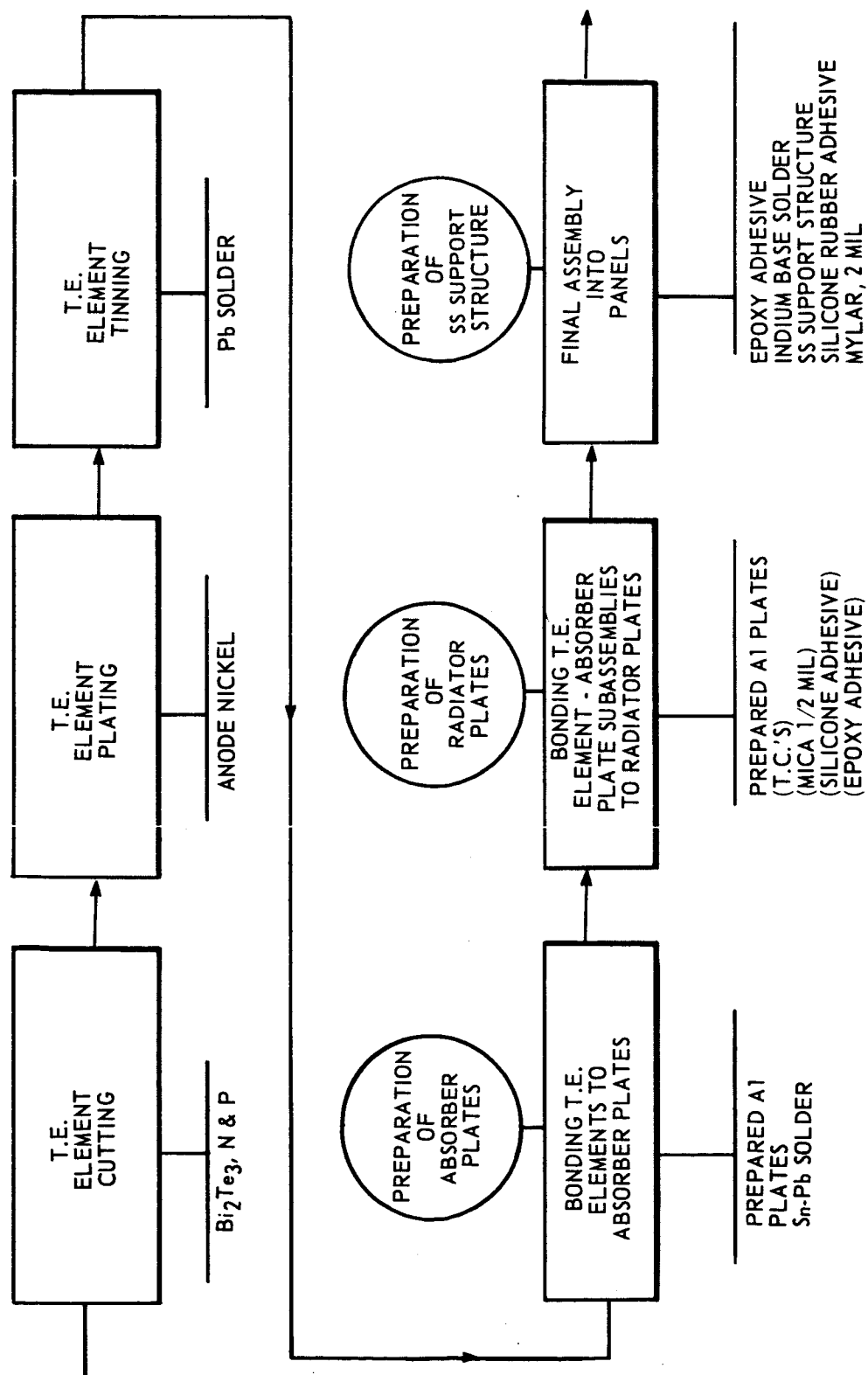


Figure 38. Flow Chart of Flat Plate Panel Fabrication Process

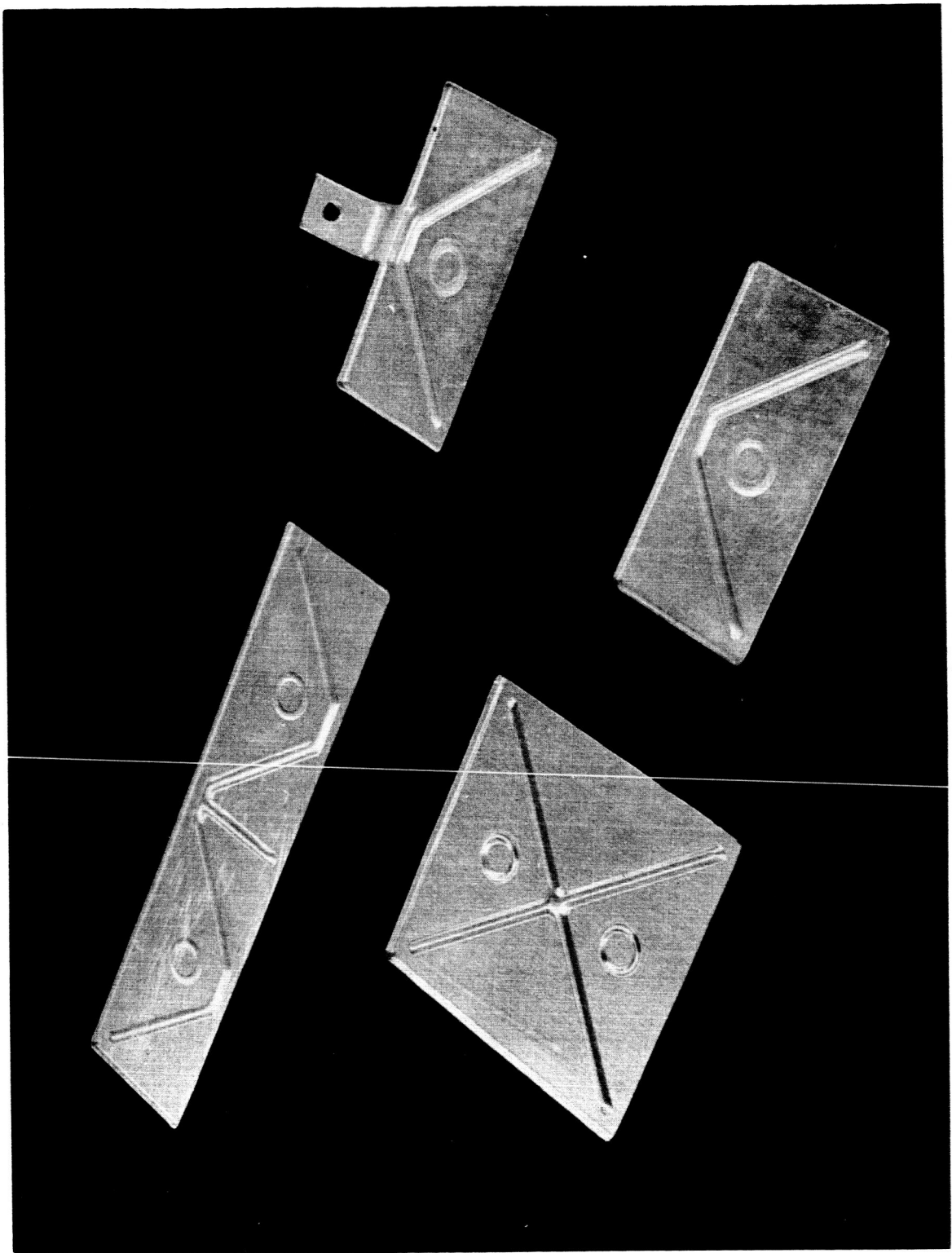


Figure 39. Absorber and Radiator Plate Forms Used with Type I Panels

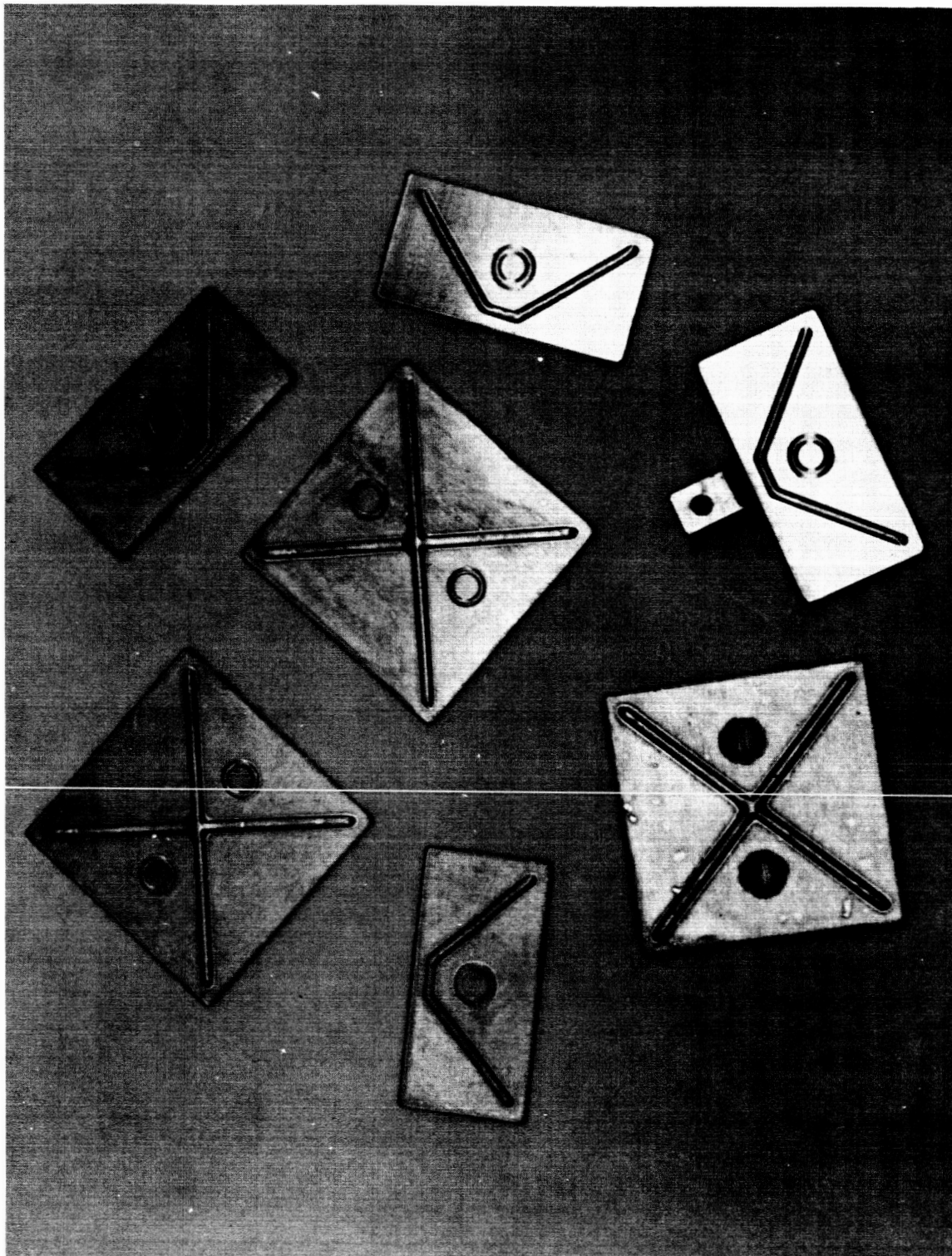


Figure 40. Absorber and Radiator Plate Forms Used With Type II-III Panels

The remainder of the processes are used for both panel type I and type II-III, however the operational sequence is different.

The process follows the flow of the thermoelectric material and is divided into six major processing steps. See figure 38. In addition there are four major subassembly steps, which describe the processing of accessory subassemblies. These are located at the end of the main process report.



## 1. THERMOELECTRIC ELEMENT CUTTING

### 1.1 Equipment

- a. Semiconductor Wafering Machine, see figure 41.
- b. Diamond slicing wheel, 5-1/2 in. dia. x 0.020 in. thick
- c. Diamond slicing wheel, 3-1/2 in. dia. x 0.010 in. thick
- d. Hot Plate
- e. Micrometer, 0 to 1 inch

### 1.2 Materials

#### 1.2.1 Direct

- a.  $\text{Bi}_2\text{Te}_3$  alloy ingots, N-type, 12 mm. dia.
- b.  $\text{Bi}_2\text{Te}_3$  alloy ingots, P-type, 12 mm. dia.

#### 1.2.2 Indirect

- a. Glycol Pthylate Adhesive
- b. Tile Mounting Blocks
- c. Acetone, C.P.
- d. Methanol, C.P.

### 1.3 Procedure

a. The  $\text{Bi}_2\text{Te}_3$  alloy thermoelectric material ingots (12 mm. diameter) are mounted to tile mounting blocks using glycol pthylate adhesive. The block is placed on a hot plate heated to  $80^\circ\text{C}$  and the adhesive, which is thermoplastic, is applied. The ingots are placed in the melted adhesive, the block is removed from the hot plate and allowed to cool.

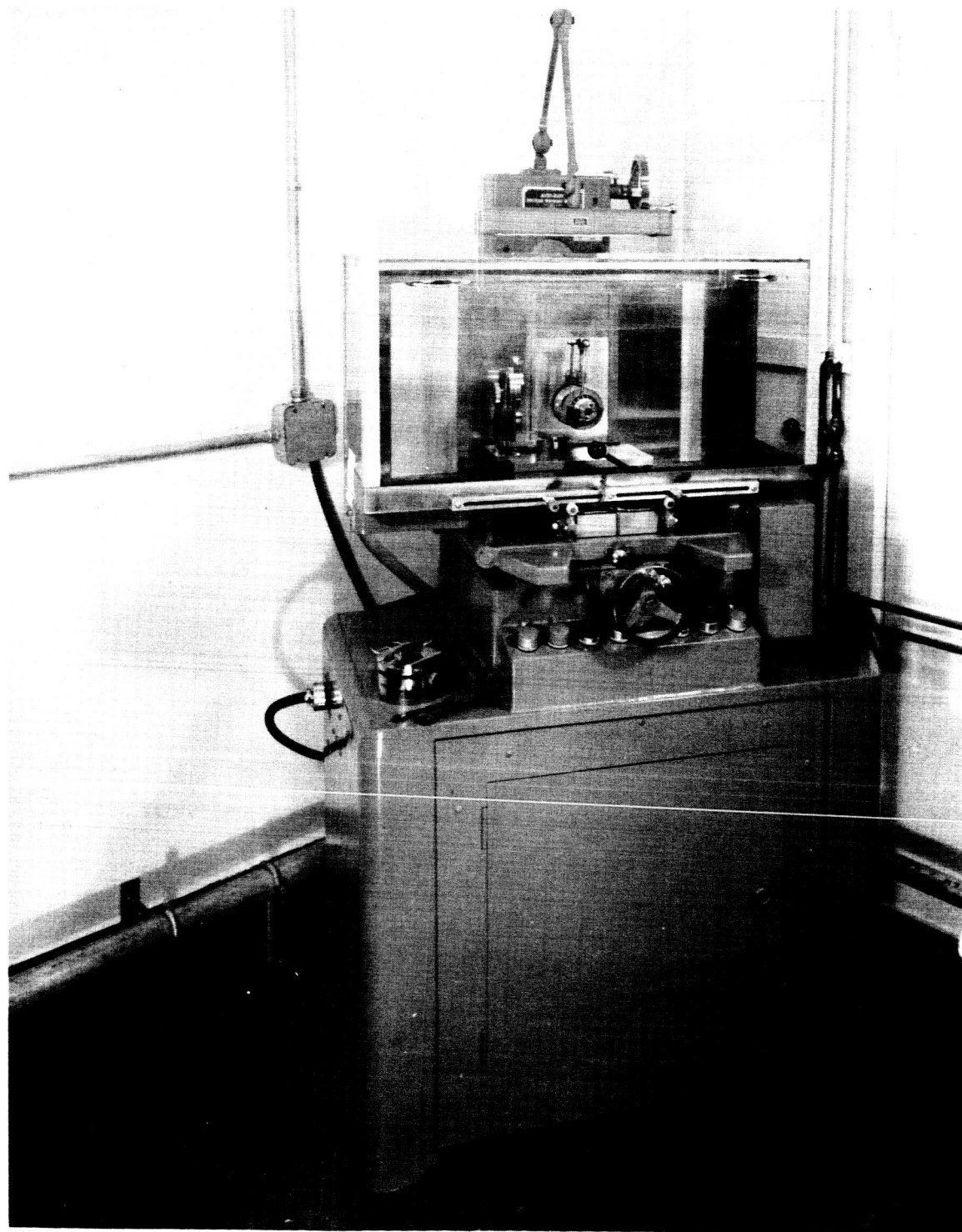


Figure 41. Semiconductor Wafering Machine

b. The mounting block containing the thermoelectric material ingots is mounted in the semiconductor wafering machine. Pellets are cut from the ingots to a length of 0.118 in.,  $\pm 0.0005$  in. with a 5-1/2 in. diameter, 0.020 in. thick diamond slicing wheel. The mounting block is removed from the wafering machine.

c. The cut pellets are removed by heating again on the hot plate. The pellets are then laid down flat on the tile mounting block in the adhesive. The block is removed from the hot plate and allowed to cool.

d. The mounting block containing the pellets is placed back in the semiconductor wafering machine and, using a 3-1/2 in. diameter, 0.010 in. thick diamond slicing wheel, diced into 0.076 in,  $\pm 0.001$  in., sections. This produces elements 0.076 in. x 0.076 in. x 0.118 in. (0.194 cm. x 0.194 cm. x 0.3 cm.). The mounting block is removed from the wafering machine.

e. The diced elements are removed by heating again on the hot plate. The adhesive is removed by immersion in hot acetone and three subsequent rinses in cold acetone. The elements are rinsed in methanol and dried.

f. Using micrometers, the dimensions of the elements are checked and those falling outside the tolerance limits are rejected.

Figure 42 shows the thermoelectric material ingots, the pellets that are cut from them, and the elements which are cut from the pellets.

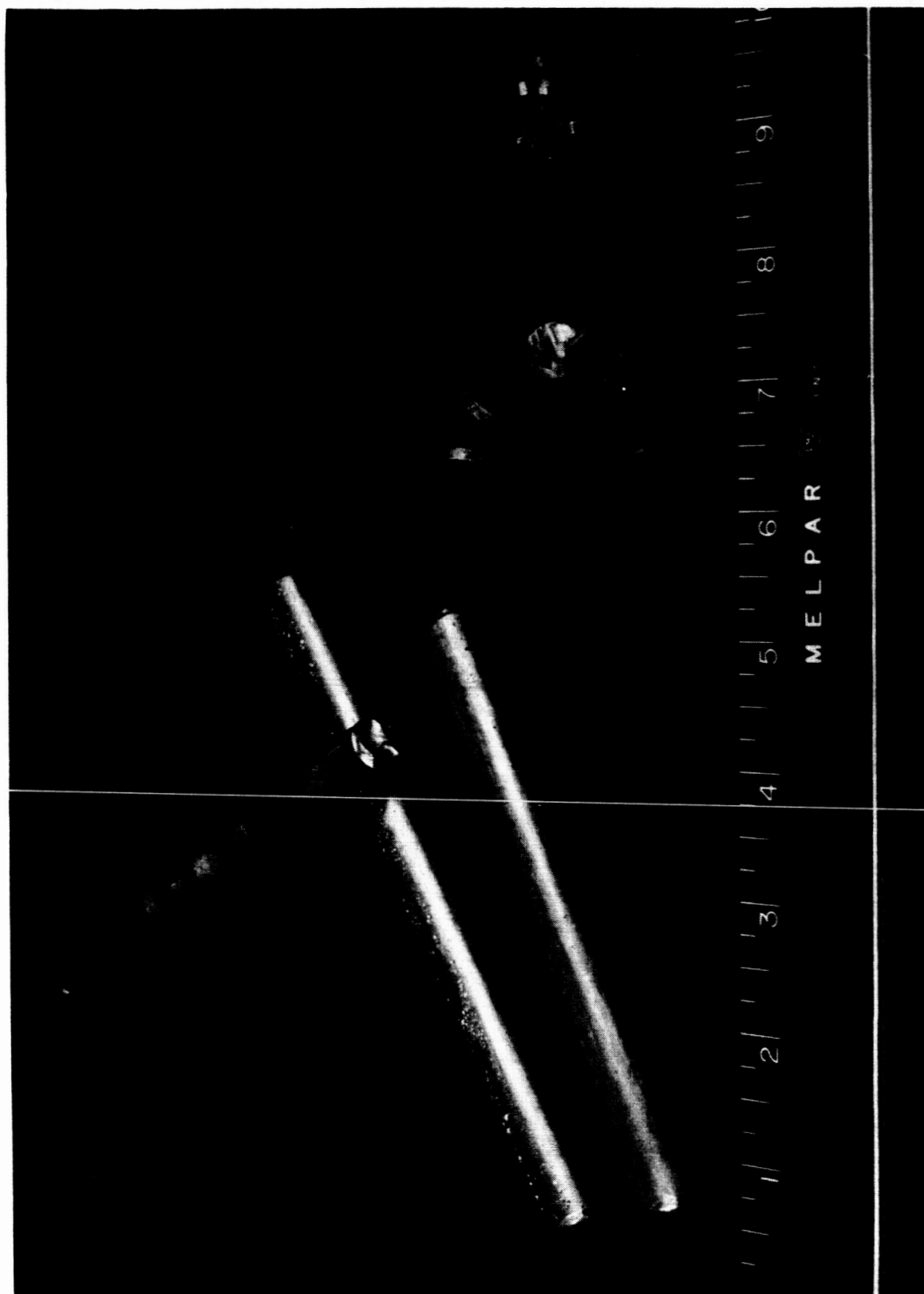


Figure 42. Thermoelectric Materials: Ingots, Pellets, and Elements

## 2. THERMOELECTRIC ELEMENT NICKEL PLATING

### 2.1 Equipment

- a. Tweezers
- b. Self-closing tweezers
- c. Holder for Airbrasive Blasting
- d. Artists Brush
- e. Microscope, Stereoscopic
- f. DC Power Supply
- g. Multiple Station Nickel Plating Apparatus, see figure 43.
- h. Airbrasive Unit, see figure 44.

### 2.2 Materials

#### 2.2.1 Direct

- a.  $\text{Bi}_2\text{Te}_3$  Alloy Elements, n-type
- b.  $\text{Bi}_2\text{Te}_3$  Alloy Elements, p-type
- c. Anode Nickel

#### 2.2.2 Indirect

- a. Metal-etch resist
- b. Metal-etch resist thinner
- c. Metal-etch resist developer
- d. Water, Deionized
- e. Methanol, C.P.
- f. Trichloroethylene, C.P.
- g. Hydrofluoric Acid, reagent
- h. Lint-free paper
- i. Silicon carbide abrasive paper, 600 grit

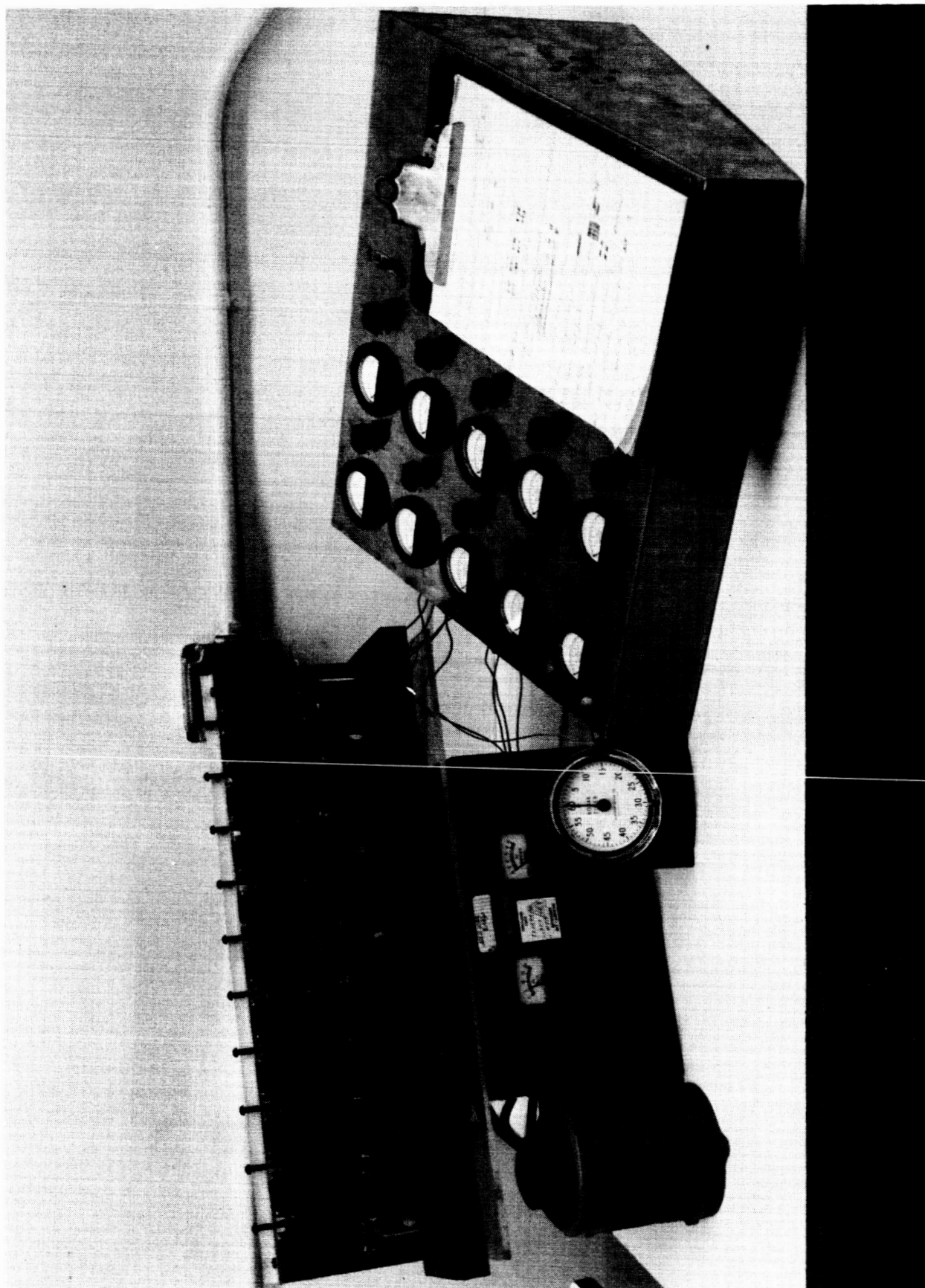


Figure 43. Multiple Station Nickel Plating Apparatus for Elements

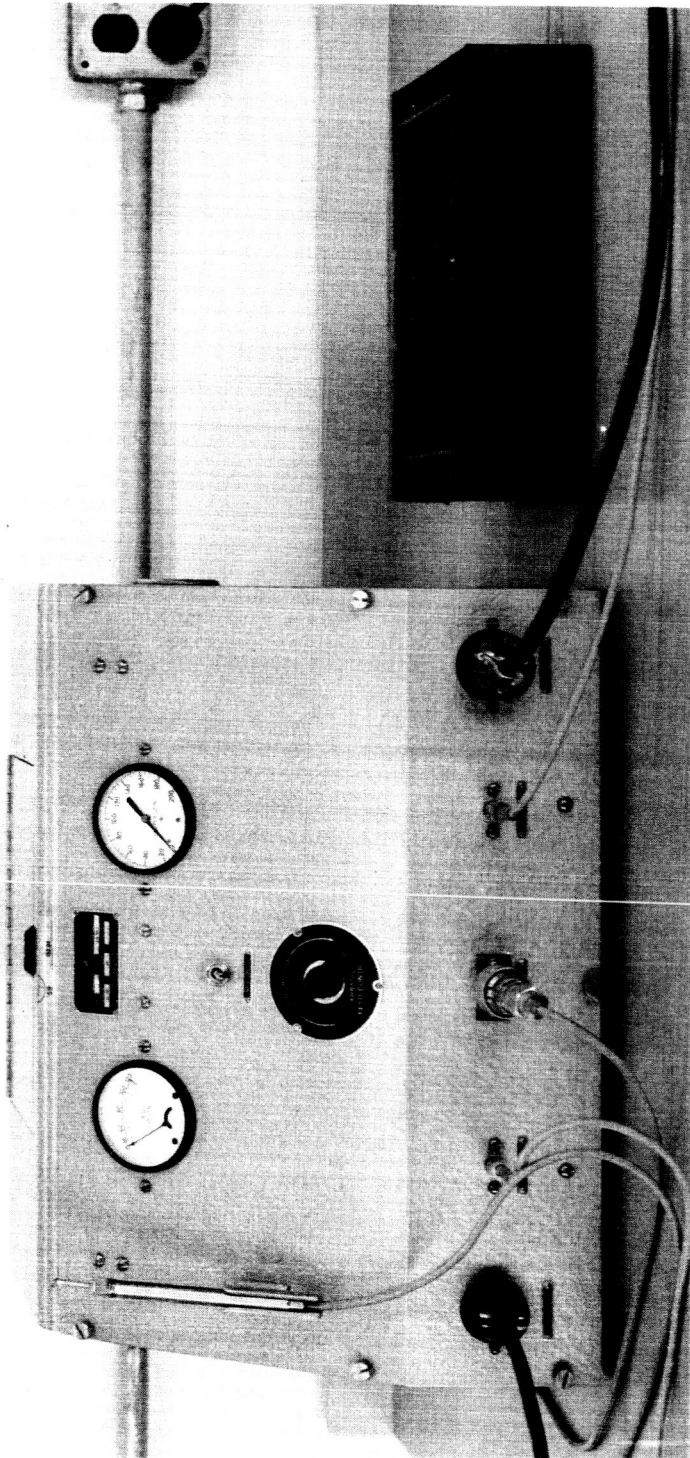


Figure 44. Airbrasive Unit

### 2.3 Procedure

a. The  $\text{Bi}_2\text{Te}_3$  alloy thermoelectric elements are examined under a stereoscopic microscope. Using tweezers to handle the elements they are checked for flaws such as cracks, pits or holes and loose slivers of material under the microscope. Stainless steel tweezers are used to handle the pellets in all operations until the pellets are placed in the nickel plated self-closing tweezers. Upon passing this visual inspection, the corners of the pellets are rounded slightly using a 600 grit silicon carbide abrasive paper with a light or soft stroke. The pellets are then centered in a three element hinged holder for roughing by blasting with an Airbrasive Unit. The ends and a short region (approximately 0.010 in.) along each side of the element adjoining the ends are blasted. (See figure 45.)

b. The pellets are now prepared for masking with metal-etch resist by etching in hydrofluoric acid for ten minutes. Deionized water is used to rinse the hydrofluoric acid from the elements. Methanol is used as a solvent after rinsing to remove the water and to help dry the elements.

c. The elements are then masked one side at a time by applying metal-etch resist (whose density is controlled by adding metal-etch resist thinner) with a small brush. The first three sides are masked to a maximum of 0.012 inch from end and a minimum of 0.007 inch from end while the elements are being held by 3C tweezers. Before the final side of the pellet is masked, the pellet is placed in a pair of modified self-closing tweezers. The fourth side of the element is then masked while sealing one of the tweezer points to the element for electrical contact.



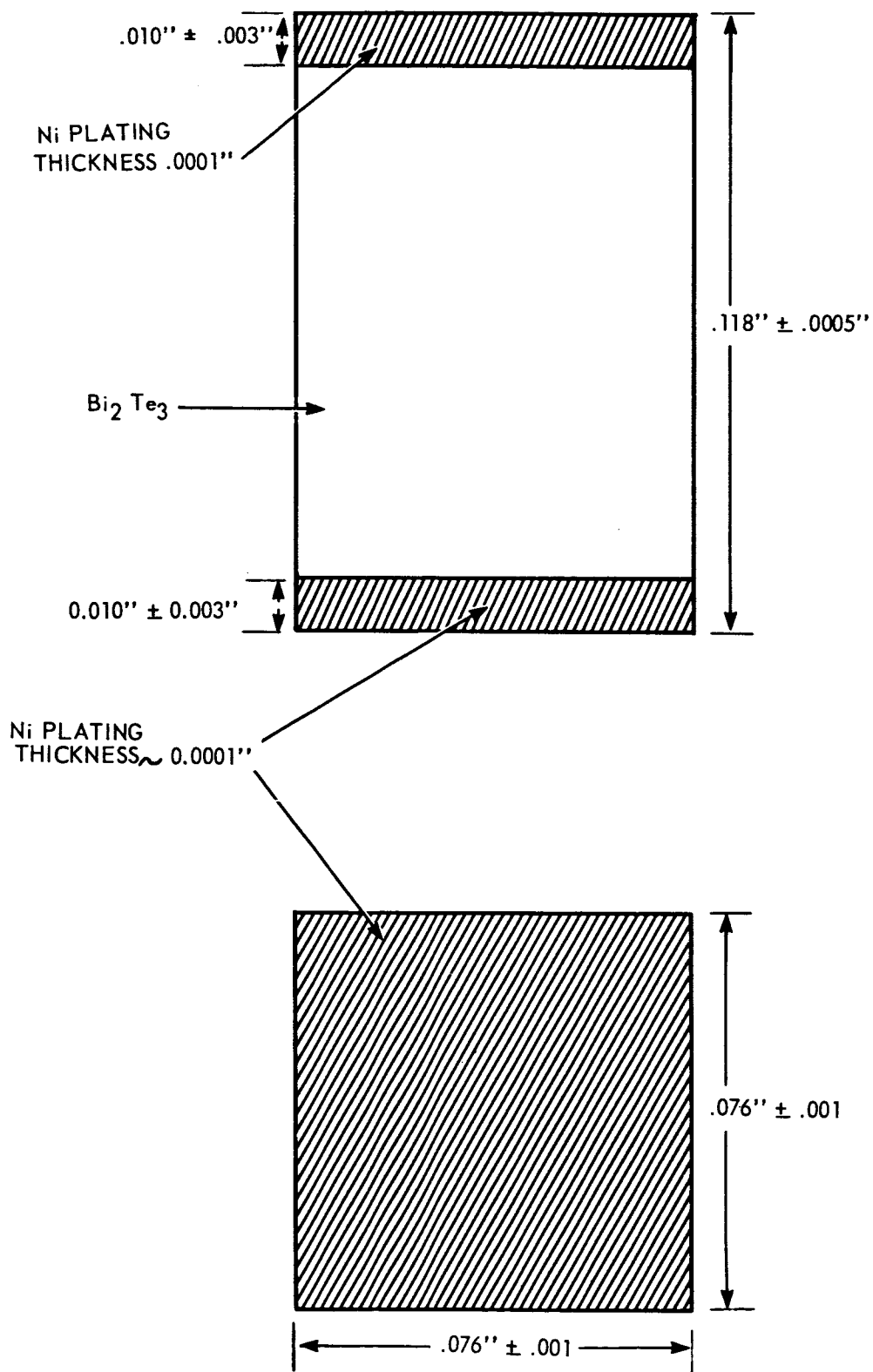


Figure 45. Drawing of Thermoelectric Element

d. When masking is complete and the metal-etch resist has dried, the holding tweezers are connected to the negative lead of the power supply. The element is lowered into the nickel plating solution and the power is applied to begin the electroplating process. For the first five minutes the current is maintained at 500 microamperes and for twenty more minutes the current is maintained at 600 microamperes.

e. Cleaning begins immediately upon removing the elements from the nickel plating solution. The elements are first rinsed several times in deionized water to remove the nickel plating solution. A methanol rinse follows.

The metal-etch resist is removed by two trichloroethylene rinses followed by ten minutes in metal-etch resist developer. It is usually necessary to wipe or mechanically abrade the element against lint-free paper to completely remove the resist. Then the pellets are allowed to dry.

f. The plated elements are inspected under a stereoscopic microscope in order to determine if they are adequately plated and to determine that no voids or cracks exist in the plating.

Figure 46 shows the thermoelectric elements in various stages of processing. From left to right are shown elements, (1) as cut, (2) blasted for plating, (3) nickel plated, and (4) tinned with lead solder.

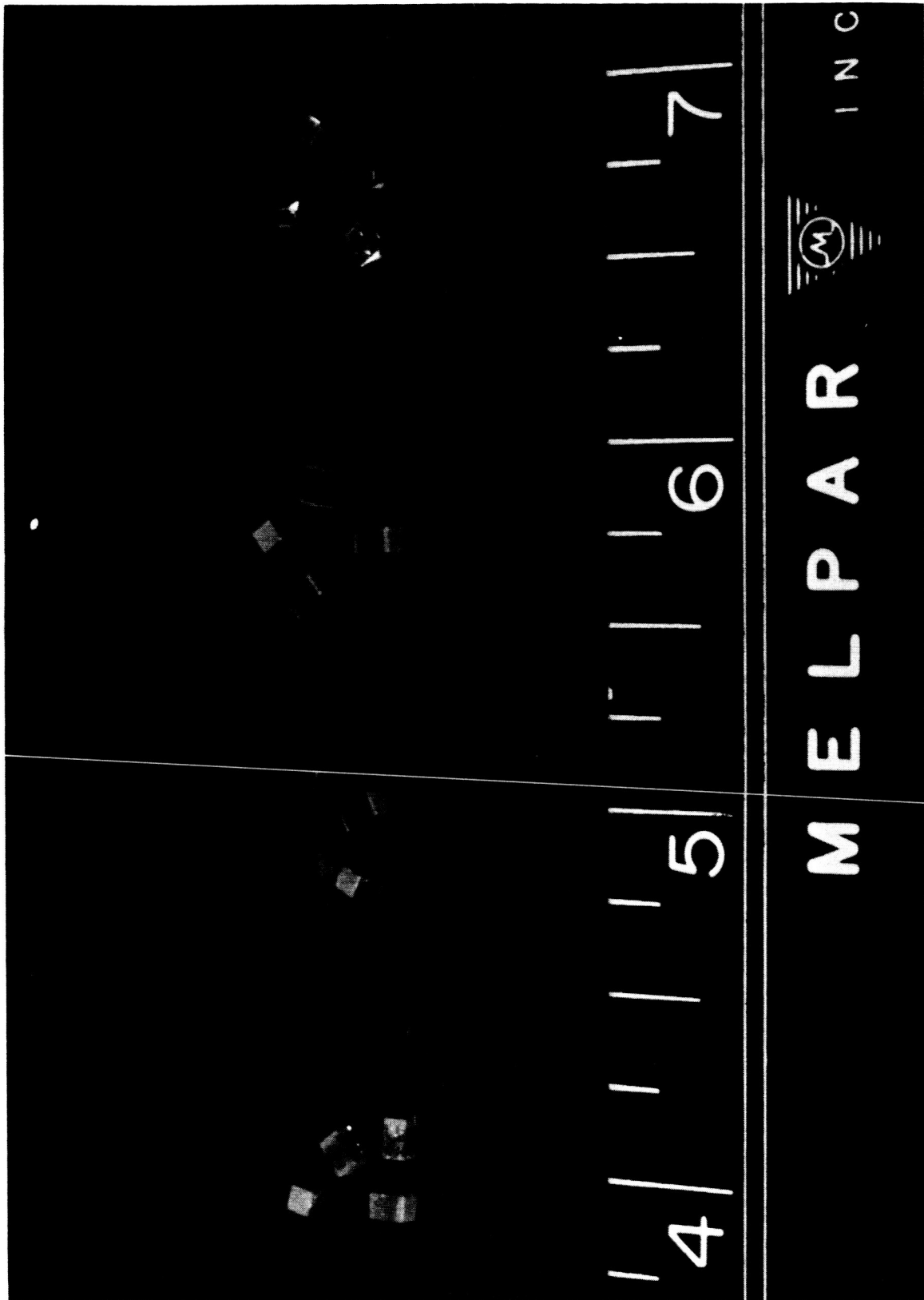


Figure 46. Thermoelectric Elements: Cut, Ends, Blasted, Plated, and Solder Contacted

### 3. THERMOELECTRIC ELEMENT TINNING

#### 3.1 Equipment

- a. Soldering Iron, with nickel tip,
- b. Microscope, Stereoscopic
- c. Tweezers
- d. Flux Applicator, glass rod, 0.040 inch dia. x 3 inch long

#### 3.2 Materials

##### 3.2.1 Direct

- a. Thermoelectric Elements, plated, n-type
- b. Thermoelectric Elements, plated, p-type
- c. Lead Solder, pure (99.9% or better)

##### 3.2.2 Indirect

- a. Flux, Divco No. 229
- b. Lint-free paper
- c. Cotton Swabs
- d. Methanol, C.P.

#### 3.3 Procedures

a. The element is inspected under a stereoscopic microscope and the more perfect end (material appearance and plating) is chosen for the hot junction.

b. The element is tinned with lead solder in the following manner. Lead is applied to the heated nickel tip of the soldering iron. Flux is applied to the plated end areas on the element using the glass rod applicator. The element is dipped into the melted solder using tweezers and removed so that a 0.005 inch high dome of solder is left on the element.

c. The element is immediately cleaned with methanol using a cotton swab and dried. The heavy oxide film on the lead solder surface is removed by wiping on lint-free paper.

#### 4. BONDING THERMOELECTRIC ELEMENTS TO ABSORBER PLATES

##### 4.1 Equipment

- a. Hot Plate
- b. Soldering Jig, see figure 22.
- c. Oven, Controlled Temperature
- d. Microscope, Stereoscopic
- e. AC Power supply
- f. AC Voltmeter, Model 400H
- g. AC Ammeter, 0-3A
- h. AC Resistance Testing Fixture, see figure 47.
- i. Micrometer, 0-1 inch
- j. Tweezers, 3C
- k. Surface Temperature Thermometer, 0-540°C

##### 4.2 Materials

###### 4.2.1 Direct

- a. Thermoelectric Elements, plated and tinned (one end), n-type
- b. Thermoelectric Elements, plated and tinned (one end), p-type
- c. Prepared aluminum absorber plates (see Subassembly step 1)
- d. Solder, 63% tin - 37% lead

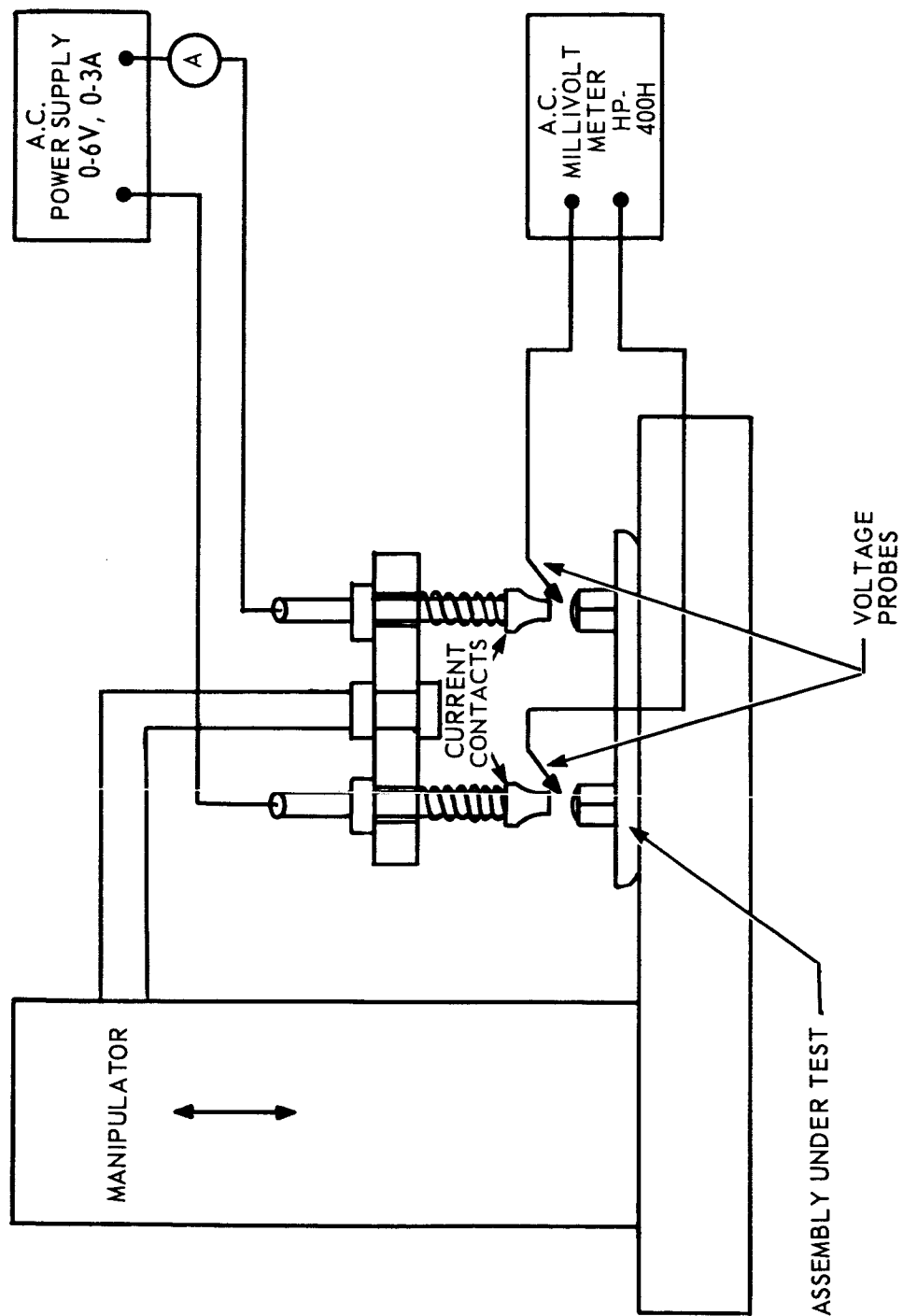


Figure 47. AC Resistance Test Fixture

#### 4.2.2 Indirect

- a. Flux, Divco No. 229
- b. Cotton swabs
- c. Methanol, C.P.
- d. Water, deionized

#### 4.3 Procedure

a. A prepared aluminum absorber plate is placed in the soldering jig. The jig is placed on the hot plate which is at a surface temperature of  $340^{\circ}\text{C}$  as measured by the surface temperature thermometer. The thermoelectric elements, one n- and p-type are placed in the element holder using tweezers and the flux is applied to the soldered end of the elements.

b. When the lead wetted areas on the absorber plate become molten, the element holder containing the elements is placed into position on the jig. As soon as the solder on the elements flows out well, the weight is added to the elements, forcing them down to within 0.001 inch to 0.002 inch from the plate. The jig is then immediately removed from the hot plate and allowed to cool.

c. After cooling, the absorber plate-element subassembly is removed from the jig and cleaned at once in deionized water and methanol. The unit is further cleaned with a cotton swab and methanol and dried.

d. At this point the absorber-plate subassemblies are placed in a controlled temperature oven for 16 to 24 hours at  $250^{\circ}\text{C}$  to eliminate any failures due to material mechanical deficiencies.

e. The absorber plate subassemblies are now tested to determine the ac resistance of the subassemblies. The free ends of the elements are next wetted with tin-lead solder and placed into the ac resistance test fixture. An ac current of one ampere is passed through a subassembly and the voltage drop is measured using a sensitive ac vacuum tube voltmeter. This test is to show up excessive contact resistance and is useful since the resistivity ranges of the materials are known. High resistance units are rejected.

## 5. BONDING ABSORBER PLATE-THERMOELECTRIC ELEMENT SUBASSEMBLY TO RADIATOR PLATES

### 5.1 Equipment

- a. Hot Plate
- b. Soldering Jig, see figure 23.
- c. AC Power Supply
- d. AC Ammeter, 0 to 3A
- e. AC Voltmeter, Model 400H
- f. AC Resistance Test Fixture, see figure 47.
- g. Tweezers
- h. Flux applicator
- i. Surface Temperature Thermometers, 0-540°C

### 5.2 Materials

#### 5.2.1 Direct

- a. Absorber Plate-Thermoelectric Element Subassemblies, see figure 48.
- b. Prepared Aluminum Radiator Plate Subassemblies (see Subassembly step 2)



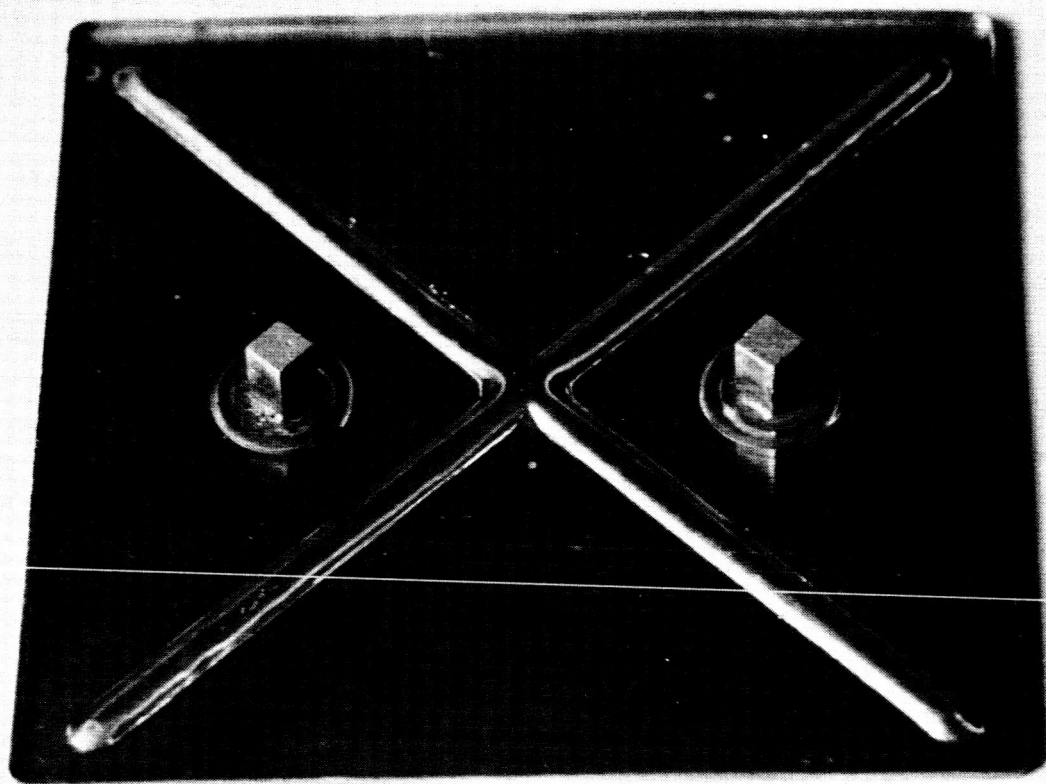


Figure 48. Thermoelectric Element, Absorber Plate Subassembly

### 5.2.2 Indirect

- a. Flux, Divco No. 229
- b. Water, deionized
- c. Methanol, C.P.

### 5.3 Procedure

a. A prepared aluminum radiator plate subassembly is placed in the bottom half of the soldering jig and flux applied to the areas of the plates where the elements are to make contact. The absorber plate thermoelectric element subassembly is placed in the top half of the soldering jig. The two parts of the jig are joined together bringing the two subassemblies into proper position with one another. The jig is placed on a hot plate at a temperature of  $200^{\circ}\text{C}$  as measured by the surface temperature thermometer. When the tin-lead solder at the radiator contacts flows, the weight is placed on the jig bringing the elements to within 0.001 inch to 0.002 inch of the radiator plates. The jig is immediately removed from the hot plate and allowed to cool.

b. After cooling, the resulting unit couple subassemblies are removed from the jig and cleaned in deionized water and then in methanol. They are removed from the methanol and allowed to dry.

c. The ac resistance of the single couple subassemblies is measured in the same way as described in step 4. High resistance units are rejected.

## 6.1 FINAL ASSEMBLY INTO PANELS

### 6.1 Equipment

- a. Assembly Jig, see figure 27.
- b. Oven, Controlled Temperature
- c. Blow Pipe Torch
- d. Tweezers
- e. AC Power Supply
- f. AC Ammeter, 0 to 3A
- g. AC Voltmeter, Model 400H

### 6.2 Materials

#### 6.2.1 Direct

- a. Epoxy Adhesive, Type A-1, with Activator A
- b. Solder, Indalloy No. 5
- c. Support Structure Subassembly, (see subassembly step 3)
- d. Silicone Rubber Adhesive
- e. Mylar Film, 0.002 inch thick

#### 6.2.2 Indirect

- a. Water, deionized
- b. Methanol, C.P.
- c. Natural Gas
- d. Silicon Rubber Adhesive Metal Primer

### 6.3 Procedure

- a. A flat aluminum plate is used as a base to hold the assembly jig. A 1/8 inch thick rubber mat is placed on top of the flat aluminum plate and the assembly jig is placed on this rubber mat. Brass pins (part of the

assembly jig) are placed into the drilled holes of the bottom of the jig (the holes are located at the position of each element). The single couple sub-assemblies are placed in the jig absorber side down using tweezers. They are oriented so that the resulting configuration will be connected electrically in series. The couples containing the thermocouples are placed in the center portion of the panel (where applicable). Two special output lead single couple subassemblies are placed at either end of the series connected configuration will be connected electrically in series.

b. Epoxy adhesive placed in the appropriate locations between the rows of single couple subassemblies using small 0.002 inch thick Mylar spacers. This is done in such a manner that the radiator plate will be mechanically one piece after curing of the adhesive. The separations where electrical connections are to be made between radiator plates are not filled with adhesive. Weights are placed on the assembly.

c. The assembly jig is placed in a controlled temperature oven and cured at 100°C for 2 hours. After curing the jig is removed from the oven and allowed to cool.

d. The weights are removed and the necessary electrical interconnections are made by soldering with Indalloy No.5 using a natural gas fired miniature blow-pipe torch. The panel regions to be soldered are pre-fluxed.

e. After making the necessary series electrical interconnections at the radiator side, the resulting panel is cleaned in deionized water and in methanol and then dried.

f. An ad resistance test is made in a manner similar to that previously described.

g. Preparatory to applying the support structure subassembly, the areas to be bonded to the support structure are treated with Silicone Rubber Adhesive Metal Primer. This is allowed to air dry for two to three hours.

h. Using silicone rubber adhesive, the support structure subassembly is bonded to the panel. This adhesive is cured under an infrared heat lamp for four hours at approximately 80°C. This completes the fabrication process for the flat plate panels.

## SUBASSEMBLY STEP I - PREPARATION OF ALUMINUM ABSORBER PLATES

### I-1 Equipment

- a. Absorber Plate Forming Die, see figure 49.
- b. Hydraulic Press, see figure 50.
- c. Hot Plate
- d. Vapor Degreaser
- e. Electroless nickel plating apparatus, see figure 51.
- f. Artists Brush
- g. Oven, controlled temperature
- h. Annealing furnace, controlled temperature and atmosphere
- i. Tweezers
- j. Flux applicator
- k. Surface Temperature Thermometer

### I-2 Materials

#### I-2.1 Direct

- a. Aluminum, alloy 1100, 0.004 inch thick foil
- b. Electroless Nickel
- c. Liquid Bright-Gold
- d. Solder, Lead (99.9% or better)

#### I-2.2 Indirect

- a. Methanol, C.P.
- b. Water, Deionized
- c. Trichloroethylene, C.P.
- d.  $\text{NH}_4\text{OH}$ , Reagent

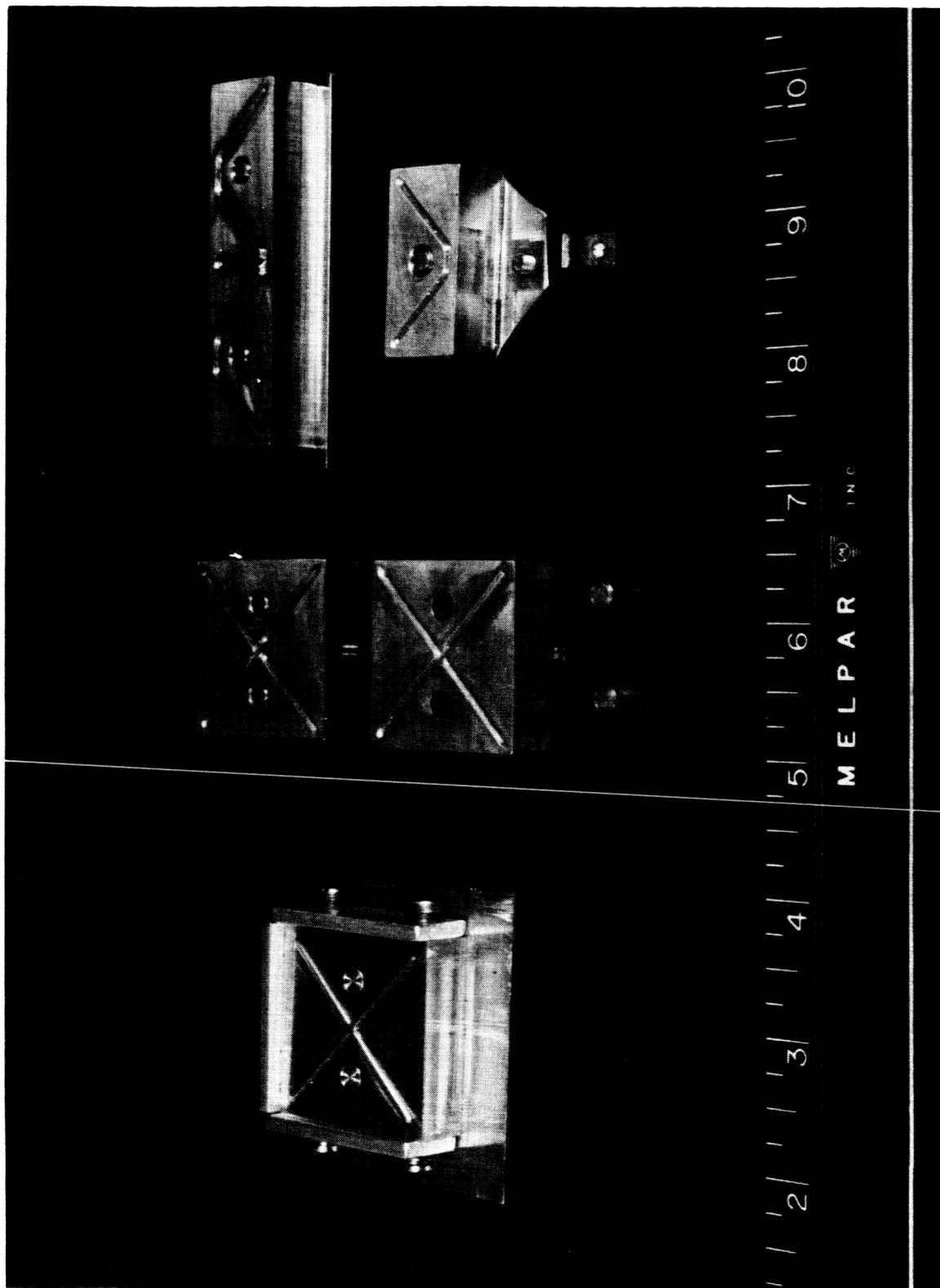


Figure 49. Absorber and Radiator Plate Forming Dies

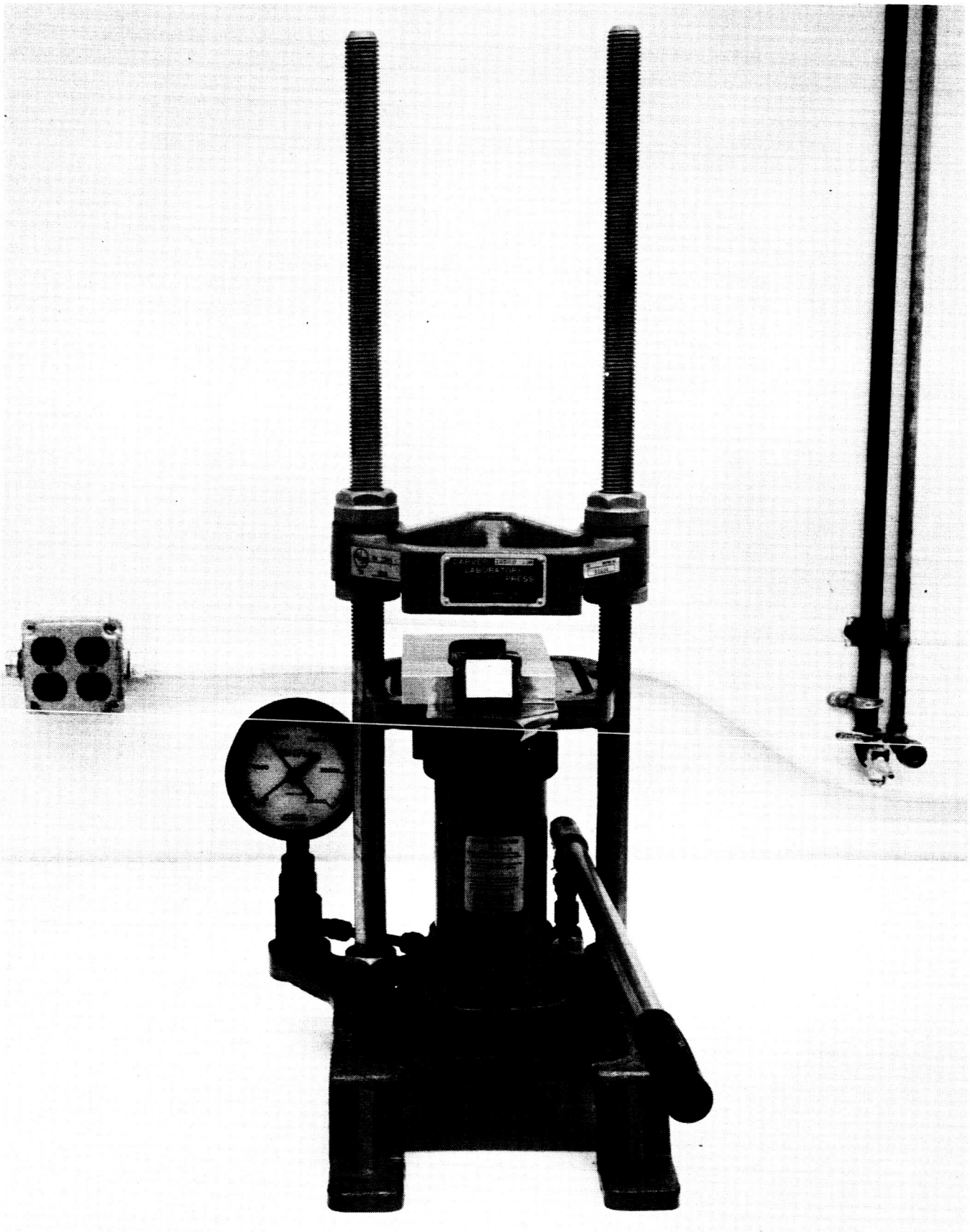


Figure 50. Hydraulic Press Used for Forming Absorber and Radiator Plates



I-35

- e. NaOH, Reagent
- f. Forming Gas (10%  $H_2$  - 90%  $N_2$ )
- g. Flux, Divco No. 229

### I-3 Procedure

a. The alloy 1100 aluminum in the form of 0.004 inch thick foil is cut into squares and formed into the shape of the absorber plates using a forming die in the hydraulic press. The formed part is removed from the die and cleaned in trichloroethylene, rinsed with methanol and dried.

b. After forming, the absorber plates are annealed in a forming gas atmosphere at  $580^{\circ}C$  for 30 minutes in the annealing furnace and then cooled slowly to room temperature. The plates must be carefully handled with tweezers throughout these operations.

c. The next operation is the cleaning prior to electroless nickel plating of the plates. The absorber plates are first degreased in a vapor degreaser containing trichloroethylene. After the degreasing they are rinsed in methanol and immersed in a cleaning etch composed of 100 grams of NaOH in 150 milliliters of concentrated  $NH_4OH$  for 10 seconds. This is followed by three rinses in concentrated  $NH_4OH$ .

d. Following the last rinse in concentrated  $NH_4OH$  the plates are transferred immediately to the electroless nickel plating bath. This should be accomplished quickly enough that the immersion in the bath takes place while a film of  $NH_4OH$  is completely covering the aluminum plates. This is to prevent oxidation of the aluminum surface due to exposure to the air. The  $NH_4OH$  film is compatible with the bath since it is one of the constituents of the bath.

The composition of the bath is as follows:

$\text{NiCl}_2 \cdot 6\text{H}_2\text{O}$	30 g/l
$\text{NaH}_2\text{PO}_2 \cdot \text{H}_2\text{O}$	10 g/l
$\text{NH}_4\text{Cl}$	50 g/l
$\text{Na}_3\text{C}_6\text{H}_5\text{O}_7 \cdot 2\text{H}_2\text{O}$	100 g/l
$\text{NH}_4\text{OH}$ to give pH = 9.0	

The plating conditions for electroless nickel plating of the aluminum plates are 7:

temperature of bath =  $90^\circ\text{C}$ ,

time = 2 minutes,

pH = 9.0

e. Upon completion of the electroless plating step, the plates are rinsed in deionized water, methanol and dried.

f. Next, the high-emissivity Liquid Bright-Gold coating is applied to the inner surface of the plates with a small artist's brush. It is flowed on and spread around on all areas of the inner surface, except where the thermoelectric elements are to be bonded. Only a small amount is necessary to achieve the desired coating.

g. The Liquid Bright Gold coating is cured and baked on at  $250^\circ\text{C}$  for 6 hours in the controlled temperature oven.

h. The final operation in the preparation of the absorber plates is the wetting of the element bonding areas with lead solder. This is accomplished on a hot plate set for a surface temperature of  $340^\circ\text{C}$ . as measured by the surface temperature thermometer. Divco No. 229 flux is applied with the flux applicator and enough lead solder is flowed on to form a thin layer over the

circular areas of the plate where the elements are to be bonded. The plates are removed from the hot plate immediately and cooled. They are then cleaned in deionized water. A drawing of the absorber plates is shown in figure 52. The preparation of the absorber plate subassemblies is complete. Absorber plates in various stages of completion are shown in figure 53.

## SUBASSEMBLY STEP II - PREPARATION OF ALUMINUM RADIATOR PLATES

### II-1 Equipment

- a. Radiator Plate Forming Die, see figure 49.
- b. Hydraulic Press, see figure 50.
- c. Hot Plate
- c. Vapor Degreaser
- e. Electroless Nickel Plating Apparatus, see figure 51.
- f. Artists Brush
- g. Oven, controlled temperature
- h. Annealing Furnace, controlled temperature and atmosphere
- i. Tweezers
- j. Radiator Plate subassembly jig, see figure 54.

### II-2 Materials

#### II-2.1 Direct

- a. Aluminum, alloy 1100, 0.008 inch thick sheet
- b. Electroless Nickel
- c. Liquid Bright-Gold
- d. Epoxy Adhesive, Type A-1 (with Activator A)
- e. Mylar Film, 0.002 inch thick

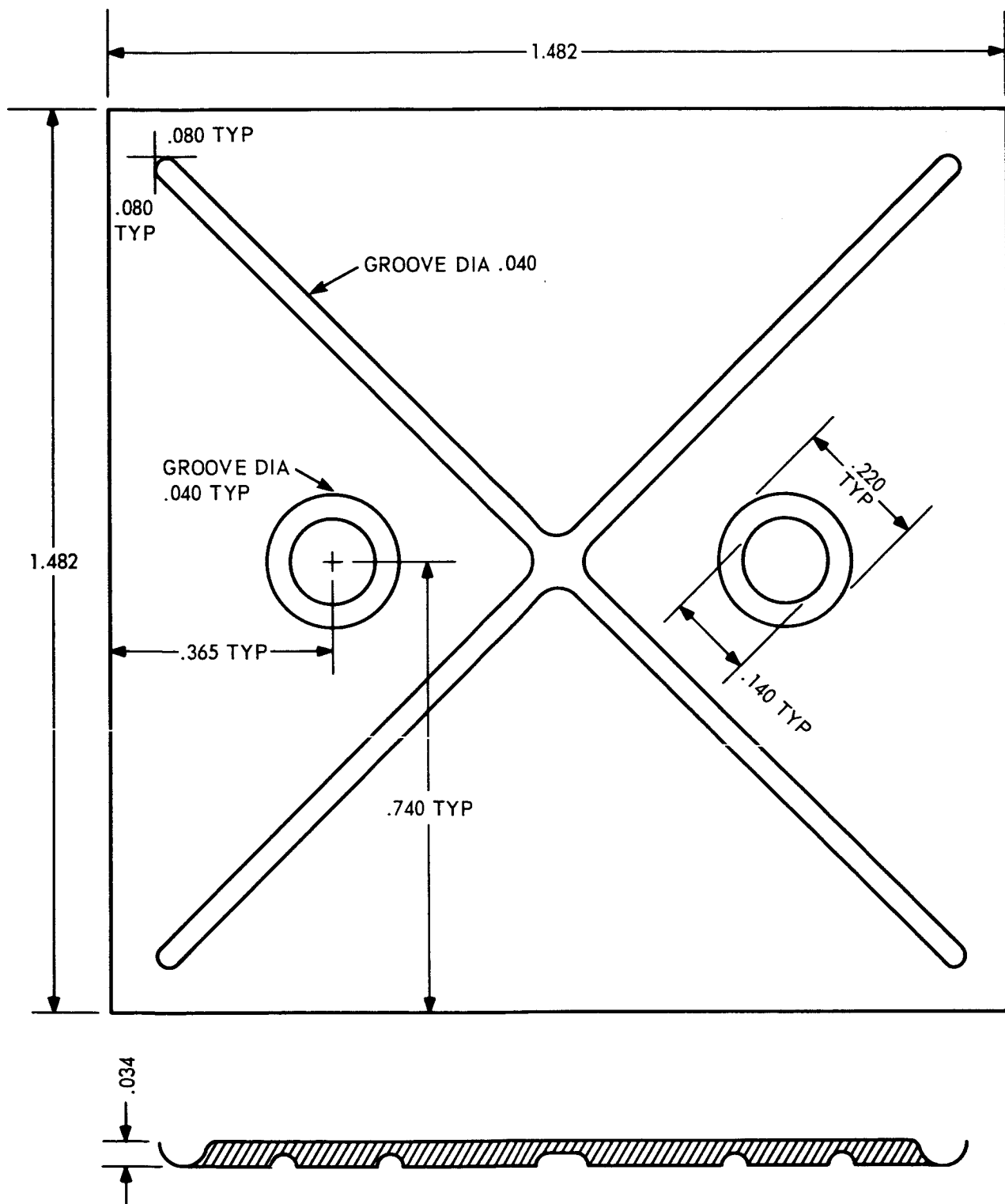


Figure 52. Drawing of Absorber Plate

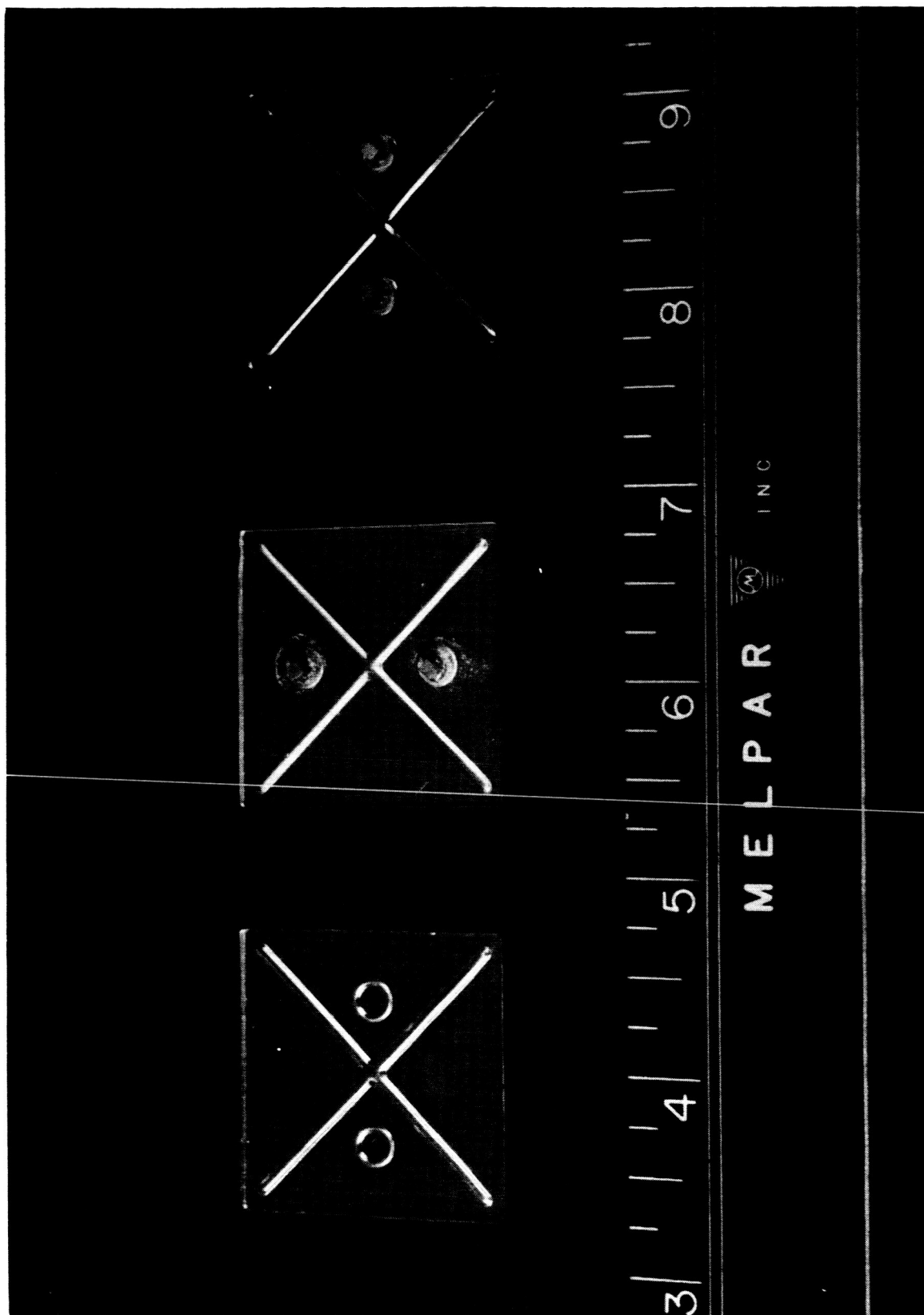


Figure 53. Absorber Plates: As Formed, with Elements Attached, and Coated with Gold

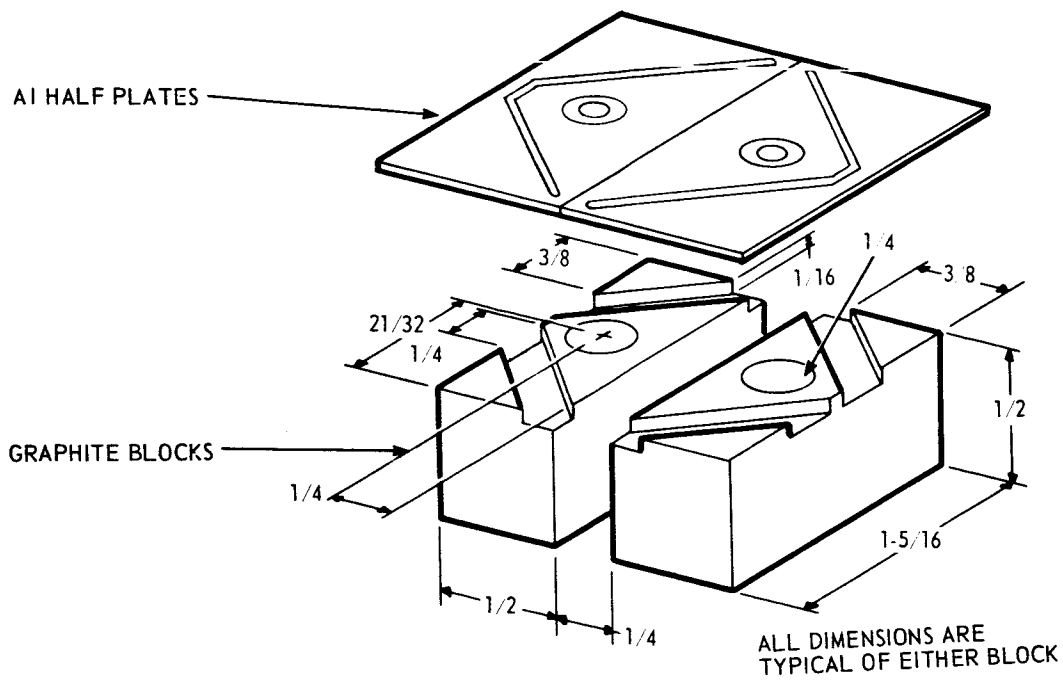
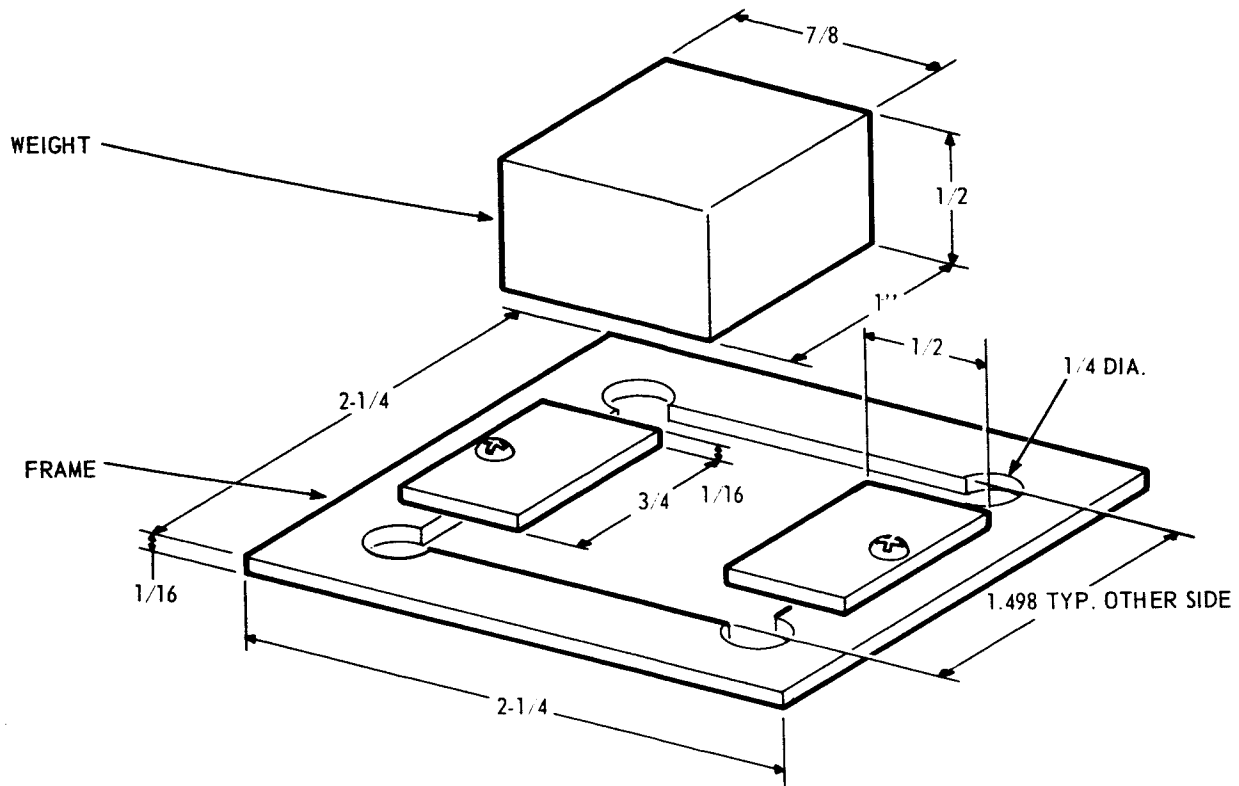


Figure 54. Assembly Jig for Radiator Plate Subassembly

## II-2.2 Indirect

- a. Methanol, C.P.
- b. Water, deionized
- c. Trichloroethylene, C.P.
- d.  $\text{NH}_4\text{OH}$ , Reagent
- e.  $\text{NaOH}$ , Reagent
- f. Forming Gas (10%  $\text{H}_2$  - 90%  $\text{N}_2$ )

## II-3 Procedure

a. The alloy 1100 aluminum in the form of 0.008 inch thick foil is cut into squares and formed into the shape of the radiator plates using a forming die in the hydraulic press. The formed part is removed from the die and cleaned in trichloroethylene, rinsed with methanol and dried.

b. After forming, the radiator plates are annealed in a forming gas atmosphere at  $580^\circ\text{C}$  for 30 minutes, in the annealing furnace, and then are cooled slowly to room temperature. The plates are handled with tweezers throughout these operations.

c. The next operation is the cleaning prior to electroless nickel plating of the plates. The radiator plates are first degreased in a vapor degreaser containing trichloroethylene. After the degreasing they are rinsed in methanol and immersed in a cleaning etch composed of 100 grams of  $\text{NaOH}$  in 150 milliliters of concentrated  $\text{NH}_4\text{OH}$  for 30 seconds. This is followed by three rinses in concentrated  $\text{NH}_4\text{OH}$ .



d. Following the last rinse in concentrated  $\text{NH}_4\text{OH}$  the plates are transferred immediately to the electroless nickel plating bath. This should be accomplished quickly enough that the immersion in the bath takes place while a film of  $\text{NH}_4\text{OH}$  is completely covering the aluminum plates.

e. Upon completion of the electroless plating step, the plates are rinsed in deionized water, methanol and dried.

f. Next, the high-emissivity Liquid Bright-Gold coating is applied to the inner surface of the plates with a small artist's brush. It is flowed on and spread around on all areas of the inner surface, except where the thermoelectric elements are to be bonded. Only a small amount is necessary.

g. The Liquid Bright Gold coating is cured and baked on at  $250^\circ\text{C}$  for 6 hours in the controlled temperature oven.

h. The last operation in the preparation of the radiator subassemblies is the joining of the separate pieces to form an adhesive bonded pair (see figure 55). This is accomplished in a radiator plate subassembly jig (see figure 54). Epoxy adhesive is used to form an electrically insulated joint between the two plates. Small pieces of mylar (0.002 inch thick) are used as spacers between the two radiator plates.

i. The epoxy adhesive is cured in the controlled temperature oven at  $125^\circ\text{C}$  for two hours. The plates are then removed and allowed to cool. Drawings of the various forms of radiator plates are shown in figure 56. The preparation of the radiator plate subassemblies is complete.

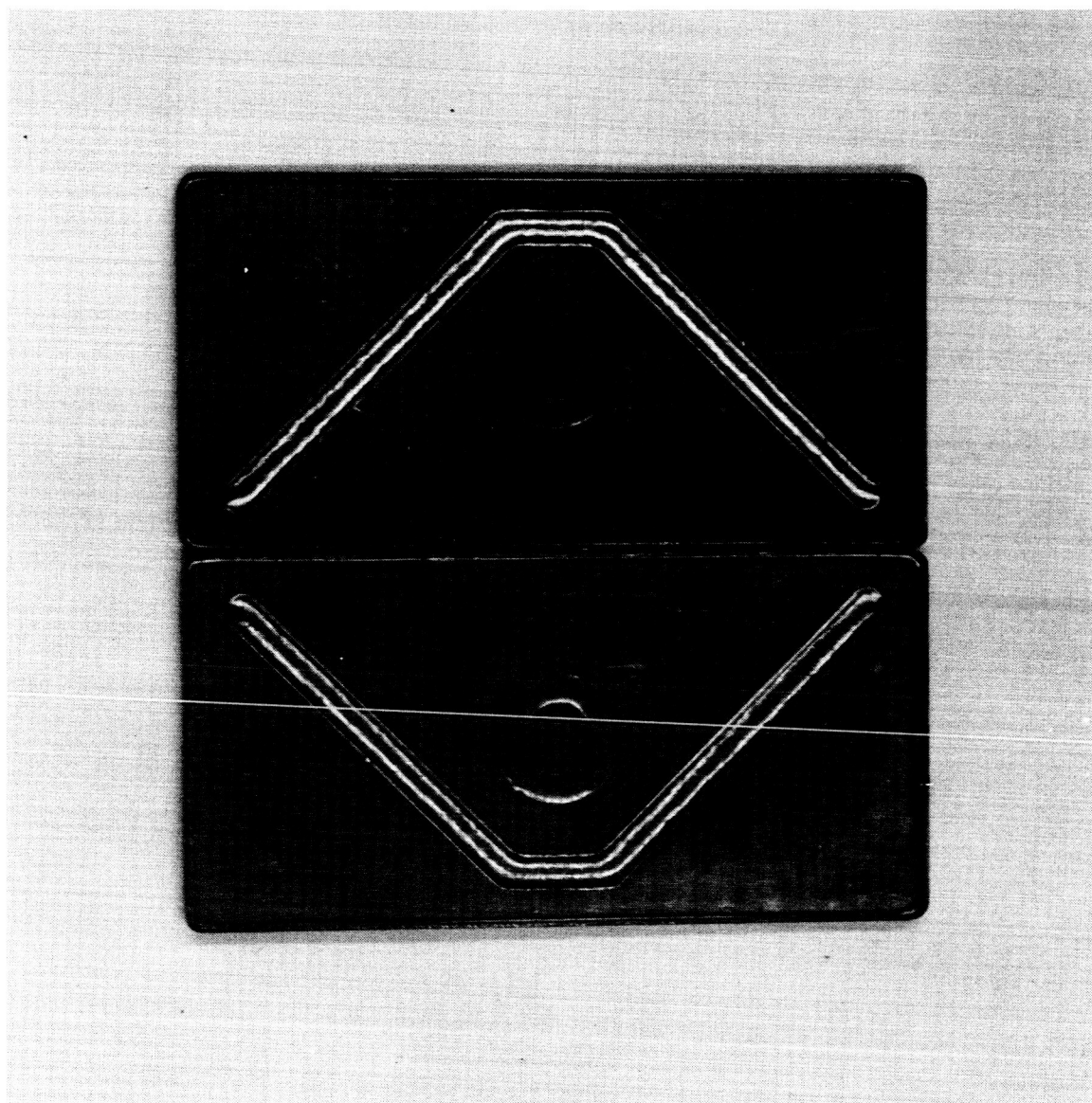
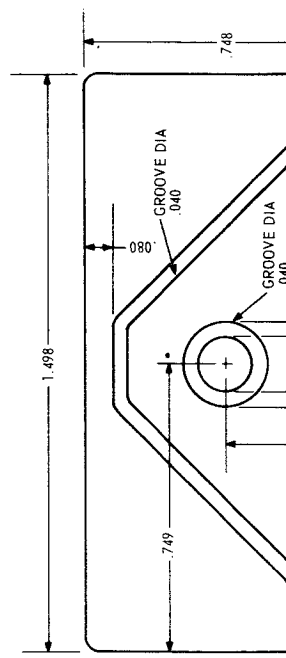
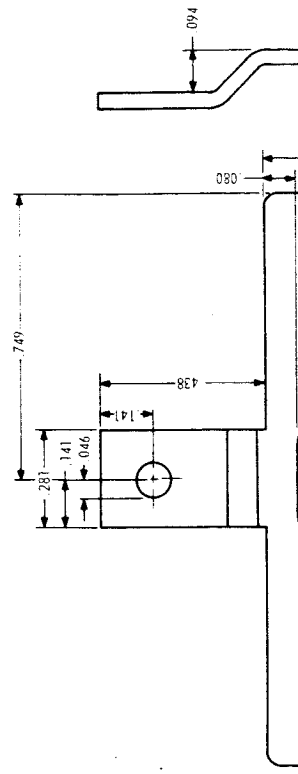
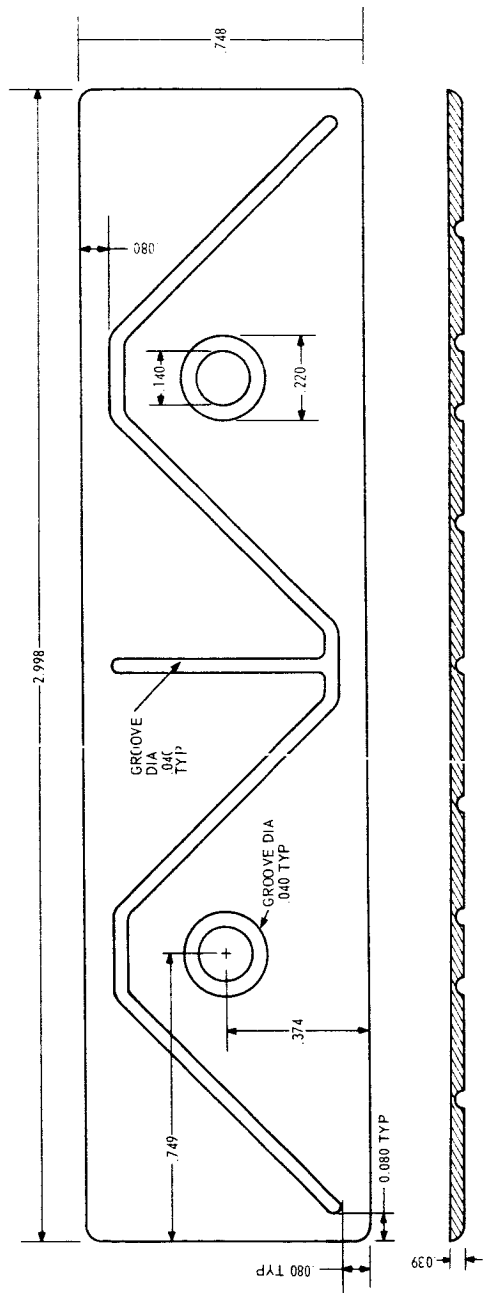


Figure 55. Radiator Plate Subassembly

LONG PLATE



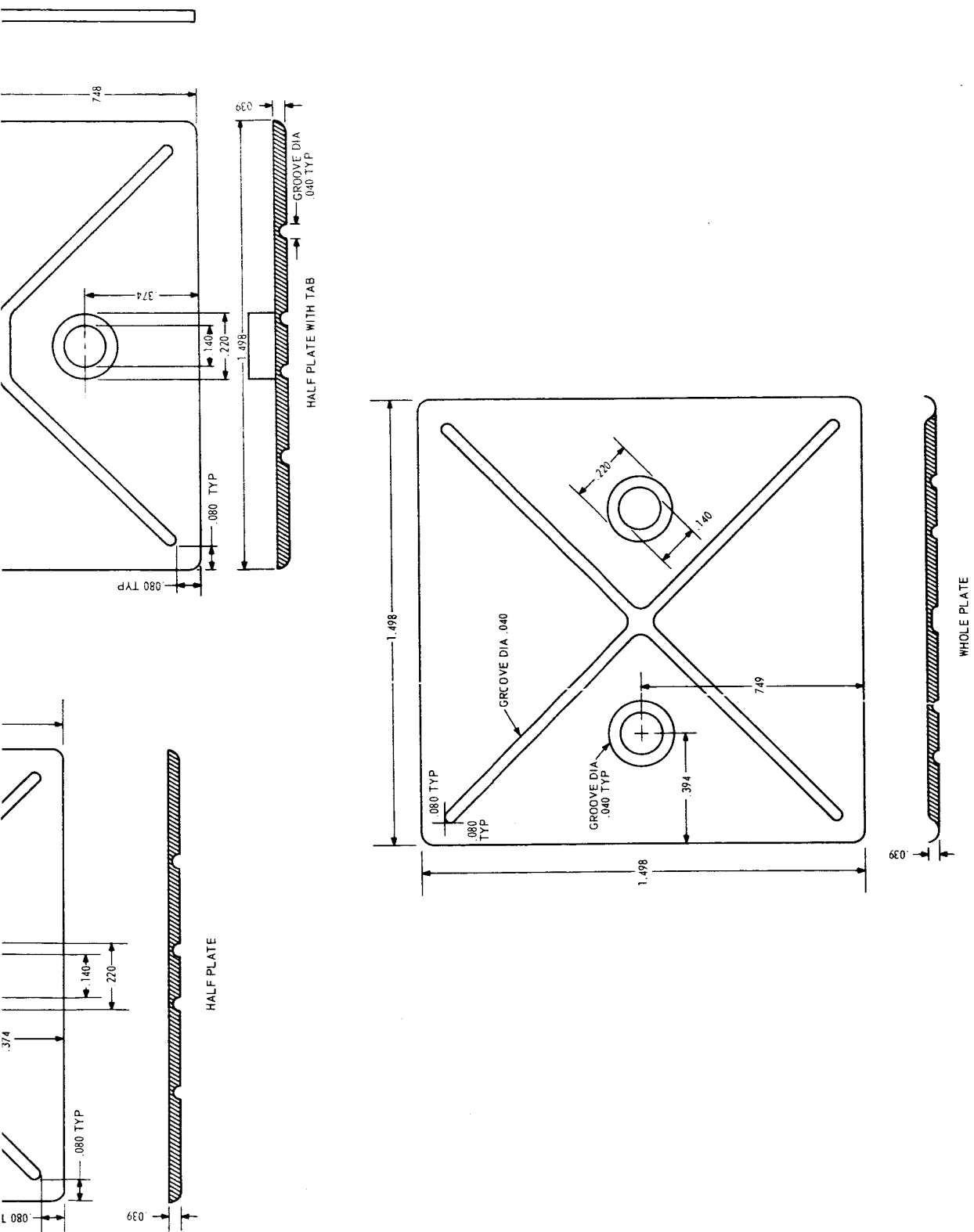


Figure 56. Drawing of Radiator Plates

## SUBASSEMBLY STEP III - PREPARATION OF THE STAINLESS STEEL SUPPORT STRUCTURE

### III-1 Equipment

- a. Graphite Soldering Jig
- b. Propane Torch

### III-2 Materials

#### III-2.1 Direct

- a. Stainless Steel Tubing, Type 304, 0.050 inch dia., 0.009 inch wall thick
- b. Stainless Steel Sheet, Type 304, 0.010 inch thick
- c. Solder (97.5% Pb - 2.5% Ag)
- d. Silicone Rubber
- e. Silicone Rubber Adhesive

#### III-2.2 Indirect

- a. Flux, Stainless Steel, Divco
- b. Silicone Rubber Adhesive Metal Primer
- c. Water, Deionized

### III-3 Procedure

a. The tubing and sheet materials are cut to the required sizes (see figure 58). Using a graphite jig to position the parts, and a propane torch, the frame of stainless steel tubing is soldered together. The low temperature silver solder is used with Divco stainless steel flux to make the joints. The stainless steel sheet mounting tabs and gussets are attached in the same way. The flux residue is removed by soaking in hot deionized water.

b. The sheet tabs and gussets are treated with silicone rubber adhesive metal primer which is allowed to dry for two hours in air at room temperature. After this, the silicone rubber adhesive is applied to these parts and the silicone rubber isolators (see figure 57) are bonded to these areas. The adhesive cures in four hours in air at room temperature. The preparation of the stainless steel support structure is complete. Figure 58 is a photograph of one of the stainless steel support structures.

#### SUBASSEMBLY STEP IV - ATTACHMENT OF TEST THERMOCOUPLES

Certain unit couple subassemblies must have thermocouples for testing purposes. This step applies to instrumental models only.

##### IV-1 Equipment

- a. Oven, controlled temperature
- b. Tweezers

##### IV-2 Materials

###### IV-2.1 Direct

- a. Thermocouples, Chromel-Alumel, 40 gauge, 6 inches long
- b. Epoxy adhesive, type A-1 (with Activator A)
- c. Silicone adhesive
- d. Mica, 0.040 inch x 0.040 inch x 0.0005 inch thick

###### IV-2.2 Indirect

None

##### IV-3 Procedure

a. Before the assembly of the thermoelectric element-absorber plate subassembly to the radiator plate subassembly, certain pieces are selected for thermocouples.

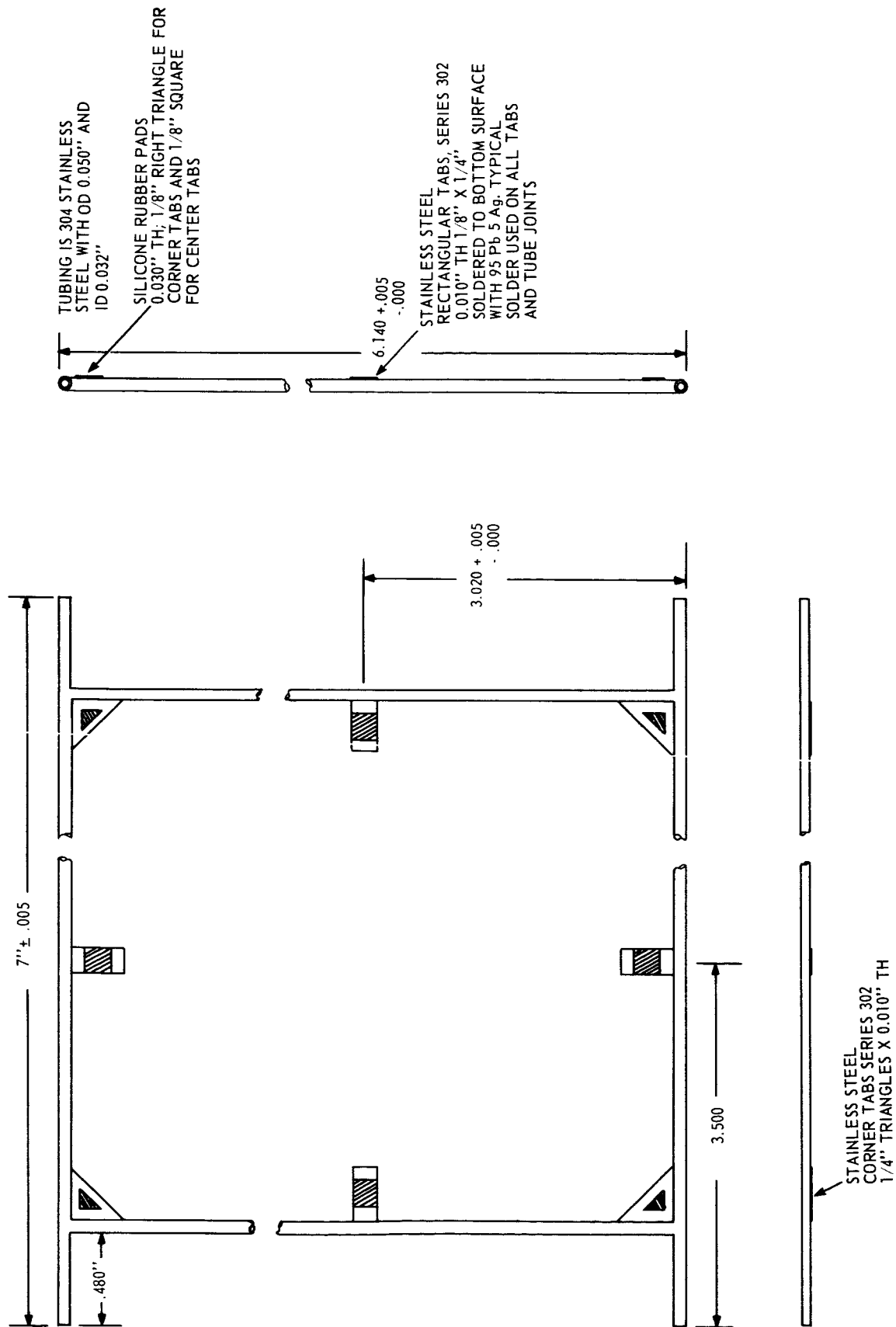


Figure 57. Drawing of Stainless Steel Support Structure

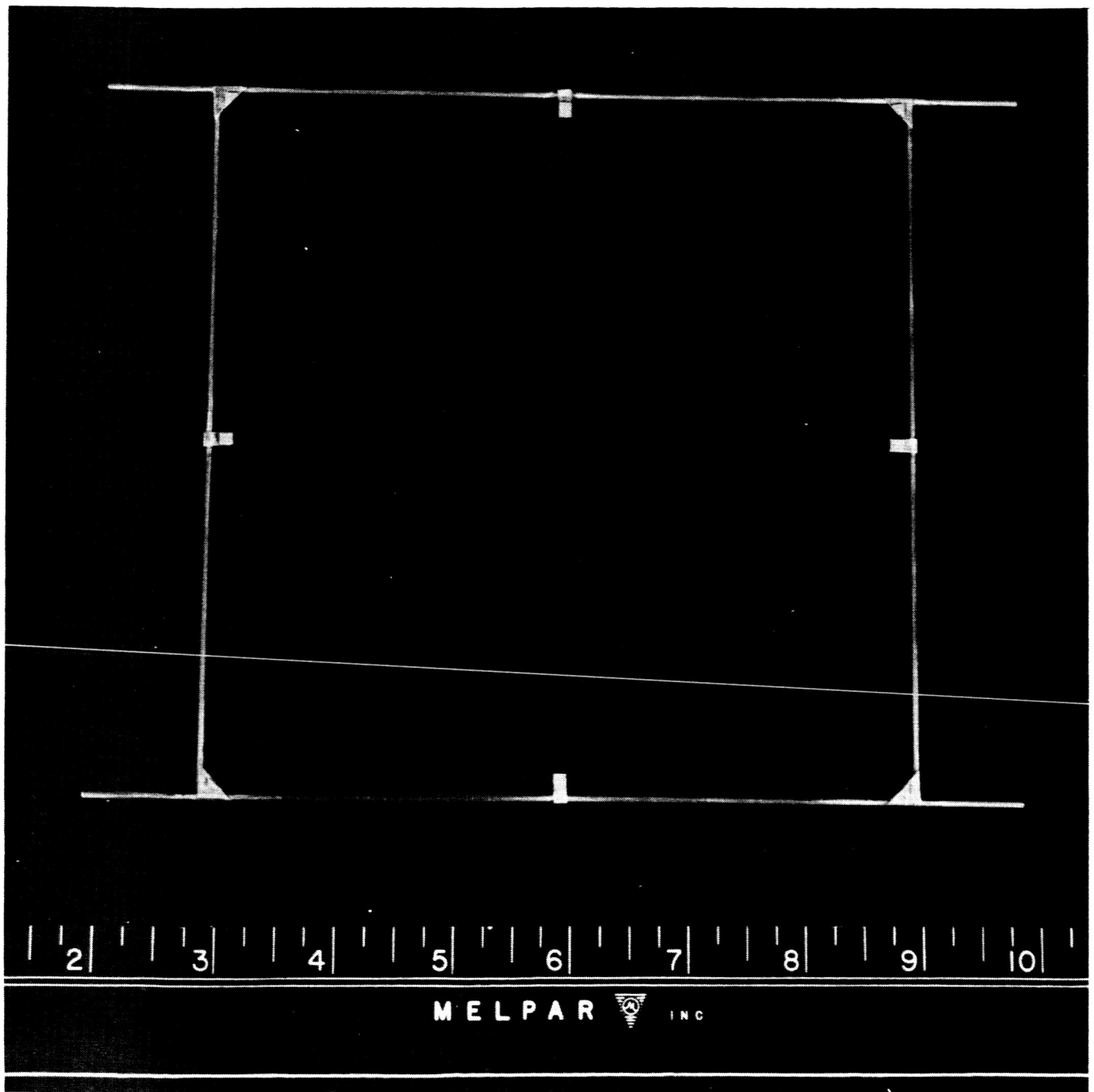


Figure 58. Stainless Steel Support Structure



b. A thermocouple, put into place with tweezers, is attached to the absorber plate with silicone adhesive. A small mica piece is used to provide electrical isolation between the plate and the thermocouple. The silicone adhesive is cured in the controlled temperature oven at 250°C for 4 hours.

c. Another thermocouple, put into place with tweezers, is attached to the radiator plate with epoxy adhesive. A small mica piece is used to provide electrical isolation between the plate and the thermocouple. The epoxy adhesive is cured in the controlled temperature oven at 100°C for 2 hours. This completes the attachment of the test thermocouples. Each instrumented model has two separate single couples with test thermocouples.